ADDIS ABABA UNIVERSITY

SCHOOL OF GRADUATE STUDIES

COLLEGE OF NATURAL AND COMPUTATIONAL SCIENCES

SCHOOL OF EARTH SCIENCES

INTEGRATED GEOPHYSICAL CHARACTERIZATION OF INJIBARA UNIVERSITY CAMPUS BUILDING SITE, INJIBARA, AMHARA, NORTH WESTERN ETHIOPIA

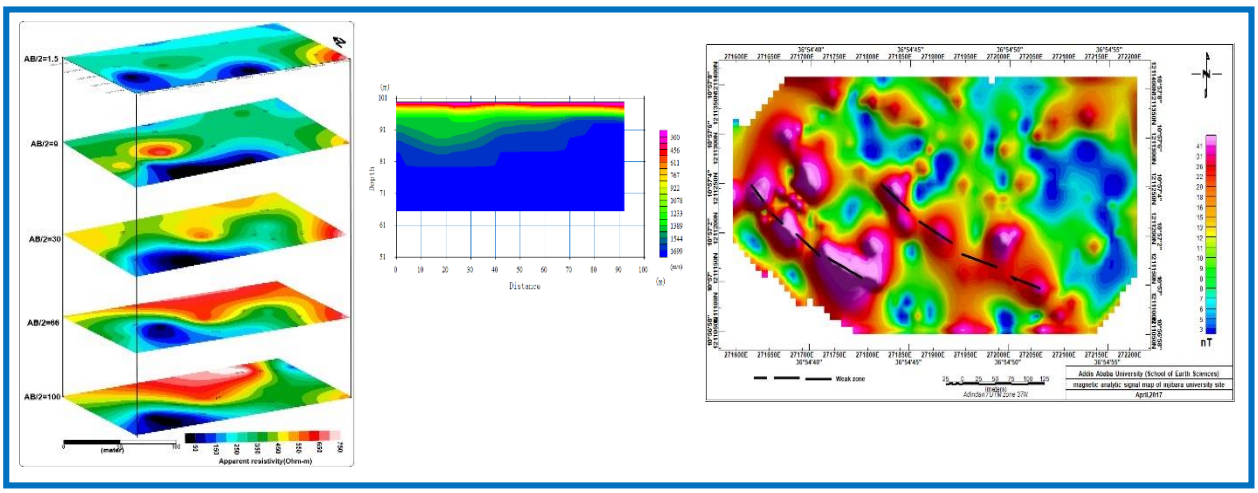

BY

ABRAHAM MULUALEM

A Thesis Submitted to the School of Graduate Studies of Addis Ababa University in Partial Fulfillment of the Requirements for the Degree of Master of Science in Earth Sciences (Exploration Geophysics)

June, 2017

Addis Ababa, Ethiopia

ADDIS ABABA UNIVERSITY

SCHOOL OF GRADUATE STUDIES

SCHOOL OF EARTH SCIENCES

INTEGRATED GEOPHYSICAL CHARACTERIZATION OF INJIBARA UNIVERSITY CAMPUS BUILDING SITE, INJIBARA, AMHARA, NORTHWESTERN ETHIOPIA

By

Abraham Mulualem

Faculty of Science

School of Earth Sciences

Approved by board of examiners:-

1. Dr. Balemwal Atnafu Signature_____

(Head, School of Earth Sciences) Date_____

2. Dr. Getnet Mewa Signature_____

(Advisor) Date_____

3. Prof.Tilahun Mammo Signature_____

(Examiner) Date_____

4. Prof.Tigistu Haile Signature_____

(Examiner) Date_____

Declaration

This is to certify that the thesis prepared by Abraham Mulualem entitled: **"INTEGRATED GEOPHYSICAL CHARACTERIZATION OF INJIBARA UNIVERSITY CAMPUS BUILDING SITE, INJIBARA, AMHARA, NORTHWESTERN ETHIOPIA**" is my original work conducted under the supervision of Dr.Getnet Mewa and has not presented to any university or institution for the award of any degree or diploma program and all sources of materials used for the thesis are duly acknowledged.

Name of the candidate	Signature	Date
Abraham Mulualem	_____	_____

This is to certify that the above declaration made by the candidate is correct to the best of my knowledge and it has been submitted for examination with my approval as university advisor.

Dr.Getnet Mewa	Signature	Date
(Advisor)	_____	_____

ABSTRACT

Integrated geophysical investigations, specifically electrical resistivity, seismic refraction and magnetic methods were conducted for engineering characterization of the foundations conditions of the Injibara University buildings construction site located in Injibara town of Amhara Regional State, NW Ethiopia. The principal objective of this research is to study the suitability of the foundation Earth materials underlying the site, where Injibara University is established.

The geophysical survey included thirteen resistivity sounding points, seven refraction seismic spreads and 153 point magnetic data. Qualitative and quantitative interpretation of the data have provided valuable geotechnical information using pseudo-depth and geo-electric section, sliced-stacked map, seismic velocity models and magnetic anomaly maps incorporated with available geologic information from the study area.

Interpretation of the geophysical data revealed that the surface geology of the area is composed of three layers. The top soil consisted of clay, silt and sand mixtures having 1-4 m thickness range is mapped over the whole area. The second layer of low resistive layer is interpreted as highly weathered and fractured vesicular basalt. The depth extent of this layer varies from about 10m on the NW end and SE parts and to about 27m around the central part. The third layer occurred in the depth range of 10-27m is characterized by relatively high resistivity and average high p-wave velocity (2550 m/s) and it is the response of the moderately weathered and fractured basaltic bed rock, which is deeper near to the center of the profiles and gets shallower towards NW end and southeastern portions. Besides, analyses of collected data have suggested the possible locations of minor structural discontinuities (may be local fractures).

The geophysical results with summary shows that the bed rock is found at shallow depth in the northwestern end and southeastern part of the study area, whereas in the near central part of the survey area the bed rock is found at a relatively high depth. Setting the building foundation is more recommended in the southeastern part of the construction site, but in the near central and northwestern part much attention should be taken in designing the foundation of the building site in order to avoid any geo-hazard consequences.

ACKNOWLEDGMENT

My first deepest gratitude goes to my advisor Dr. Getnet Mewa for his follow up, constructive comments, encouragement, guidance and reviewing the thesis and providing all the information for the completion of this thesis work. During the time that I engaged in field work, he acted like not only my advisor but also like my father and colleague. I am running out of words to express my thanks to him that he has done for me.

Secondly, I would like to thank Institute of Geophysics, Space Science and Astronomy (IGSSA) staffs for allowing me to use the geophysical instruments for my fieldwork and Arba Minch University for the permission and support during my graduate study.

Special thanks go to Prof. Tilahun Mammo, Prof. Tigistu Haile and Dr. Abera Alemu for their fruitful and supportive discussions on various theoretical aspects of the geophysical methods. I have learned many things from you.

My special thanks also go to my best friend Mr.Melese Temesgen for his incredible support and assistance in the field data collection. I never forget throughout my life his support in the field, he scarifies specially his very valuable time to help me.

I would like to thank the PhD and MSc. candidates of the geophysics stream at the School of Earth Sciences of Addis Ababa University, especially Mr.Mengistu Bacha,Mr. Tefera Alemu and Mr. Haileyesus for assisting me in processing resistivity and magnetic data using different software. I am also glad to thank Mrs.Hanna Muluneh, Mr.Mandefro Mengistu, Mr.Yonas Muluneh, Mrs.Dagmawit Ferede, Bahiru Mandefro and Birtukan Alemye who helped me in different issues.

I am very thankful to Injibara University administrators for the permission to enter into the campus and support during field work in providing the site plan.

Finally, my sincere thanks go to my parents who helped me a lot in finalizing this thesis work within the limited time frame.

Table of Contents

List of Figures

List of Tables

List of Appendices

Appendix-1

Appendix-2

Appendix-3

Appendix-4

Appendix-5

Acronym

masl	meter above sea level
m	meter
Km	Kilometer
Ω-m	ohm-meter
Hz	Hertz
Fig	Figure
GPS	Global Positioning System
IGRF	International Geomagnetic Reference Field
ADSWE	Amhara design and supervision Works enterprise
NE	Northeast
NW	Northwest
RMS	Root Mean Square Error
SE	Southeast
SW	Southwest
UTM	Universal Transversal Mercator
VES	Vertical Electrical Sounding
2D	Two Dimensional
WEP	Northwestern Ethiopian plateau

CHAPTER I

1. INTRODUCTION

1.1 General background

Construction of sustainable civil engineering structures, whether simple or complex ones, requires profound knowledge about the characteristics of subsurface Earth materials, particularly the physical peroprties of the underlying rocks/soils, distribution of tectonic elements, contents of moisture / fluid within them etc. Discontinuities in the form of bedding planes, joints, faults and folds highly determine the physical strength (deformation characteristic) of rocks. Similarly, properties of materials filling voids (openings), such as pure/mineralized water, air or both in unconsolidated soils or fractured rocks influence their physical characteristics. Therefore, the stability of civil engineering constructions depends on the correct assessment of the various physical and geotechnical properties of the underlying earth materials where the structures are intended to be erected (Johnson, 1991).

However, constructions undertaken over formation with insufficient bearing capacities often result in unexpected failures, manifested in the form of cracks, settlements, displacements or total collapses. Particularly, those structures erected over areas where expansive soils (such as clays) are widely distributed demand special attention as their shrinking and swelling characteristics can easily cause damages due to their property variations as a result of moisture / fluid content fluctuations associated with seasonal changes.

Therefore, geotechnical investigation of any construction sites is essential to obtain reliable inputs that enable to develop economically and technically feasible structural designs incorporating mitigation measures to anticipated geo-hazard events.

Like elsewhere in the world, Ethiopian public officials require geotechnical investigation data acquired in accordance with the Ethiopian Building construction Code with accompanying recommendations prior to issuing a building permit in order to protect the safety of the public the surrounding environment (Ethiopian building code, 1995).

Unlike drilling, pitting and trenching, geophysical methods are environmentally safe and also do not cause any significant damages/ concerns to the communities. Geophysical measurement responds to change in the physical, chemical, mechanical, elastic, radioactivity or thermal

properties of the underlying earth materials. Because of such divers characteristics usually one or more of the properties correspond to certain features of earth materials, i.e., contact, discontinuity (fracture/fault zones). Unlike direct sampling, such as drilling or pitting and sending samples to laboratories for analyses, geophysical methods respond to different parameter in different ways and deliver information in a short time with minimum expenses.

For engineering applications seismic refraction, electrical resistivity and magnetic methods are widely used to map the subsurface structures. These methods depend on the acoustic impedance, ground resistivity and magnetic susceptibility contrast of the subsurface materials respectively.

The unique tectonic setting of Ethiopia results in complex geological and geo-morphological setups where along with these and continuously deteriorating environmental conditions, the country is very vulnerable for such geo-hazard risks, as volcanic, seismic, land slide and alike. Every year Ethiopia allocates quite a substantial amount of budget to the expansion of infrastructures: roads, bridges, dams and building complexes. Particularly, to expand access to education the construction of universities is taking place in different parts of the country and among these is the Injibara University.

To study the foundation conditions at site and evaluate its suitability for erecting a four story building to be used as dormitory for student, subsurface investigations were carried out employing electrical resistivity, magnetic and seismic refraction methods with an ultimate objective of generating inputs for civil applications.

1.2 Project Site Description

1.2.1 Location, accessibility and geomorphology

The research area, Injibara University site, is situated, in Awi Zone, Amhara Regional State about 447km NW of Addis Ababa (Figure1.1). It is bounded by UTM coordinates 271602-272203m Easting and1211020- 1211378m Northing, and is generally characterized by flat to gently sloping topography bounded by mountains and small hills from the western and southern side (Figure 1.2). It has an average elevation of about 2552m amsl and located about 1.5 km SW of Injibara town, just on the Injibara-Chagni asphalt road.

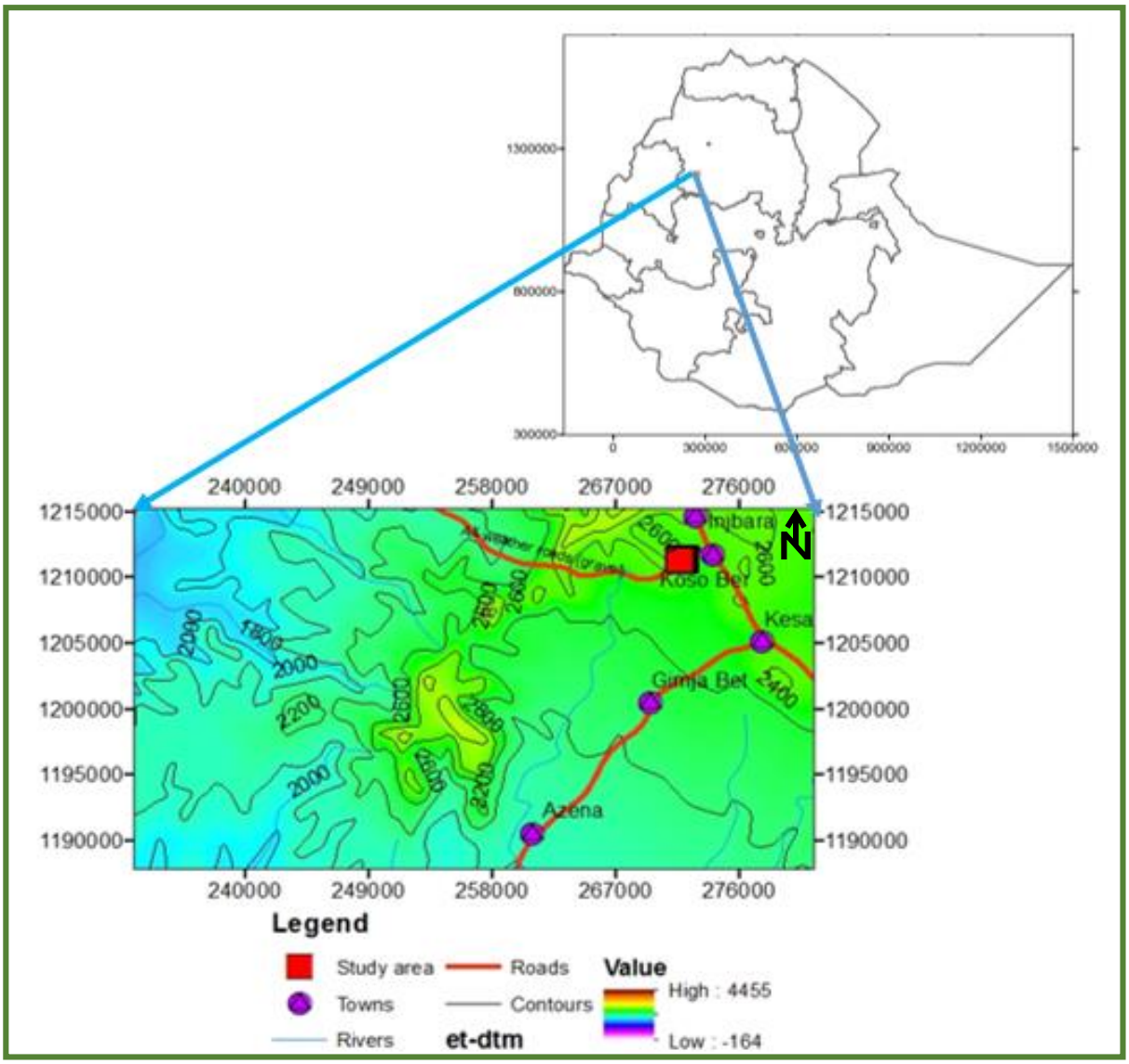

Figure1.1. Location map of the study area

Figure 1.2. Partial view of the construction site

1.2.2. Physiography, drainage and climate

The present landscape of the research site and its surroundings is a result of volcanic, tectonic, erosion, deposition and related processes. Accordingly, three main geomorphologic features characterize the study area and its surrounding areas namely: plateau, low land plain and mountains (figure1.3). The plateau occupies a wide area forming flat to undulating landform that is slightly incised by small gullies with seasonal flows; the low land (plain) have relatively small coverage that also includes the current study area, whereas the mountainous landform represents the areas on northern and western parts of Injibara and are characterized by highly dissected landscape.

Indigenous plants and hybrids cover the surrounding areas, but except few isolated trees there is no vegetation cover within this specific study site. The prominent rivers/streams over the area are Mesni, Sutena and Zerket. Besides, such perennial streams as Ayo and Ayma are flowing that finally join the Abay River (ADSWE, 2008).

Based on annual and monthly mean temperatures, changes in seasonal rainfall, types of natural vegetation and altitudes, the climate of the project area is categorized to dega and cool temperate regime (Table1.1). Fluctuation of rainfall, which is the crucial input in the hydrological cycle, determines the quantity/volume and distribution of surface and sub-surface water resources. Often the impact of rainfall variability is evident on surface water sources within a short time, and unlike this it's the impact on subsurface water resource is more complex and requires much longer time.

The main rainy season in the area lasts from June to September, whereas from October to May it is totally dry, but it get remarkable rainy days even within the dry month specified above.

Table 1.1: International Climatic classification based on altitude (ADSWE, 2016).

Altitude (masl)	Mean annual Temperature(^{o}C)	Description	Local name
> 3300	<10	Cool	Kure
2300-3300	10-15	Cool Temperate	Dega
1500-2300	15-20	Temperate	Woina-Dega
500-1500	20-25	Warm Temperate	Kola
< 500	>25	Hot	Bereha

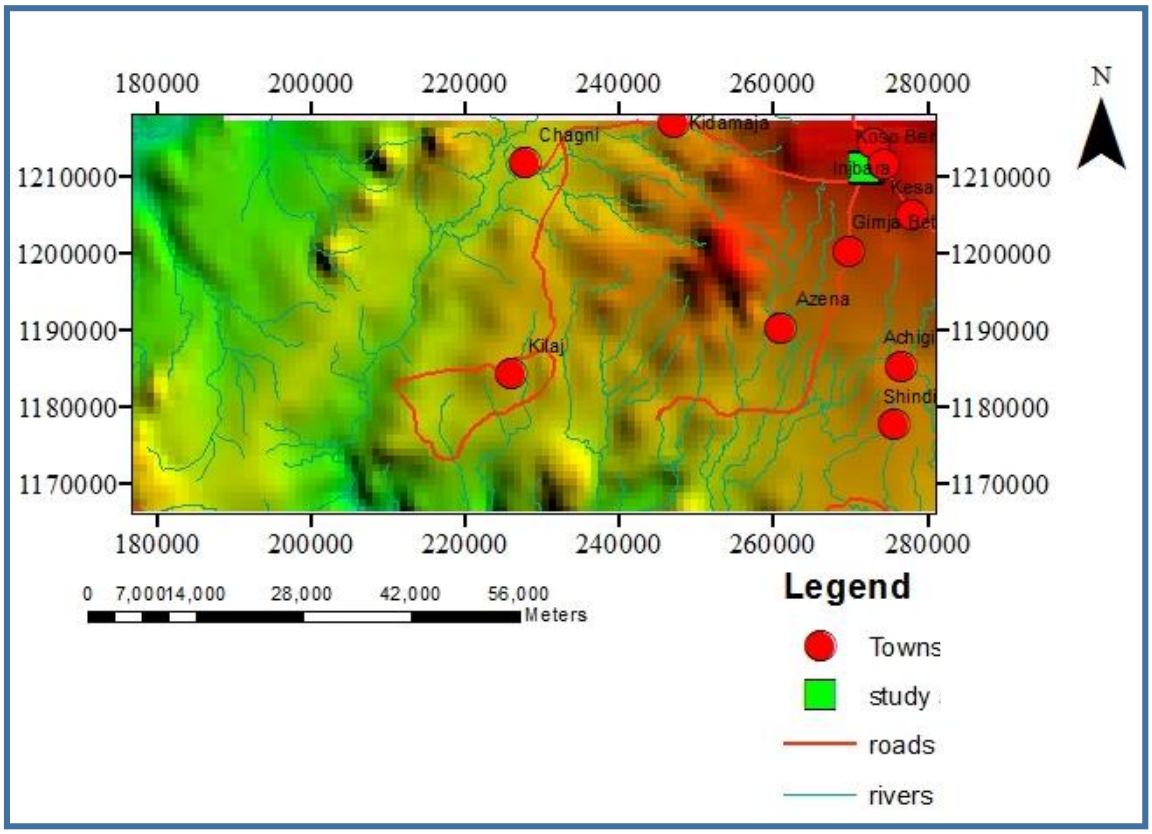

Figure1.3. Physiographic map of the study and its surroundings

1.3 The research problem

Severe damages on buildings, roads and other major infrastructures occur primarily due to insufficient investigations and understanding of the subsurface structures that serve as input for the preparation of design of civil engineering structures. Therefore, in this study geophysical methods were applied to collect more continuous information allowing to study the subsurface characteristics, i.e., compositional variation, depth to competent bedrock, thickness of saturated beds, and depth to groundwater table, location and extents of structural discontinuities. Often these geological features have significant impact on the stability of building foundation. In doing so, crucial information can be collected probably missed during geotechnical tests relied mainly on test pit results. It is only detail knowledge and due consideration of the subsurface geological characteristics that helps to avoid, if not minimize, construction failures and reduce economic loses and human sufferings.

With the above considerations, attempt is made to address the fundamental research problem through integrated analyses of electrical resistivity, seismic wave velocity and magnetic property measurements/determinations as well as available geotechnical information.

1.4 Research questions

In view of the problem stated above, the research questions that are required to be addressed can be briefly formulated as follows:

1. How much is the approximate depth to the competent bedrock and what morphology it has within the research area?
2. How does the local geology and structures vary both laterally and vertically over the construction site?

In order to answer the above research questions general and specific objectives are formulated and addressed using standard survey methodologies that are discussed in detail in the following.

1.5 Research objectives

1.5.1 General objective

The principal objective of this research is to study the suitability for foundation of the Earth materials underlying the Injibara University campus construction site, by employing geophysical survey techniques.

1.5.2 Specific objectives

To deal with this general objective, this research has planned to address the following specific objectives:

- Determine depth and the thickness of individual layers (strata) of the subsurface over selected areas of the construction site and their probable effect on the building foundation
- Map any structural discontinuities (fractures, faults, weak zones) and infer their possible impacts on the safety of buildings;
- Estimate depth to groundwater table (if it exists within the limit of depth of investigation) or to any saturated bed;
- Determine the depth to the competent bed rock that serve as good foundation for building construction;
- Provide recommendations on the foundation conditions in relation to their suitability for building construction in in the site.

1.6 Expected outcome and significance

The outcomes of this research are assumed to be essential to evaluate the foundation conditions of the Injibara University construction site and within its premises identify possible locations with strong bearing capacities. In addition, structural disturbed zones and lithological zone likely with poor bearing-capacity, shallow groundwater table, and other important features will be delineated.

The research outcomes are presented as plan maps, pseudo-depth and geo-electric sections reflecting the main features of the underlying earth materials in a form that they were easily understand by any user.

1.7 Limitation of the study

In this thesis work, all efforts have been made to carry out the study in a systematic manner, well equipped with geophysical instruments to collect field data. Besides, limited secondary data has been acquired from some offices. However, as it happens in similar research works, this study has also faced number of limitations, of which the following were the primary limitations:

- Major financial constraint for logistics and daily expenses didn't allow to extend the field duration so as collect more data over the entire area in a systematic manner.
- Inconveniences encountered in the project area to carry out field data acquisitions (too many noise sources, limitations to extend electric cables and seismic cables, presence of metallic objects in some places, etc.).
- Insufficient secondary data, like drilling and detail geology, providing comprehensive information useful for data interpretation collected from this particular locality.

1.8 Research Methodologies

1.8.1 Methodologies

The success of any research work is highly determined by appropriateness and feasibility of the methodologies employed to achieve the objectives. In this case, to deal with both the general and specific objectives stated earlier, both primary and secondary data are used. Secondary data sources obtained from different government offices, literatures related to geophysics, geological, hydro- and engineering geological investigations are thoroughly reviewed.

In general, the methodology used in this research work involved three steps, which are classified as desk study, field data collection and Data processing and analysis.

1.8.1.1 Desk Study

Identifying and reviewing of previous data/information that have relevance to the current research work was the first step, which includes the following activities:

- ✓ Identification and interpretation of topographic and geological maps.
- ✓ Reviewing published and unpublished maps, reports to get insight into the geological, hydro-geological, engineering geological and geophysical peculiarities of the study area.
- ✓ Interpretation and develop conceptual models that serve as input to prepare refined field survey methodology.

1.8.1.2 Field data collection

Field work, which is the most important part of this research work, has been executed. Under this step all the necessary primary geological and geophysical data have been collected as follows:

- Acquisition of magnetic data at average station spacing of 15-20m following selected traverses and at random points considering accessibility conditions employing the GSM-19T proton precision magnetometer.
- The magnetic data were collected by establishing a base station and at each station magnetometer reading, position, time and elevation were recorded. Each base station was recovered (revisited) every an hour.
- Electrical resistivity sounding using SARIS Terrameter with schlumberger electrode arrays. The interval between successive sounding stations varies from 45-190m.
- Seismic refraction data acquisition was carried out employing 48-channel Dolang Seismograph. In this research only 24 and 12-channels with vertical geophones depending the accessibility of the site, where active construction is taking place. The geophones were laid down at a spacing varies from 4 to10m. Seismic refraction data have been collected along seven spreads with the spread length varying from 60 to 120m.

1.8.1.3 Data processing and analysis

The primary data collected from the field work was processed and analyzed using different software packages. These important and widely used software include the Oasis Montaj V6.4.2, Arc GIS 10.1, WinResist, SeisImager/2D, Surfer 10, MapInfo and IPI2win. Using these software packages data were presented for qualitative and quantitative interpretations that finally enabled to produce the results in the form of geophysical anomaly maps, sections and profiles.

The generalized Flow chart of methodological approach used for this study is described in Figure 1.4.

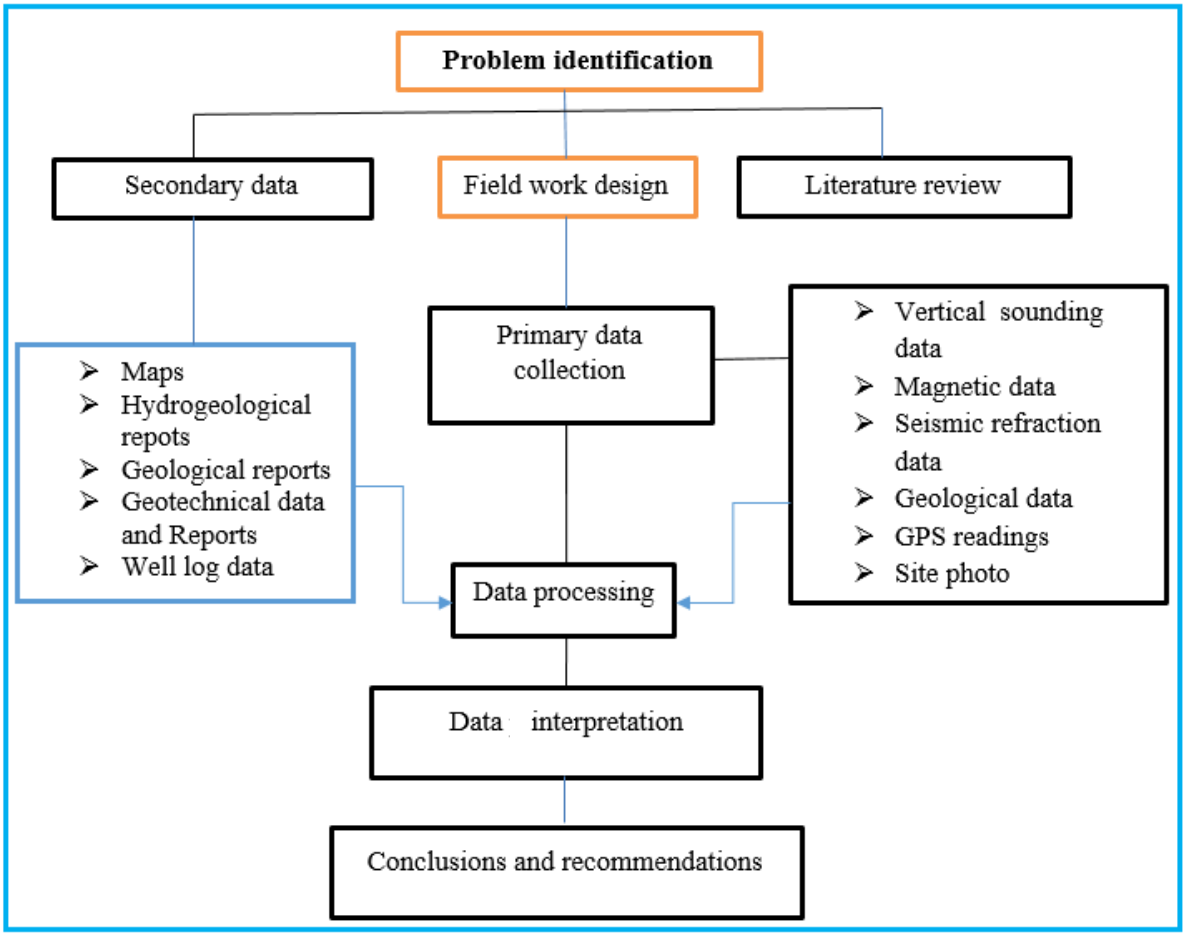

Figure1.4.Flow chart of the methodological approach employed during the present research work.

1.9. Instrumentation

Different geophysical instruments were utilized to collect data so as to achieve the objective set for the current research.

1.9.1 SARIS TERRAMETER

Scintrex Automatic Resistivity Imaging System (SARIS) was employed used for electrical resistivity sounding survey data acquisition. It is a portable terrameter with a digital readout that automatically displays apparent resistivity (in Ω-m), current (mA), voltage difference (mV) and standard deviation (SD). The accessories included stainless steel electrodes used as current and potential electrodes and wire reels.

1.9.2 Proton Precession Magnetometer

The GSM-19T proton precession magnetometer is a widely used modern equipment with high accuracy (1nT) and resolution (0.2nT). It measures the Earth's total magnetic field (nT).

1.9.3 Dolang 48-channel seismograph

Equipment used to perform the seismic refraction survey included the system unit (MOM) with an electrical timing signal, lap top computer to control the data acquisition process and display recorded signals, seismic cables, geophones to detect signals from the energy source and a 10kg sledge hammer as seismic energy source. Geophones are devices to transform seismic (mechanical) energy into an electrical voltage. A geophone consists of a coil wound on a high-permeability magnetic core and suspended by leaf springs in the field of a permanent magnet. If the coil moves relative to the magnet, voltages are induced and current will flow in any external circuit. The current is proportional to the velocity of the coil through the magnetic field, so that ground movements are recorded, not ground displacements (Milsom, 2003). Contact between the ground and the geophone is achieved by inserting the spike attached to the base of the geophone vertically into the ground.

The refracted seismic signals are received by geophones that are connected to a multi-core seismic cable with contact positions located at increasing distances from the source.

1.9.4 Global Positioning System (GPS)

The locations of sounding points, geophone position, shot points and magnetic observation stations i.e., Easting, Northing and elevations, were determined using the Garmin GPS map 62 receiver, which provides readings with an accuracy of ±2-3m.

1.10 Review of previous works

Few papers and reports concerning geology and hydrogeology of the area and vicinity have been written.

1. Amhara Design and Supervision Works Enterprise has conducted electrical resistivity survey in order to study the nature of the subsurface geological formation and delineating probable zones of saturation (aquifers).According to this study the dominant geological structures in the study area are lineaments, local faults and medium to large spacing fractures with three major sets trending N-S, SE-NW and NE-SW direction. Fractured and weathered vesicular basalt and inter-granular pore space are the major water bearing zones.
2. In 2016 MH Engineering Plc-Consulting Engineers and Architects has conducted a direct geotechnical method of investigation to collect information on the geotechnical properties of the geological formations within the specific site and to inspect construction material. According to their report, they have 20 dug test pits of about 3m in selected site and for each test pit visual description and laboratory analysis on selected soil samples collected from the excavated test pits have been conducted.

   From the laboratory test analysis they determine particle size distribution, liquid limit of soils , plastic limit and plasticity index of soils, natural moisture contents and free swell indices. Generally, by considering sub-surface condition, depth of moisture fluctuation zone, laboratory results and anticipated structural load from each structure category and bearing capacity values they give the following recommendations:

   - Footing foundation system is recommended
   - The foundation width should not be less than 1m
   - Floor slab should be placed on well compacted granular fill
   - Use allowable bearing pressure of 450Kpa if hard rock strata are encountered. The foundation depth should be 1.2-1.5m beyond the natural ground level.
   - Use allowable bearing pressure of 350Kpa if weathered or decomposed rock strata is encountered as foundation material. The foundation depth should be 1.5-1.8m beyond the natural ground level.
   - Use allowable bearing pressure of 300Kpa if very stiff cohesive or dense sand is used as foundation material. The foundation depth should be 2.0-2.4m beyond the natural ground level.
   - Use allowable bearing pressure of 250Kpa if medium stiff cohesive or medium dense sand is used as foundation material. The foundation depth should be 2.5-2.8m beyond the natural ground level.

- Use allowable bearing pressure of 200Kpa if soft cohesive or loose sand is used as foundation material. The foundation depth should go up to 3m.

1.11 Structure of the thesis

The whole body of this thesis work comprises of six chapters. Each chapter with its corresponding sections and subsections develop distinct information. Chapter one of the thesis describes the introduction part which include general description of the study area, statement of the problem, objective, methodology, limitation and previous work. The second chapter includes geology, hydrogeology and seismicity of the study area. In chapter three topics covered is theoretical background of the geophysical methods employed in the investigation. Chapter four covers the topics of data acquisition, processing and presentation. The interpretation of the different results is included in chapter five. The last chapter includes the conclusions and recommendations of the overall work of the thesis.

CHAPTER II

2. GEOLOGY, HYDROGEOLOGY AND SEISMICITY OF THE AREA

2.1. Regional Geology

According to Solomon Gerra (2000), the distribution of lithological varieties shows that Ethiopia is covered by about 18% Proterozoic crystalline basement 25% Mesozoic sediment and 56% Cenozoic volcanic and sediments.

Here, three major geological terrains recognized in Ethiopia are:

a) Proterozoic crystalline basement
b) Late -Paleozoic to Mesozoic marine and continental sedimentary rocks
c) Cenozoic, basic and felsic volcanic and associated sedimentary rocks

The study area is dominated by volcanic rocks therefore, the Cenozoic, basic and felsic volcanic and associated sedimentary rocks have been reviewed in the following subsections.

2.1.2. Cenozoic Volcanic rocks

The various volcanic rock units in the area cover large part of the north central and eastern part of the area forming a typical plateau topography and rarely rugged ridge chains in the NE corner. Relatively minor occurrences of the Tertiary Lower and upper basalt units and occur in the west and south part of the area unconformably overlying the Precambrian basement and Paleozoic – Mesozoic sedimentary rocks. The study area is included in the bure map sheet (NC-37/5) which is produced by geological survey of Ethiopia. The Tertiary volcanic rocks succession in the Bure map sheet comprises the following major rock units from bottom to top; Lower and Upper basalt units, trachyte flows and plugs , thin scoraceous basalt flows and scoraceous basaltic cones. Their grouping is made wholly based on their field characteristics; that are composition and texture, relative stratigraphic position and their geomorphic characteristics. The Lower and Upper basalt units show horizontal stratification and nowhere tilting of the volcanic rocks observed. The Lower basalt is named because it is found at the base of the Cenozoic volcanic succession of the area and the Upper basalt because it lies above the lower basalt (EIGS, 2008).

2.1.2.1 Lower basalt

The Lower basalt occurs at the base of the Tertiary volcanic rocks pile or succession of the

area and hence named Lower basalt. This unit commonly forms gently to moderately steep topographic features and rarely short cliffs. It shows both vertical and lateral variations in many aspects. Generally, it is dark gray to light-brownish gray and yellowish-brown and when it is moderately weathered often shows purplish and reddish brown color and fine grained rock. It is commonly jointed rock. Joints occur as vertical, horizontal, columnar with four to five faces and also as irregular joint sets (EIGS, 2008).

2.1.2.2 Upper basalt

The unit is usually exposed as a continuous or sheet-like, patchy or small blocks and fragmental outcrops. It usually forms the top most part of the plateau or the hills in the map area. The upper basal is relatively thinner than the lower basalt and its measured thickness reaches about 610 m. It is commonly exposed above 2400 m elevation.

Megascopically the upper basalt is dark gray to grayish and when weathered it is yellowish-brown to reddish white or purplish in color. It is fine to aphanitic, porphyritic with plagioclase, olivine, pyroxene and rarely amphibole phenocrysts. The abundance of the phenocrysts varies within the section. Green, coarse plagioclase laths of up to 1.5 cm long and hornblende are observed on the top of Gebezez Mariam and Chare hills and Bongit Tsion hills and are seen concentrated on the rock surface. The Tub is scarcely vesicular basalt and when occurs the vesicles are smaller in size (usually less than 5 mm) and are partially filled by calcite and zeolite minerals. It is commonly silicified and epidotized rock. At places it shows spheroidal and elephant skin weathered surfaces (EIGS, 2008).

2.1.3 Volcanics of North Western Ethiopian plateau

In the northwestern Ethiopian plateau, the volcanic succession is emplaced on the sub horizontal Mesozoic transgressive and regressive sedimentary strata. This volcanic plateau does not fit the popular image of a continental flood basalt province in that it is not a thick monotonous, rapidly erupted pile of un deformed flat lying tholeitic basalts. Instead, it is made up of several distinct volcanic centers with different magmatic character and with a large range of ages (Kieffer et al., 2004).

The major volcanic units of the northwestern Ethiopian Plateau (WEP) include:

- The Oligocene flood volcanic (Trap series)
- Miocene- Pliocene shield volcanoes
- Volcanic plugs and domes
- Quaternary volcanic

2.1.3.1. Trap series

In the northwestern Ethiopian plateau the flood volcanic succession includes basaltic lava flows, basaltic tuffs, as well as a considerable volume of rhyolitic, trachytic and phonolitic products (Mohr and Zenettin, 1988). Intermediate lavas are lacking and the volcanism is of a distinctly bimodal basalt rhyolite type a feature common to most continental flood basalt provinces. In their mineralogical composition most of the flood basalt are aphyric to sparsely phyric and contain phenocrysts of plagioclase and clino pyroxene with or without olivine. They have tholeitic to transitional chemical composition (Mohr, 1983).

2.1.3.2Tarmaber formation

The flood volcanism was succeeded by emplacement of large shield volcanoes and by continental rifting (Mohr, 1983). A number of large shield volcanoes developed on the surface of the volcanic plateau overlying the thick sequence of flood basalt. These volcanoes are conspicuous features of the Ethiopian plateau and distinguish it from other well known, but less well preserved flood basalt provinces such as the Deccan and Karoo. According to Kieffer et al., (2004) currently about 20 % of the surface of the plateau is covered by shields, the summits of the shields are about 1.5km above the flood basalt. They also calculated that the volume of the shields was about 20% of that of the flood basalts that is about 4x104km3.

Like the flood volcanics the shield volcanoes are bimodal and contain sequences of alternating basalts, rhyolitic and trachytic lava flows, tuffs, and ignimbrites, particularly near their summits. The lava flows of the shield volcanoes are thinner and less continuous than the underlying flood basalts. They also are more porphyritic, containing abundant and often large phenocrysts of plagioclase and olivine. The Simen shield is tholeitic and surmounts tholeitic flood basalts while Choke and Guguftu are alkaline and overlies alkaline flood basalts (Kieffer et al., 2004).

2.1.3.3 Volcanic plugs and domes

A conspicuous feature of the volcanic landscape in the northern Ethiopia volcanic plateau is the presence of numerous volcanic plugs. These structures are relicts of central conduits of volcanoes exposed by erosion of less resistant volcanic formations. They have felsic compositions and have been linked to the felsic volcanic rocks of the Ethiopian plateau. They have silica saturated, alkali rich trachytic composition. Their compositions are distinct from those of felsic rocks within trap sequences that are rhyolitic.The plugs are not the feeders to the trap volcanism but instead may be related to overlying shield volcanoes (Dercq et al., 2001). The Plugs are compositionally distinct from the majority of felsic volcanic rocks of the

plateau, which have rhyolitic compositions, and from more recent felsic volcanoes. Instead, they resemble the trachytic sills and flows that are intercalated with pyroclastic rhyolites (tuffs and ignimbrites) in the upper units of shield volcanoes (Tarmaber formation).

2.1.3.4 Quaternary volcanics

Quaternary alkali basalts occur related to local rift structures north south trending extensional faults. Volcanic cones and flows of scoraceous basalts are well preserved in the Lake Tanagraben. These basalts are considered Pleistocene in age. The volcanic rocks of the lakeTana area are usually described as olivine alkaline basalts, which may have a thickness up to 1300m (Mohr, 1971). In the recently compiled geological map of Ethiopia described the rocks as plateau basalts, consisting of quaternary alkaline basalts and trachytes.

The region south of Lake Tana exposes Quaternary volcanic rocks composed of vesicular alkali basalt and cinder cones, indicating the volatile rich nature of the host magma**.** The host lavas are basaltic in composition and are dated 0.39± 0.03 Ma (Hofmann, 1997). The basalts occur as massive, vesicular and fragmented rocks. They are aphyric to sparsely porphyritic containing phenocrysts of in order of decreasing abundance olivine, plagioclase, clinopyroxene and occasionally nepheline set in a fine- grained matrix composed of the same phase as the phenocryst assemblage.

2.1.4 Recent (Quaternary) Sediments

The recent Quaternary superficial deposits occur relatively extensively in the central north and eastern part of the area mainly developing from the underlying Tertiary volcanic rocks. They are grouped in to elluvial soil and alluvial soil cover.

2.1.4.1 Elluvial soil

In geology, eluvium or eluvial deposits are those geological deposits and soils that are derived by in situ weathering or weathering plus gravitational movement or accumulation. The process of removal of materials from geological or soil horizons is called eluviation or leaching. The eluvial soil covers most of the plateau area and is generally, red to reddish brown silty to sandy soil commonly containing basalt rock fragments. Its exposed thickness reaches up to 5 m. The red and reddish-brown color of the eluvial soil may indicate its in situ development from the underlying basaltic rocks.

2.1.4.2. Alluvial soil

Alluvial soil is a fine-grained fertile soil deposited by water flowing over flood plains or in river beds. Alluvial deposit, alluvial sediment, alluvium, alluvion - clay or silt or gravel carried by rushing streams and deposited where the stream slows down.

The alluvial soil cover occurs along river and stream valleys and its surroundings and marshy areas. It is commonly black cotton soil and rarely dark brown silty soil. The exposed thickness of the alluvial soil along the Bir river valley is about 8 m thick (EIGS, 2008).

2.2. Local geology of the study area and its surroundings

The geology of the study area and its surrounding is dominated by the following rock units, scoraceous basalt, Vesicular basalt, scoria, trachyte and recent alluvial deposits.

Vesicular Basalt*:* This rock unit is covered large part of the study area and it is clearly out cropped at Ayo river bank and Mesni,Sutena and Zerket stream banks and beds. Ridges surrounding Injibara town are also covered by this unit. Weathering and fracturing are affecting this unit and it is not filled by secondary minerals. Previously drilled well data result indicates this unit gives potential amount of water to the wells.

Figure 2.1. Vesicular basalt at Mesni river bed

Scoraceous Basalt: Dark to brown color, weathering, fracturing and vesiculation are the major characteristics of this unit. This unit is dominantly observed at Ayo river bank and Sutena stream bed.

Figure 2.2. Weathered and fractured scoraceous basalt at Sutena stream bed

Scoria: This unit is found in western part from the study area and it is clearly out cropped along Injibara-Chagni road cut. It is weathered and its thickness reaches up to 15 meter. This unit is important for ground water storage and conductance, however it is not suitable for engineering foundation purpose.

Figure 2.3. Scoria unit at the road cut overlaid by deposits

Trachyte: this unit is found in western ridges of Injibara town that cover small area and it is characterized as fractured, weathered and reddish in color.

.

Figure 2.4. Clay unit covering the Injibara University construction saite

Alluvial deposits: Alluvial deposits are covering low land plain part of the study area and it consists of clay, silt, sand, gravel, cobbles and boulders which are basaltic origin. The clay unit covers large part of the study area. Gravels, cobbles and boulders are dominant on the beds of streams and its thickness varies from place to place.

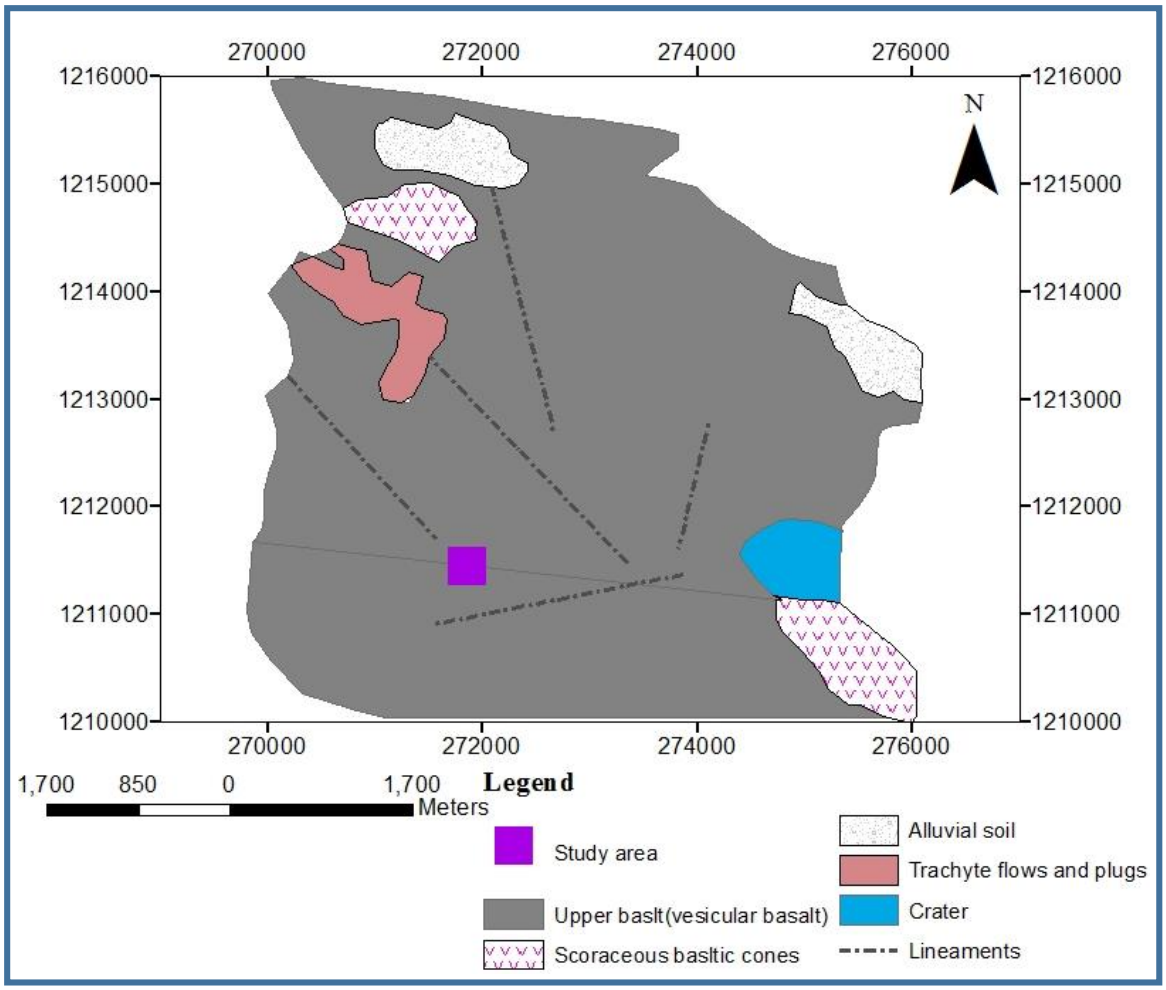

Figure 2.5. Geological map of the study area and its surroundings modified from Bure map sheet

2.3 Local Geological Structures

The dominant geological structures observed on the area are lineaments, local fault, and medium to large spacing fractures with three major sets trending N-S, SE-NW and NE-SW direction.

Figure 2.6. Local fault at Mesni stream bed

2.4 Hydrogeology of the Study Area

Fracturing, vesicles, inter granular pore space, contacts between different lithological units and lineaments are the major conduits and storage of ground water in the area. In addition to these catchments of Ayo Perennial River and Mesni, Sutena, and Zerket perennial streams have significant contributions for ground water recharge on the area (ADSWE, 2016).

2.5 Seismicity of the Area

Based on seismicity, Ethiopia is divided into five zones of approximately equal seismic risks depending on the known distribution of earthquakes (Ethiopia Building Code Standard, 1995). These are no damaging zone (0 zone), less damaging zones (Zones 1 and 2) and zones of major damaging (zone 3 and 4). From the seismic hazard map of Ethiopia, the project site falls in zone zero (0) as shown in Figure 2.7. This map is based on the amplitudes of the ground acceleration to be expected during 100 years return period. According to the building code, the ground acceleration ratio (α^0) depends on the seismic zones.

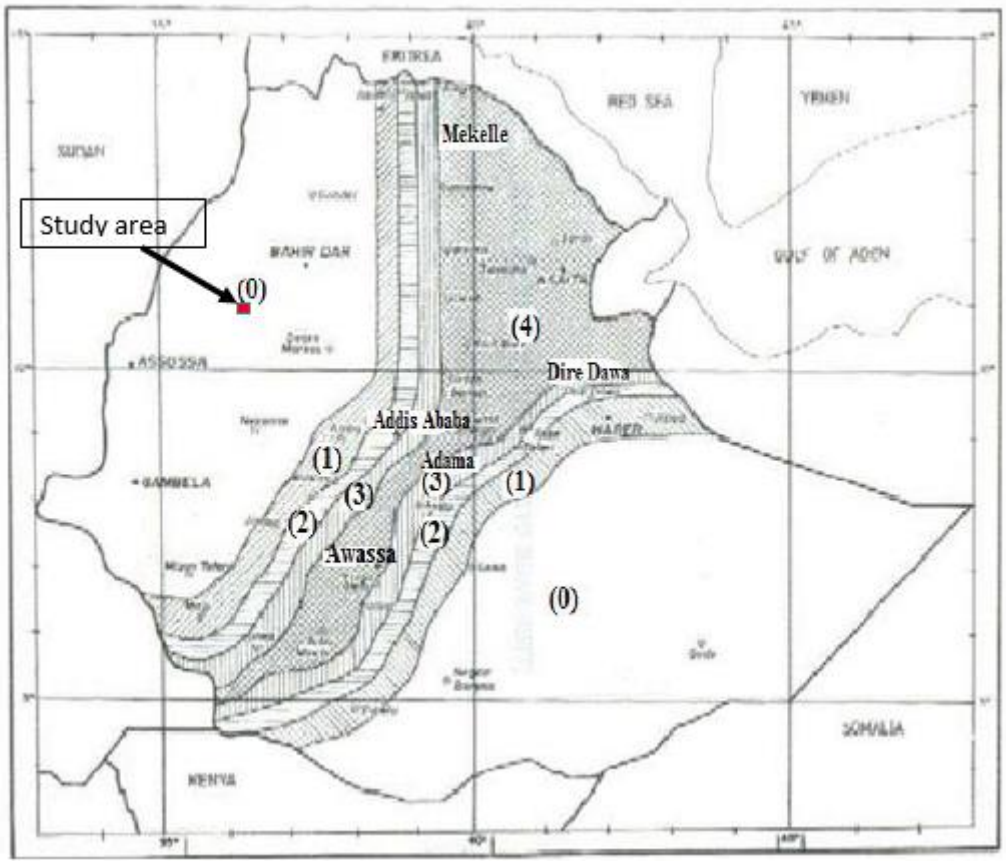

Figure 2.7. Seismic hazard map of Ethiopia (Ethiopian Building Code Standards, 1995)

CHAPTER III

3. THEORETICAL BACKGROUND OF THE GEOPHYSICAL METHODS OF INVESTIGATION

3.1 Preamble

Geophysical survey methods have wide scope of utilization, there is always one physical property for which a particular method is exceptionally sensitive. And few, if any, geophysical methods provide a unique solution to a particular geophysical situation. It is possible to obtain a very large number of geophysical solutions to some problems. However, a number of geophysical methods may be applied simultaneously (integrated geophysical exploration) in solving certain geophysical problems, and such approach, greatly reduces the problem of ambiguity, which is the inherent drawback in the interpretations of results from one method, by complementing the information gap from the additional methods. In this work electrical, seismic refraction and magnetic methods have been applied and the theoretical background of each method is presented in the following sections.

3.2 Electrical Resistivity Method

Resistivity method is mostly used in engineering and hydro-geological investigations to investigate the shallow subsurface geology. In the resistivity method, artificially generated electric currents are introduced into the ground and the resulting potential differences are measured at the surface. Deviations from the pattern of potential differences expected from homogeneous ground provide information on the form and electrical properties of the subsurface inhomogeneity (Kearey et al., 2002).

The purpose of electrical resistivity surveys is to determine the subsurface resistivity distribution by making measurements on the ground surface. From these measurements, the true resistivity of the subsurface can be estimated. The ground resistivity is related to various geological parameters such as the mineral and fluid content, porosity and degree of water saturation in the rock. Electrical resistivity surveys have been used for many decades in hydrogeological, mining and geotechnical investigation (Loke, 1999).

The method has been used to locate fault zones, zones of deep weathering and cavities. It can also be used in the exploration of alluvial deposits where permeable gravel and sand beds can be distinguished from low permeability clays or rock. This capability has been applied in searches for foundation materials at civil construction site (McCann et al., 1987).

3.2.1 Basic principles

Resistivity of rocks generally depends on the water content (porosity), the resistivity of the water, the clay content and the content of metallic minerals (Bernard, 2003). The following considerations help in the determination of the resistivity of rocks.

a) A hard rock without pores or fractures is very resistive to the flow of electric current. This is generally observed in hard fresh Precambrian rocks.
b) Dry sand without water is very resistive.
c) Porous or fractured rock bearing free water has resistivity, which depends on the resistivity of the water and on the porosity of the rock.
d) Impermeable clay layer, which is wet, has low resistivity but may not contain enough yields for successful groundwater exploitation.

In resistivity measurements, highest resistivity are associated with igneous rocks. Sedimentary rocks tend to be most conductive due to their high fluid content. Metamorphic rocks have intermediate resistivity. Granites and quartzite have high resistivity ranges; sandstone and shale have intermediate resistivity ranges (Bernard, 2003). The resistivity therefore in a particular geological environment has an influence on the aquifer resistivity. Numerical values for various types of water are outlined (Table 3.1).

In resistivity measurements current is injected into the ground via electrodes and the resulting potential is measured also by electrodes in the ground. The outer electrodes show the current electrodes for injecting current into the ground and the inner electrodes are the potential electrodes connected to the voltmeter.

3.2.2 Types of resistivity surveys

There are two basic types of resistivity investigations namely, profiling and depth sounding investigations. Resistivity profiling is used to detect lateral changes and depth sounding is used to investigate the changes in resistivity with depth. The basic difference between these two aspects of measurements is that in profiling measurements are taken at the various stations on the profile. Therefore stations are selected based on the general relative measurements along the profile. With sounding the equipment is positioned at a station and measurements are taken to a target depth. In a general principle sounding measurements are carried out after profiling.

Table 3.1 Resistivity's of different rocks types (from Loke, 1999)

Rock types	Resistivity (Ω-m)
Metamorphic/Igneous rocks	$5 \times 10^3 - 10^6$
Slate	$6 \times 10^2 - 4 \times 10^7$
Gneisses	8-10x103
Marble	$1 \times 10^6 - 1 \times 10^7$
Quartzite	$1 \times 10^6 - 1 \times 10^8$
Basalt	$5 \times 10^3 - 1 \times 10^5$
Andesite	$5 \times 10^3 - 1 \times 10^5$
Sedimentary Rocks	
Sandstone: · Saturated with fresh water · Saturated with saline water	$1 \times 10^5 - 1 \times 10^6$ $3 \times 10^1 - 2 \times 10^2$ 1-10
Clay: · Saturated with fresh water · Saturated with saline water	$1 \times 10^3 - 1 \times 10^5$ $1 \times 10 - 1 \times 10^2$ 1-10
Gypsum	$1 \times 10^5 - 1 \times 10^7$
Shale	$20 - 2 \times 10^3$
Limestone	$50 - 4 \times 10^2$
Unconsolidated (colluvial and alluvial)	Varies based on their parent rock

3.2.2.1 Vertical electrical resistivity sounding

The procedure involved in vertical electrical sounding is primarily based on the assumption that the subsurface has a horizontal stratification. The measurements are taken with gradually increasing distances of the current electrodes (the potential electrodes remain constant at some stations). As the distance between current probes is increased, there is also an increased in the depth at which the current penetrates below the surface of the ground increasing the depth of investigation (Figure3.1). In this way, an estimate of the vertical resistivity distribution below the center of the array is determined. These are usually plotted as depth against resistivity, so that the resistivity at different depths are analyzed.

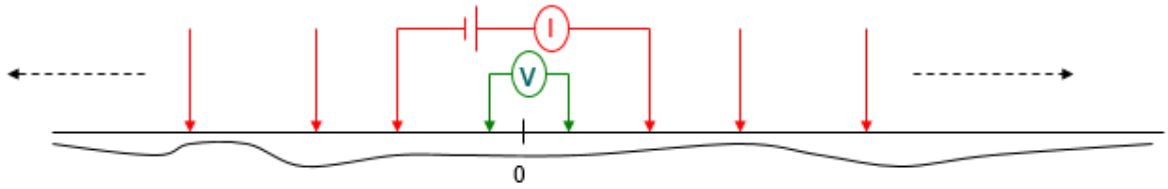

Figure3.1. Schematic plan for Electrical resistivity sounding (Loke, 2001)

3.2.2.2 Electrical resistivity profiling

Profiling provides information about lateral variations, usually with some information about vertical variations. Wider electrode spacing results in deeper penetration. In profiling, readings are taken at regular intervals along a profile (Figure3.2). The profile is usually pegged at regular interval distances. The general variations of resistivity at the individual stations are used to select anomalous stations for further investigations or drilling. Profiling results are presented as resistivity against distances corresponding to the stations. In this situation the resistivity at the stations are displayed so that anomalous stations can be observed.

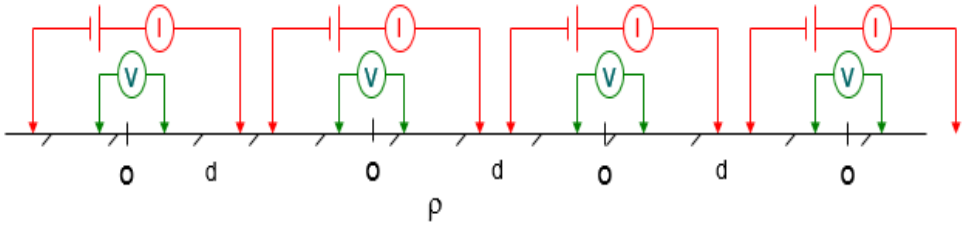

Figure3.2.Schematic plan for electrical resistivity profiling (Loke, 2001)

3.2.3 Types of arrays

The choice of the best array for a field survey depends on the type of structure to be mapped, the sensitivity of the resistivity meter and the background noise level (Loke, 2001). Some common arrays that are commonly used for electrical resistivity measurements surveys are:

- Schlumberger
- Wenner
- Dipole-dipole Arrays

Among the characteristics of an array that should be considered are the sensitivity of the array to the vertical and horizontal changes in the subsurface resistivity, the depth of investigations, the horizontal data coverage and the signal strength.

The typical methodology in conducting resistivity investigation begins by some pre-modeling to determine the type of array to be selected and electrode spacing. Choosing the type of array in investigations is not only an important factor to ensure success, it also determines the efficiency of the investigation. In resistivity profiling investigations, cables and electrodes are moved long distances and therefore the arrays chosen will be those which make movement simple and rapid as possible as well as efficient in delineating targets (Loke, 2001).

3.2.3.1 The Schlumberger array

Where only two electrodes are moved is appropriate for use because of speed and convenience. The interpretation material for the Schlumberger array also makes it attractive for depth sounding. Site selection is extremely important with the Schlumberger array because it is sensitive to conditions around the closely spaced inner electrodes.

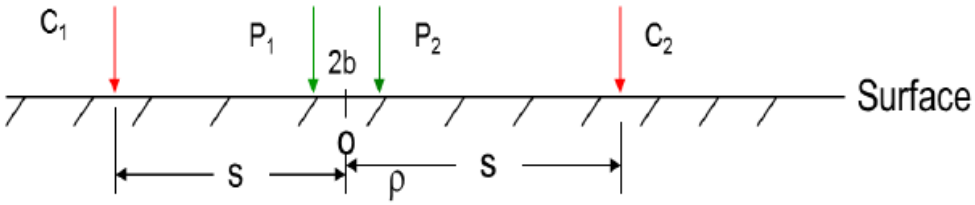

Figure 3.3.The electrode arrangement of the Schlumberger Array

3.2.4 Data acquisition in electrical resistivity

For measuring the ground resistivity, a current has to be transmitted with electrodes, while the potential created on the surface by the circulation of this current into the ground is measured with other electrodes. Increasing progressively the distance between the transmitting and the receiving electrodes permits an increase in the depth of investigations.

The resistivity depends on hydrological-hydrogeological conditions, the chemical composition of the water, the dissolved ions in it, the porosity of the formation, the possible fractures, the temperature and pressure and the topography. Resistivity depends on many factors and it doesn't comprise a distinguishing property of specific formations, since the resistivity variability may have a large range in the same formation. Interpretation of resistivity measurements therefore must be carried out with regards to the available geologic information of the area including geologic maps, drilling information on aquifer depth, aquifer thickness and static water levels.

3.2.5. Interpretation of VES Data

The interpretation problem for VES data is to use the curve of apparent resistivity versus electrode spacing, plotted from field measurements on bi-log scale graph paper, to obtain the parameters of the geo-electrical section: the layers resistivity and thicknesses. From a given set of layer parameters, it is always possible to compute the apparent resistivity as a function of electrode spacing (the VES curve). Unfortunately, for the converse of that problem, it is not generally possible to obtain a unique solution. There is interplay between thickness and resistivity; there may be anisotropy of resistivity in some strata; large differences in geoelectrical section, particularly at depth, produce small differences in apparent resistivity; and accuracy of field measurements is limited by the natural variability of surface soil, rock and by instrument capabilities. As a result, different sections may be electrically equivalent within the practical accuracy limits of the field measurements.

3.2 The Seismic Method

3.2.1 Overview of Seismic Waves and Velocity

A single shot seismic record has direct, refracted and reflected waves. In an environment with faulted zone in the bedrock, diffracted waves are also recorded. In this work only refracted seismic waves are made use of.

Seismic waves are in the form of packets of elastic strain energy that travel from a naturally or artificially generated source. It has two major components, the Body and Surface waves (Reynolds, 2011). Body waves propagate through the whole internal structure of the earth. It comprises of the compressional (primary (P)) wave and shear (secondary (S)) wave .P-waves are longitudinal and cause the particle of the medium to vibrate in the same direction as the wave propagate but s-waves are transverse and cause the particles of the medium to vibrate perpendicular to direction of propagation of the wave. In the same medium, p-wave travels faster than s-wave.

Surface waves are in the form of Rayleigh and these waves travel along the surface of the Earth with a more complicated particle motion and are responsible for damages during the release of energy earthquakes (Sherif, 2002). The velocities with which seismic pulses move are determined by the density (ρ), the bulk (K) and shear moduli (μ) of the medium through which they pass. The seismic velocities are given by the following relations:

$$V_P = \sqrt{\frac{K + 4/3\mu}{\rho}} \tag{3.1}$$

and between the shear wave propagation velocity V_s and elastic constants;

$$V_S = \sqrt{\frac{\mu}{\rho}} \tag{3.2}$$

In near surface seismic exploration geophysics, elastic p-wave velocity is normally utilized but developments in recent years combine s-waves with p-waves for lithostratigraphic characterization (Telford and Sherif, 1990).

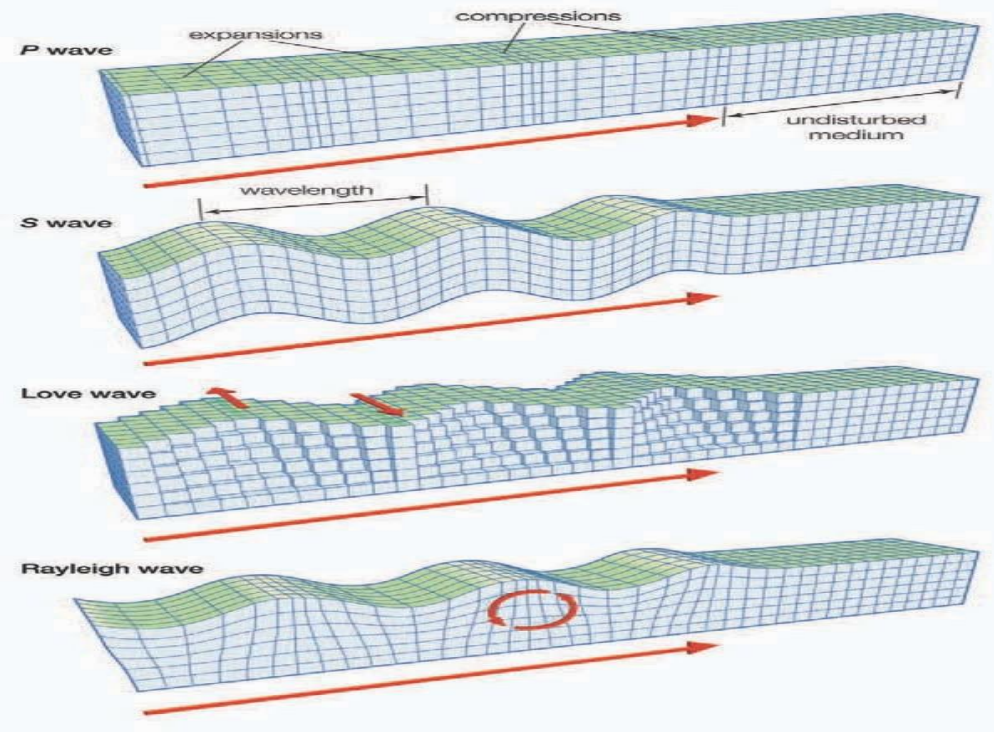

Figure 3.4. The main types of seismic waves: P, S, Love, and Rayleigh waves

3.2.2 Seismic Refraction Method

In a homogeneous earth layer, a wave travels in a straight path but changes direction as it enters a different acoustic layer (Figure 3.5). The ratio of the sine of the incident angle to the sine of the angle of refraction is equal to the ratio of the velocity of the first layer to that of the second layer given by equation 3.4. As the incident angle increases, the refracted angle in the second layer also increases. Critical refraction is reached when the angle of refraction in the second layer equals 90^o as the incident angle is further increased. At critical refraction, the refracted ray travels along the interface separating the two acoustic layers.

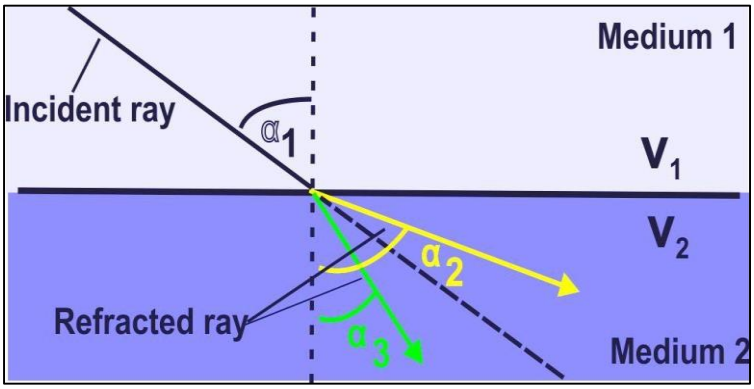

Figure 3.5. Schematic diagram of a p-wave travelling in different media

3.2.2.1 Travel time Curve, Velocity and Layer Thickness

The time taken for seismic pulse to arrive at the receivers (geophones) are plotted against the distance of the receivers from the shot location in order to compute the velocities of layers present using the slopes of the T-X curves (figure 3.6). The direct wave plot passes through the origin and has velocity V1 given by the inverse of its slope. The distance from the shot location to the point the refracted waves start arriving at the geophones is the critical distance (X_{crit}). From the crossover point (X_{cross}), the refracted waves take over as first arrivals.

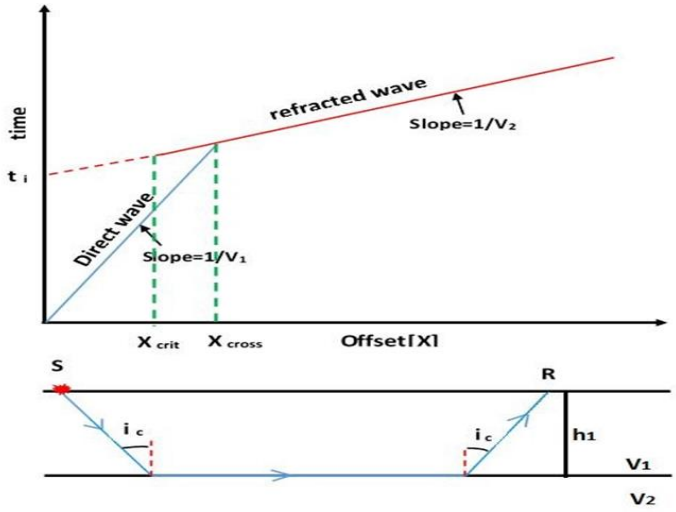

Figure 3.6. A travel time curve of seismic refraction first arrivals.V1 and V2 are velocities of the first and second layers respectively (Emmanuel, 2015)

3.2.2.2The Basic Principles of Refraction

The seismic refraction method uses the seismic energy that returns to the surface of the Earth after traveling along ray paths through the ground, to locate refractors that separate layers of different

seismic velocity (Alhassan, 2010), therefore the primary application of seismic refraction technique is to determine the depth to bedrock and bedrock structure. It is based on the time-arrival of the seismic energy generated by a source recorded at a variety of distance.

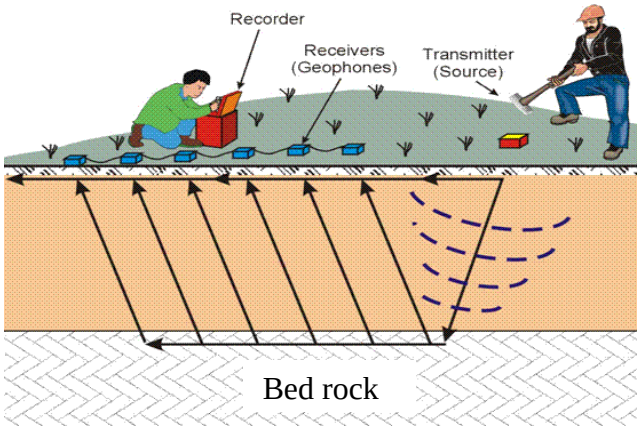

Figure3.7. Acquisition of seismic refraction data

The refraction seismic is an output of three basic principles and the methods of trigonometry and geometry. These are the applications of Snell's law, Fermat's and Huygens principles.

Snell's law: says "the directions of refracted and reflected waves traveling away from a boundary depend on the direction of the incident wave and the speeds of the waves. Look at the following equation (3.3) and equation (3.4) below.

$$\frac{\text{Sin i}}{\text{Sin r}} = \frac{V1}{V2} \qquad (3.3)$$

Equation (3.4) is called Snell's law where i and r are the angles of incident and refracted rays respectively. V_1 and V_2 are speeds of the incident and refracted rays inside the two layers. At critical refraction (when angle r=90^0 and i=ic), the refracted wave is produced by an incident wave traveling along the ray that reaches the boundary at the critical angle of incidence ic. For this case of critical refraction, sin r=sin 90=1, the Snell's law can be written as

$$\text{Sin } i_C = \frac{V1}{V2} \qquad (3.4)$$

Which shows how the critical angle depends on the wave speeds.

There are three consequences of Snell's law;

1) If the velocity of the two layers V_1 and V_2 are equal, the two angles i and r are equal and there will be no refraction.

2) If V_1 is greater than V_2, angle i will be greater than r and as a result the refracted wave always goes down. It doesn't go up. This is the main problem of seismic refraction method for

rock layers with low velocity at depths. And this problem is called velocity reversal problem.

3) This third consequence is very important for the seismic refraction method. When V_1 less than V_2 i.e., when the velocity increases towards depth, r will be greater than i as a result there will be a refracted wave from the depth to the surface and then recorded by Seismometers (geophones).

Fermat's principle: says "elastic waves travel between two points along paths requiring the least time".

This particular path requiring the least time is the path predicted from Snell's law.

$$\frac{V1}{V2}=\frac{\sin i1}{\sin i2} \qquad (3.5)$$

Consequence of Snell's law

a) If $V_1 = V_2 \rightarrow i = r$, then there is no refraction.

b) If V1> V2→i> r, then there is no way one can record the refracted waves.

c) If V1< V2→i< r, then the refracted waves go up to the surface.

Huygen's principle: waves in a homogeneous medium spread out from a point source as expanding spheres. Huygen's principle states "every point on a wave front is the source of a new wave that also travels out from it in spherical shells. If the spherical waves have a large enough radius, they can be treated as planes. Lines perpendicular to the wave fronts, called wave paths or rays, can often be used to describe the wave propagation more conveniently than wave fronts.

3.2.3 Geometry of Refraction waves

3.2.3.1 The Single Layer Refraction

When the seismic waves reach a boundary between two substances or rock layers in which the wave speeds are different, they divide into waves that bounce, or reflect, from the boundary and other waves that pass, or refract, across the boundary.

For simplicity let's consider a single refractor with two homogeneous layers (Figure 3.8).

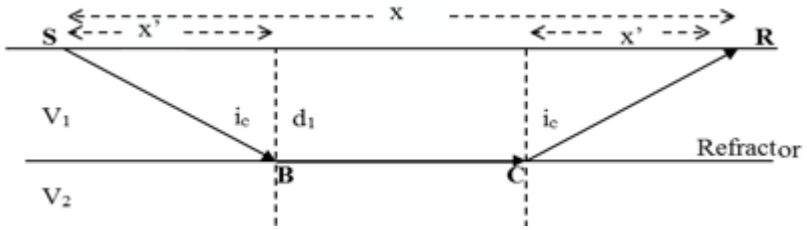

Figure 3.8. Travel-time of direct & refracted waves from a shot point in two-layer system

(Emmanuel, 2015)

The time taken for the direct wave to reach the receiver R from the source S in Figure 3.8 is given as:

$$T_1=\frac{X}{V1} \quad (3.6)$$

And for the refracted wave

$$T2=\frac{SB}{V1}+\frac{BC}{V2}+\frac{CR}{V1} \quad (3.7)$$

$SB=SR=d1/cosi_c$, $x'=d1tani_c$ and $BC=x-2x'=x-2d1tani_c$

Thus, it can be rewritten as

$$\mathbf{T_2}=\frac{\boldsymbol{2d1}}{\boldsymbol{V1}}+\frac{\boldsymbol{x-2d1tanic}}{\boldsymbol{V2}} \quad (3.8)$$

Using Snell's law it becomes

$$T_2=\frac{2d1}{V1}(1-\sin^2 ic)+\frac{X}{V2} \quad (3.9)$$

Then substituting cosic= $\sqrt{1-\sin\text{^}2}ic$ and $\sqrt{(1-\sin^2 i_c}$ and $\sin^2 i_c=\frac{{V_1}^2}{{V_2}^2}$,finally

$$T_2=\frac{2d1}{v1v2}\sqrt{v2^2-v1^2}+\frac{X}{V} \quad (3.10)$$

The gradients of the two travel time curves (T1 and T2) can be obtained by differentiating as follows.

$$\frac{dT1}{dx}=\frac{1}{v1} \quad \text{and} \quad \frac{dT2}{dx}=\frac{1}{v2} \quad (3.11)$$

This implies that the velocity of the two layers V_1 and V_2 can be obtained from the slopes of the travel time curves. There are two ways of obtaining the depth (d_1) to the refractor. Intercept time method and crossover distance methods.

Intercept time (t_i) method

The intercept time t_i is the point at which the straight line representing the refracted waves intersects the vertical axis of the travel time graph.

Recalling equation (18), at $T_2 = t_i$, x is zero, thus

$$t_i=\frac{2d1}{V1V2}\sqrt{(V2^2-V1^2} \quad (3.12)$$

$$d_1=\frac{tiv1v2}{2\sqrt{V2^2-V1^2}} \quad (3.13)$$

The crossover distance method

The distance at which the two straight lines intersect is called the crossing distance x_c. A geophone placed at this distance would receive both the direct wave and the refracted wave at exactly the same time. For all distances beyond x_c, the refracted wave will be the first arrival, and the direct wave will become a later arrival and before the x_c direct waves arrived first.

3.2.4 Geophysical inversion

Geophysical inversion is a method which finds a model that gives a response similar to the actual measured values. The model is an idealized mathematical representation of a section of the earth and it has a set of model parameters of physical quantities which are estimated to be from the observed data. All inversion methods essentially try to find out model to the subsurface whose response agrees with the measured data. In this particular study, the model is done by SeisImager/2D software which is a powerful refraction seismic processing package. It has three separate inversion techniques. These are the time-term method, reciprocal method and tomography. In this study, the time-term and tomographic inversion are used to generate a three layer velocity model.

3.2.4.1The Time-term Method

The time-term technique is a linear Least-Squares approach to determining the best descrete-layer solution to the data. The math behind this technique is comparatively simple. Referring to the figure below.

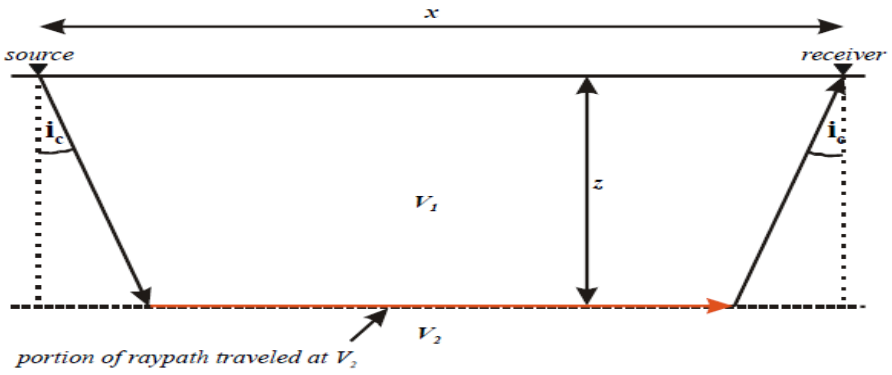

Figure3.9.Parallel refractors

We define the "slowness" S as the inverse velocity:

$S_1 = \frac{1}{V1}$ (3.14)

$S_2 = \frac{1}{V2}$ (3.15)

From Snell's Law

$$\sin ic = \frac{S2}{S1} \tag{3.16}$$

The total travel time t from source to receiver is then,

$$t = 2S1\cos(ic)\, z + xS2 \tag{3.17}$$

Now, if we define

c = 2S1cos(ic), then

$$t = 2cz + xS2 \tag{3.18}$$

And z and S2 are unknown.

The above example assumes that the refractor is parallel to the ground surface.

If we expand this to the general case – non-parallel, curved surfaces, as shown below – we end up with three unknowns rather than two, e.g. z1, z2 and S2.

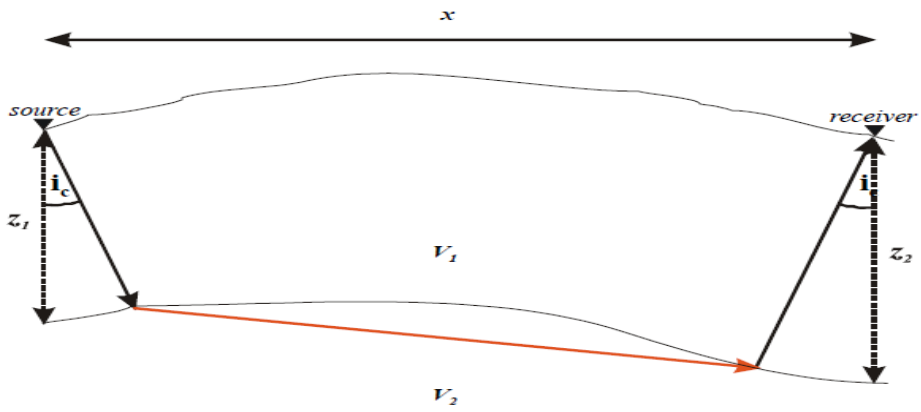

Figure 3.10. Non-parallel, curved surface refractors

Now, we have

$$t = cz_1 + cz_2 + xs_2 \tag{3.18}$$

Generalizing, we get

$$t_j = \sum_{k=1}^{n} c_{jk} z_k + x_j s_2$$

In matrix form, we get

$$\begin{bmatrix} c_{11} & c_{12} & . & . & c_{1n} & x_1 \\ c_{21} & c_{22} & c_{23} & . & c_{1n} & x_2 \\ c_{31} & c_{32} & c_{33} & . & \vdots & \vdots \\ . & . & . & . & . & . \\ c_{m1} & c_{m2} & c_{m3} & . & c_{mn} & x_n \end{bmatrix} \begin{bmatrix} z_1 \\ z_2 \\ \vdots \\ z_n \\ s_2 \end{bmatrix} = \begin{bmatrix} t_1 \\ t_2 \\ t_3 \\ . \\ t_m \end{bmatrix}$$

Where *m* = number of travel times, and *n* = number of receivers (depths to be calculated). We can now solve the matrix for *z1…*zn *and S2*.

3.2.4.2 The Reciprocal Time Method

The reciprocal time method is a much more "hands on" approach than the time-term method. Fewer assumptions are made, and the interpreter interacts with the software to a much greater degree, providing much more input. Generally, the reciprocal method should be used when the desired result needs to be as detailed as possible. The reciprocal method generally requires more data because of its use of "delay times", which require a refracted arrival from each direction. Ideally, data is acquired such that a delay time can be computed beneath each geophone. The depth is then computed from the delay time and the velocity.

3.2.4.3The Tomographic Method

The tomographic method, involves the creation of an initial velocity model, and then iteratively tracing rays through the model, comparing the calculated travel times to the measured travel times, modifying the model, and repeating the process until the difference between calculated and measured times is minimized. The math is quite complex; what is presented here assumes a working understanding of upper-level calculus and linear algebra. The essential goal is to find the minimum travel time between source and receiver for each source-receiver pair. This is accomplished by solving for *l* (ray path) and *s* (inverse velocity or "slowness"). Since we know neither, the problem is under-constrained, and we must use an iterative, least-squares

3.3 Magnetic method of prospecting

3.3.1 Introduction

The magnetic method is a geophysical technique that measures variations in the earth's magnetic field to determine the location of subsurface features. Magnetometers are instruments required for magnetic surveys. Magnetic surveys may be undertaken from the air or on the ground. The data are then taken back to the office to be processed and presented as a magnetic map. The magnetic method is relatively easy to perform and inexpensive as it requires little data processing or manipulation.

The magnetic method mostly has come into use for identifying and locating masses of igneous rocks that have relatively high concentrations of magnetite. The method is especially effective to map structural features like geological faults, fractures and/or contact zones which often

serve as potential hosts for a variety of minerals and/or buried magnetic objects such as pipelines. Magnetic field variations can be interpreted to determine an anomaly's depth, geometry and magnetic susceptibility. The main disadvantages are that subsurface information is obtained only if there are buried ferromagnetic materials and the interpretation of magnetic anomalies is nonunique. This nonuniqueness means complementary data (e.g., other geophysical data or drillhole data) are required to determine the sources of the magnetic anomalies.

3.3.2Principles and elementary theory

Magnetic method is based on the fact that when a ferrous material is placed with in the earth's magnetic field, it develops an induced magnetic field. The induced field is superimposed on the earth's field at that location creating a magnetic anomaly. Detection depends on the amount of magnetic material present and its distance from the sensor. The anomalies are normally presented as profiles and or as contour maps. Magnetism is based on the physical property of the materials and the magnetic properties of materials are expressed by the physical quantities. If two magnetic poles of strength p1and p2 are separated by a distance r, a force exists between them is given by

$$F = \frac{P_1 P_2}{4\pi\mu r^2} \tag{3.19}$$

Where μis the magnetic permeability of the medium separating the poles; p1and p2are pole strengths and r the distance between them. The force is attractive if the poles are of different sign and repulsive if they are of like sign.The *magnetic field B* due to a pole of strength *p* at a distance *r* from the pole is defined as the force exerted on a unit-positive pole at that point.

$$B=\frac{p}{4\pi\mu r2} \tag{3.20}$$

3.3.3 The Earth's Magnetic Field

Ninety percent of the Earth's magnetic field looks like a magnetic field that would be generated from a dipolar magnetic source located at the center of the Earth and aligned with the Earth's rotational axis. The strength of the magnetic field at the poles is about 60,000 nT. If this dipolar description of the field were complete, then the magnetic equator would correspond to the Earth's equator and the magnetic poles would correspond to the geographic poles. The remaining 10% of the magnetic field cannot be explained in terms of simple dipolar sources.

As far as exploration geophysics is concerned, geomagnetic field is of three parts (Kearey et al., 2002).These are: the main field, the external field, and variations of the main field.

3.3.3.1 The Earth's main field

This field represents the main components of the geomagnetic field and is believed to be originated in the Earth's outer core. This field varies relatively slowly and its magnitude on the earth's surface is given in terms of the geomagnetic field elements. The total field vector *B* has a vertical component *Z* and a horizontal component *H* in the direction of magnetic north. The dip of *B* is the inclination *I* of the field and the horizontal angle between geographic and magnetic north is the declination *D*. *B* varies in strength from about 25000nT in equatorial regions to about 70000nT at the poles (Kearey et al., 2002).

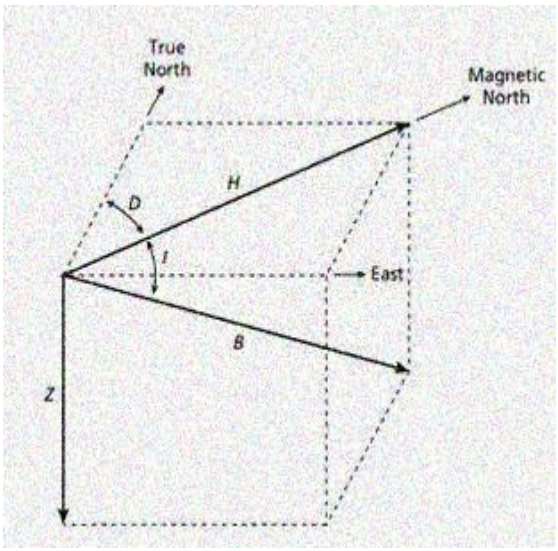

Figure3.11.The geomagnetic elements

B = Total magnetic field vector

H = Horizontal component of the total field vector

Z = vertical component of the field vector

D=Declination

I = Inclination

Where, $B^2 = H^2 + Z^2$

$I = \tan^{-1}(Z/H)$

$D = \tan^{-1}(H_E/H)$, H_E = East component of

3.3.3.2 The external magnetic field

Most of the remaining small portion of the geomagnetic field appears to be associated with electric currents in the ionized layers of the atmosphere (Telford et al., 1990). The time variations of this field portion are much more rapid than for the main field and is caused by external activities.

3.2.3.3 Anomalous magnetic field

The sources of local magnetic anomalies cannot be very deep because of the Curie temperature. Thus local anomalies must be associated with features in the upper crust (Telford et al., 1990). Generally the total magnetic field can be expressed by

$$B_T = Bext + Bint = Bext + B_D + Brm \quad (3.21)$$

Where B_T is the total magnetic field, Bext is external magnetic field,

B_D is dipole field, which is mainly generated by the fluid outer core and Brm is the field of rock magnetism.

3.3.4 Temporal variations of the Earth's magnetic field

The magnetic field of the Earth varies with time. As a result, the temporal variation of the Earth's magnetic field can be explained in terms of three temporal variations.

I. **Diurnal variations**

Magnetic effects of external origin cause the geomagnetic field to vary on a daily basis to produce diurnal variations. Under normal conditions (quiet days) the diurnal variation is smooth and regular and has an amplitude of about 20-80nT, being at a maximum in Polar Regions (Kearey et al., 2002). This variation should be accounted for when conducting magnetic surveys. Therefore, surveys have to be planned so as to allow for corrections to be made for diurnal variations.

II. **Secular variations**

These are a long term variations in the main magnetic field that are most probably caused by fluid motion in the earth's outer core. They are monitored by measuring changes in I, D and B at observatories. Because these variations occur slowly with respect to the time of completion of a typical exploration magnetic survey, these variations will not complicate data reduction efforts of the acquired field dat.

III. **Magnetic storms**

Magnetic activity in the ionosphere will abruptly increase. The occurrence of such storms correlates with enhanced sunspot activity. The magnetic field observed during such times is highly irregular and unpredictable, having amplitudes as large as 1000nT. Exploration magnetic surveys should not be conducted during magnetic storms. This is because the variations in the field that they can produce are large, rapid, and spatially varying. Therefore, it is difficult to correct for them in acquired data (Kearey et al., 2002).

3.3.5 Magnetics Properties of Rocks

Most engineering and environmental magnetic studies involve taking readings over soil, which in most situations has a low magnetic susceptibility, will not concerned with anomalies caused by magnetic susceptibility variations within the soil. However, the magnetic susceptibilities of a soil reflect their source rocks, as soils derived from mafic igneous rocks tend to have high magnetite content (Sharma, 1997). The magnetic prospecting potentially locates subsurface rocks having high magnetic susceptibilities by mapping variations in the strength of the magnetic field at the Earth's surface.

Magnetic susceptibility is a significant variable in magnetic prospecting playing the same role as density in gravity prospecting. The susceptibility of a rock usually depends on its magnetite content. The volcanic rock shows higher susceptibility than common sedimentary rocks. Accordingly, sedimentary rock, acidic volcanic rock, intermediate one and basic one shows ascending magnetic susceptibility. Weathering generally reduces susceptibility because magnetite is oxidized to hematite, but some laterites are magnetic because of the presence of magnetite and remanently magnetized hematite (Telford, Geldart and Sheriff, 1990).

3.4.6 Magnetic surveying

Magnetic exploration can be carried out on land, at sea, and in the air. As a result magnetic surveys either directly seek magnetic bodies or they seek magnetic material associated with an interesting target. Land surveys are usually done with portable proton precession magnetometers. Profiles or networks of points are measured in the same way as for gravity. It is important to survey perpendicular to the strike of an elongate body or two-dimensional modeling may be very difficult. It is necessary to tie back to the base station at 2-3 hour intervals, or to set up a continually- reading base magnetometer. This will give diurnal drift and detect magnetic storms. In magnetic surveying the operator must: record the time at which readings were taken for drift correction, stay away from interfering objects (e.g., wire fences, railway lines, roads), not carry metal objects (e.g., mobile phones), and take multiple readings at each station to check for repeatability.

3.4.7 Magnetic data reduction

To remove all causes of magnetic variation from the observations other than those arising from subsurface geology it is necessary to make correction of magnetic data.

3.4.7.1 Diurnal variation correction

The effects of diurnal variation may be removed in several ways. On land the magnetometer is read at a fixed base station periodically throughout the day. The differences observed in base readings are then distributed among the readings at stations occupied during the day according to the time of observation. Magnetometers do not drift and base readings are taken solely to correct for temporal variation in the measured field (Kearey et al., 2002).

3.4.7.2 Geomagnetic correction

In order to produce a magnetic anomaly map of a region, the data have to be corrected to take in to account the effect of latitude and to a lesser extent longitude (Reynolds, 1997). Survey data at any given location can be corrected by subtracting the theoretical field value B_{th}, obtained from the International Geomagnetic Reference Field (IGRF) from the measured value, B_{ob}. Therefore, the magnetic anomaly ΔB, obtained by subtracting the diurnal correction (∂BD) and geomagnetic correction (B_{th}) is given by

$\Delta B = B_T - \delta B_D - B_{th}$

3.4.8 Magnetic Data Enhancement techniques

These enhancement techniques are used to increase the perceptibility of magnetic anomalies that are related to bodies of interest. This is not important in all types of shallow magnetic surveys as the anomalies due to iron and highly magnetic rocks that produce high magnetic anomalies. However, enhancement techniques highly used in detailed magnetic surveying for faults and geologic mapping where magnetic anomalies may have small amplitude and obscured by nearby anomalies.

Recently, the enhanced analytic signal technique has been shown to be a superior edge detection method than the traditional first and second derivative techniques (Sharma, 1997).

The enhanced analytic signal technique produces a result that is not dependent on magnetic inclination as the traditional methods.

3.4.8.1Analytical Signal

This quantity is defined as a complex function that its real component is horizontal gradient and its imaginary component is vertical gradient(Salem and Ravat,2006).The amplitude of the analytic signal can be derived from the three orthogonal gradient of the total magnetic field using the expression:

$$|A(x,y)| = \sqrt{(\frac{\partial M}{\partial x})^2 + (\frac{\partial M}{\partial y})^2 + (\frac{\partial M}{\partial z})^2} \quad (3.22)$$

Where A(x,y) is the amplitude of the analytical signal at(x,y) and m is the obseved magnetic anomaly at (x,y). This signal exhibits maxima over magnetization contrasts, independent of the ambient magnetic field and source magnetization directions (Salem et al., 2002).

3.4.8.2The Tilt Angle Derivative

Interpreting of magnetic data is used to determine the magnetic source parameter such as location of boundary and depth based on the use of derivatives of magnetic field.

Tilt angle is defined as

$$\theta = \tan^{-1}[\frac{\partial M/\partial Z}{\partial M/\partial h}] \quad (3.23)$$

where $\frac{\partial M}{\partial h} = \sqrt{[(\frac{\partial M}{\partial X})\text{^}2 + (\frac{\partial M}{\partial y})\text{^}2\,]}$ and $\frac{\partial M}{\partial x}, \frac{\partial M}{\partial y}$ ***and*** $\frac{\partial M}{\partial z}$ are first order derivatives of the magnetic field (m) in the direction of x,y and z.The tilt derivatives vary markedly with inclination but for inclinations of 0° to 90°its zero crossing is located close to the edges of the model structure (Miller and Singh, 1994).

CHAPTER IV

4. DATA ACQUISITION, PROCESSING AND PRESENTATION

4.1 Introduction

In this research electrical resistivity, seismic refraction and magnetic methods were applied to address the main objectives stated in section 1.5. The data were acquired and analyzed using different updated software to get the relevant information for subsurface condition of the building site. The detailed data collection, processing, presentation and procedure for the present study are given below.

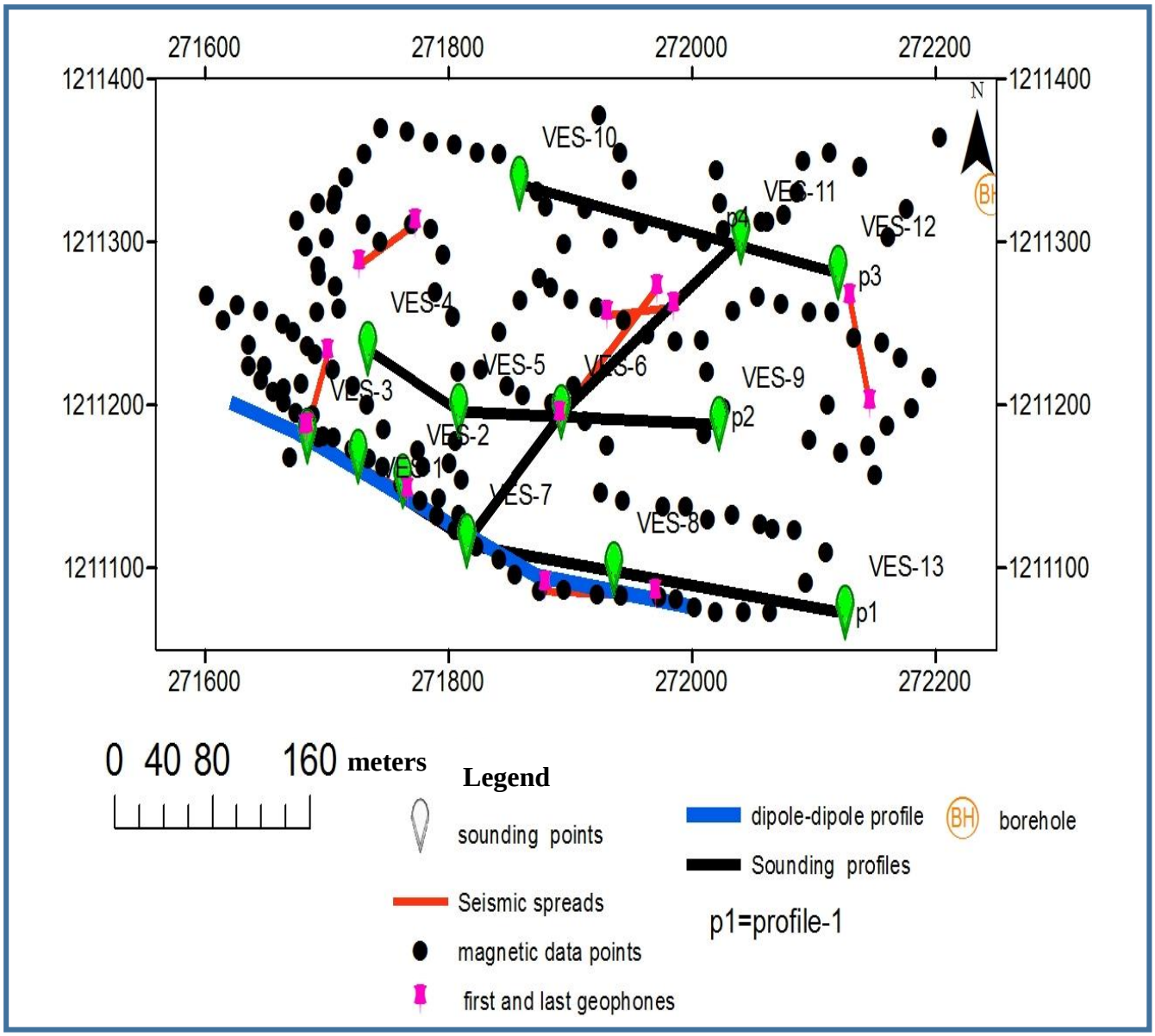

Figure 4.1. Distribution of geophysical survey stations with the location of a nearby borehole

4.2 Electrical Resistivity survey

4.2.1 Field data acquisition and Instrumentation

The electrical resistivity survey was carried out employing Vertical Electrical Sounding techniques.

A.Vertical Electrical Sounding (VES)

In this case the Schlumberger array was used to study the vertical resistivity variation by systematically expanding the separation between the current electrodes maintaining the center of array fixed for a number of successive measurements. This configuration is less sensitive for lateral inhomogeneities. A total of thirteen vertical electrical sounding survey stations along four profiles were conducted to understand the subsurface conditions of the site (Figure4.1). This technique was implemented by injecting electrical current (I) into the ground by means of two current electrodes and measuring the resulting potential difference (ΔV) by another pair of potential electrodes placed close to the center of the array. Using the measured values of I and ΔV, the apparent resistivity (ρa) at the measurement point were determined using the Ohm's law:

$$\rho = k\frac{\Delta V}{I} \tag{4.1}$$

Where,

$K = \dfrac{2\pi}{\frac{1}{AM} - \frac{1}{AN} - \frac{1}{BM} + \frac{1}{BN}}$ and k referred to as array coefficient or geometric factor that takes an account of the mutual arrangement the current and potential electrodes;

The survey lines were oriented in NW-SE and NE-SW directions and in each case the maximum spacing of the current electrodes (AB/2) was 150m. At AB/2=20 and 30m repeated readings were taken at two different potential electrode positions (MN/2) in order to to examine the data quality and also assess any possible effect of anisotropic character of the underlying formations.

Figure 4.2. Field setup of the Vertical Electrical Sounding data acquisition

B. Dipole-Dipole Profiling

Dipole-Dipole configuration was chosen for its superiority in delineating lateral resistivity heterogeneities. Data were systematically collected along a NW-SE oriented traverse that passes through the location where students' dormitory building will be erected. The data acquisition was made using a dipole length of 20m for three dipole levels (n=1, 2, 3).

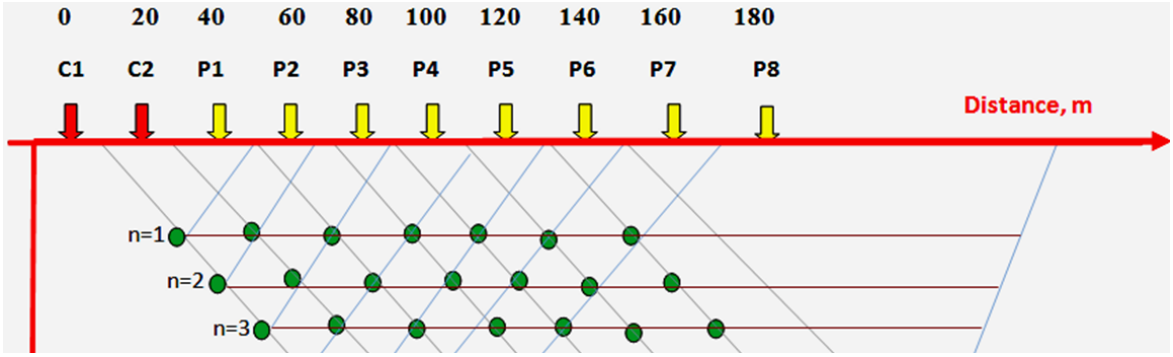

Figure4.3.Schematic field setup illustrating the principle of multi-level dipole-dipole profiling

Data was collected every 20m sampling interval; hence a maximum dipole separation of 60m is assumed to be fairly sufficient to reveal the lateral and vertical resistivity variations within the depth range, at least, 20-25m from the surface.

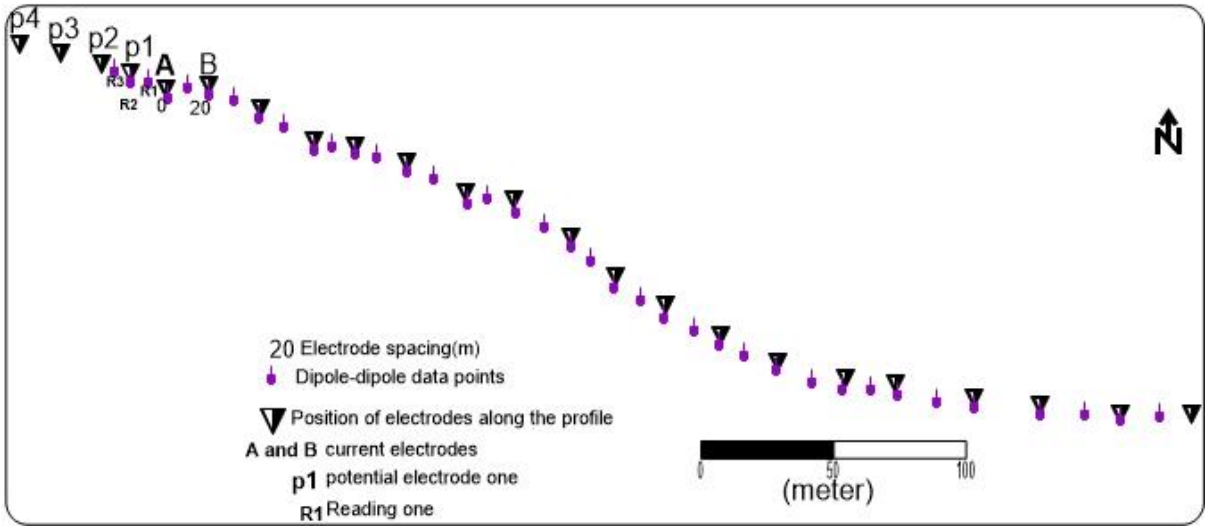

Figure 4.4. Electrodes field setup and data points in dipole-dipole profiling survey

The Sintrex-Made SARIS (Sintrex Automatic Resistivity Imaging System) having a maximum power of 100W was used both for resistivity sounding and profiling. This instrument automatically displays ρ_a values along with Standard Deviation (SD), Current (I) and Primary Voltage (V_p) on its digital screen (Figure 4.3).

Figure4.5.Front panel of the SARIS Terrameter.

The locations, i.e., Easting, Northing and elevations, of each sounding stations were determined employing the Garmin *GPSmap 62* receiver, which provides readings with an accuracy of ±2-3m.

4.2.2 Data Processing and Presentation

The apparent resistivity values obtained from the instrument were plotted on a bi- logarithmic graph sheets. In this case, ρa values on the ordinate (y-axis) and AB/2 values on the abscissa (x-axis) were plotted. Data were processed using IPI2win and Win RESIST software programs in order to determine the layer parameters (resistivity and thickness/depth) that were used as

input for further processing and plotting using Oasis montaj, Surfer 10 and MapInfo softwares and then interpretations carried out . During data processing using IPI2win and WinRESIST software iterations continued until best fitting was attained between the practical and theoretical curves, and in this case an RMS error of 1.7-4% was achieved. Then the values were used to construct the geo-electric sections and based on which data interpretations were made. Generally, good correlation between the field data and the interpreted model sections are obtained and this may be assured by an RMS error of 1.7 to 4% obtained for the sounding data. Several reinterpretations for modeled soundings curves were performed to get better model parameters and the iteration process was finalized when the root mean square (RMS) errors was less than 5%.

In the sounding curves, a 3 to 4 layer of the subsurface is seen and it well represents the subsurface condition of the construction site with the AB/2=150 m used for the survey. The layer parameters acquired by the WinResist and IPI2win softwares for each sounding point were then used to construct the geoelectric sections of each Profile using MapInfo, Surfer 10 and Oasis montaji softwares. In addition, pseudo-depth section maps and sliced-stack map are constructed using Surfer 10, Oasis montaj(6.4.2) softwares from the apparent resistivity data collected in the field.

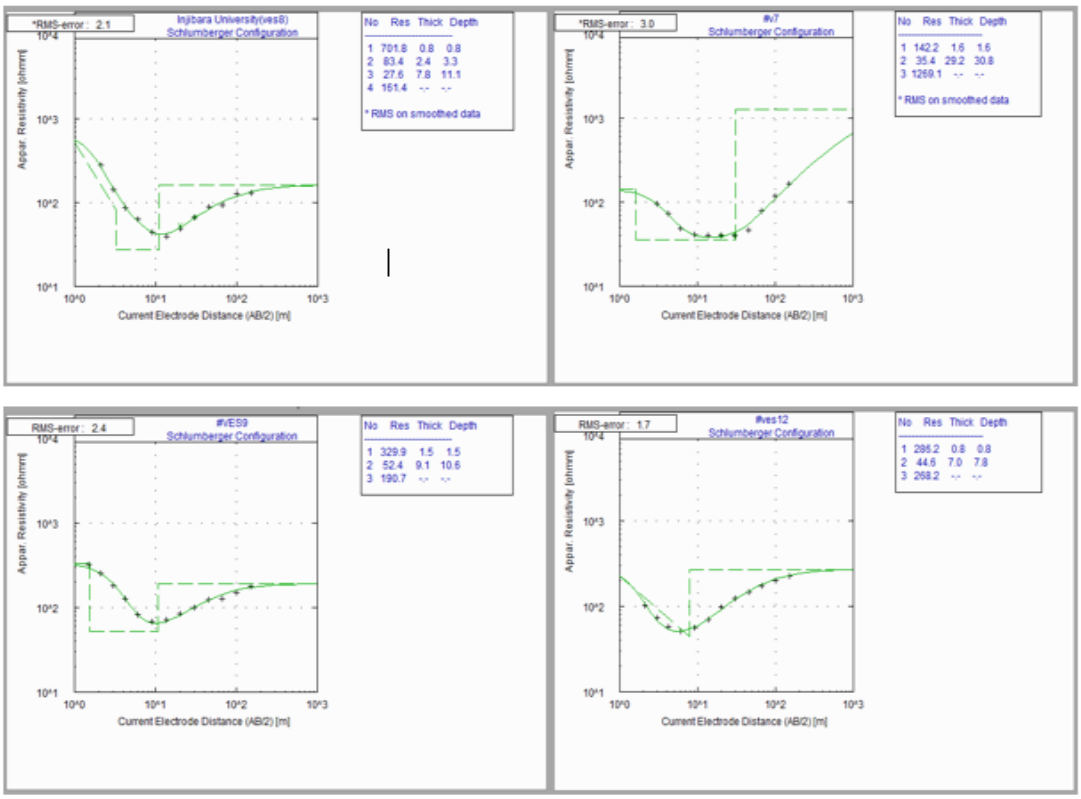

Figure 4.6. Samples of interpreted VES curves

Meanwhile, the dipole-dipole data were transferred into the Microsoft Excel and saved in ".dat" format. Then, data were read, processed and inverted using the RES2DINV (ver3.55.99). The RES2DINV inverts the measured and calculated apparent resistivity data to give an inverted model resistivity section that corresponds to true resistivity of the subsurface Earth materials. A typical plot that results from the inversion process is displayed in Figure 4.7.

The plot shows the measured (top), calculated (middle) apparent resistivity sections, as well as the inverted resistivity model section (bottom) that was used to perform data interpretation and analyses. The model quality and match between the raw and calculated apparent resistivity values are indicated by a Root Mean Square (RMS) error parameter. This value is given by the difference between apparent resistivity and calculated resistivity. The RMS error in % for the present study 14.7% with 3 iterations.

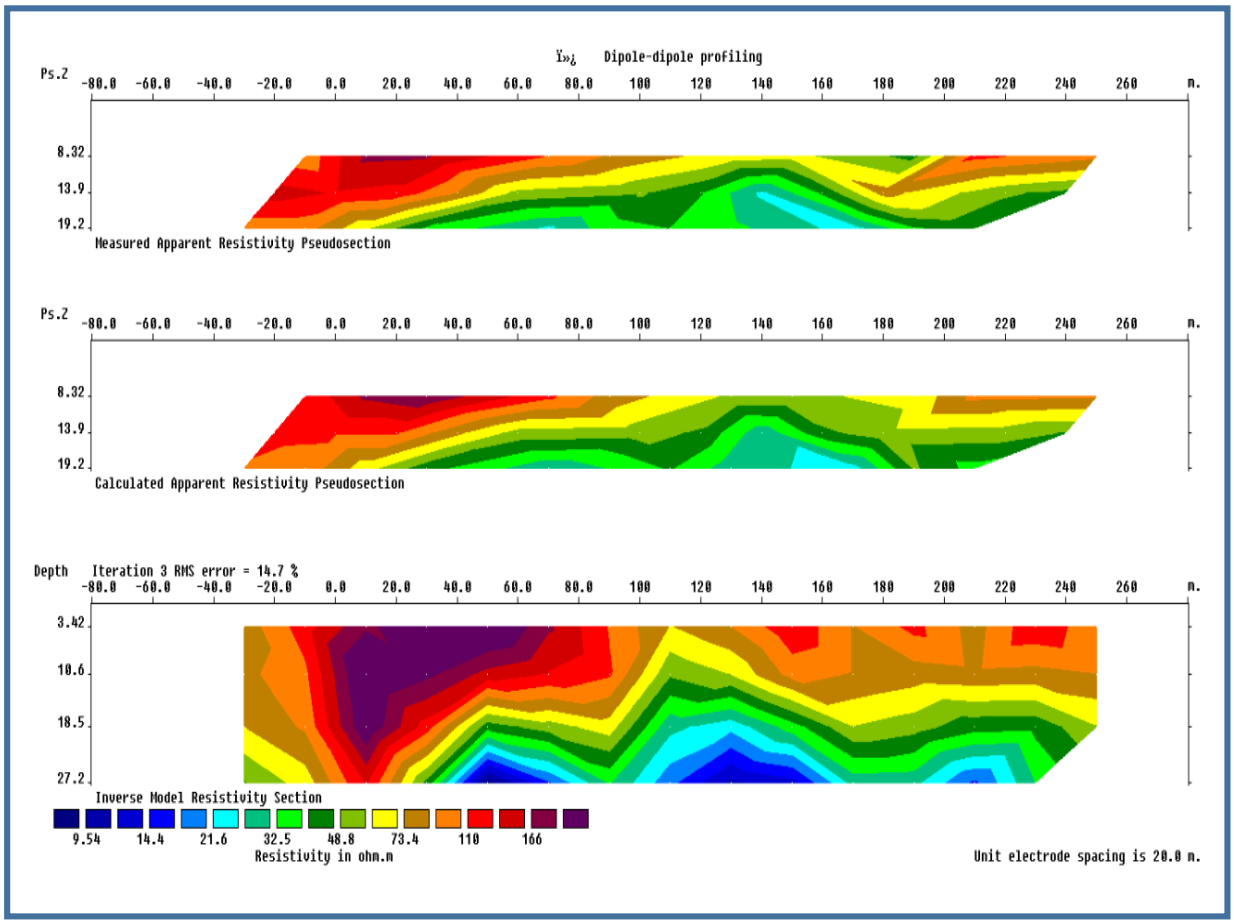

Figure 4.7.Measured, calculated and inverted Inverse model resistivity sections

4.3 Seismic Refraction Survey

4.3.1 Data acquisition and Instrumentation

The objective of refraction seismic survey was to determine the velocity of elastic waves propagation along different paths within the subsurface and indirectly assess the density characteristics. Every wave reaching the geophone produces a momentary impulse on a record of ground vibration called seismogram.

The survey was made employing the 48-channel Dolang Seismograph. However, in this study only 12 and 24 channels were used at geophone spacing of 4-10m. A 10kg sledge hammer was used as source generate elastic waves propagation along seven lines (Figure4.5), i.e, having a length of 55-110m.The sledge hammer was connected to the seismograph using the trigger cable to arm the seismograph as the impact is done. At each geophone and shot point location coordinates and elevation data were recorded using Garmin GPSmap 62.

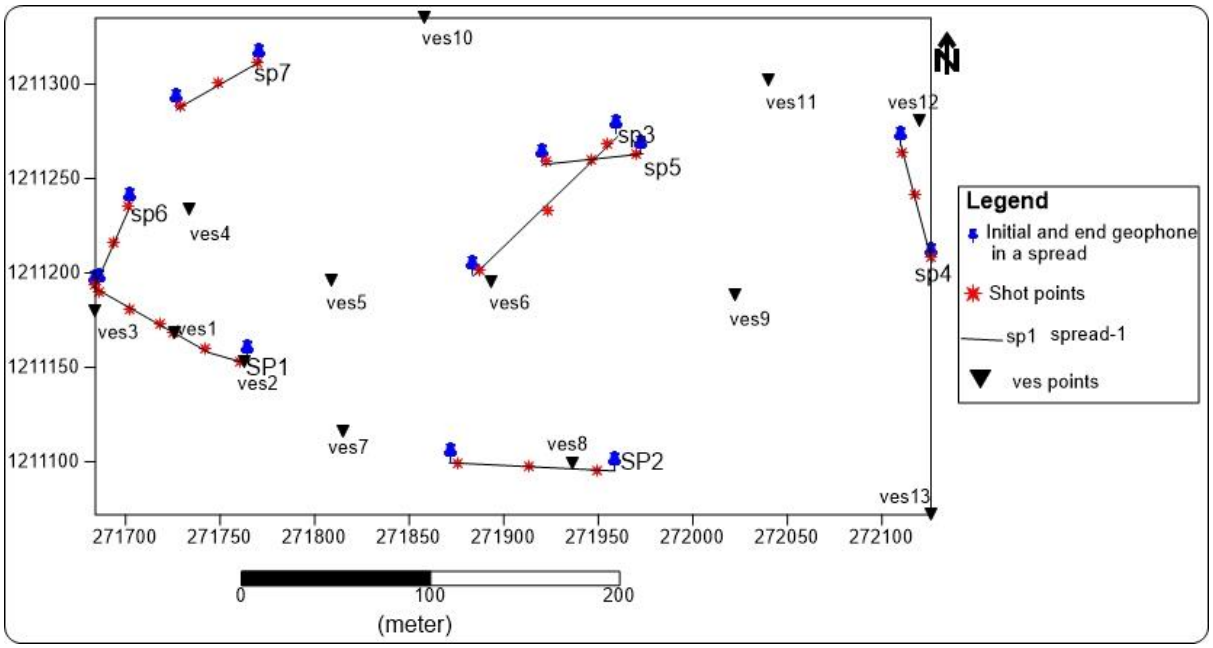

Figure 4.8. Seismic refraction survey lines (spreads)

The geophones were laid on the ground at regular interval measured by a tape meter. Geophone spacing is determined based on accessibility conditions and the detail of the required information. The field procedure employed was an in-line spread in which the source and the geophones were placed in a straight line. The geophones were connected to the seismograph via seismic cables. The source was activated at three different points for the six spreads and

six different points for one spread along the spread. The locations of the shots were 2m, 22m, 42m, 50m, 70m and 90m on spread 1 and 4m, 44m and 82m on spread 2.

Figure 4.9. Field setup, data acquisition and instrumentation of seismic refraction survey.

4.3.2 Processing and presentation of seismic refraction data

The seismic refraction data were processed using the software programs PickWin95 and Plotrefa from the SeisImager software package. Raw field data in 'seg2' format were imported into PickWin95 and the first arrivals of the P-waves were chosen. A band pass filter frequency of 56.9Hz low cutoff and 409.6 Hz high cutoff were applied to take out the low and high frequency noise. These cutoff frequencies were chosen considering the range of seismic frequencies and observing the seismogram (waveform). This was performed for each of the shot points along the spreads. Then, the first arrival picked data were imported into Plotrefa, and a plot of time versus distance was generated (Fig. 4.9). Plotrefa automatically checks

reciprocal times for multiple shot locations. It is best if the root mean square (RMS) error is less than 5%. Most of the data points in the spreads have RMS values below 5%; however, there are some data points with higher RMS errors. Data processing requires much care and experience as noise can be deceptive in picking first breaks. The main noise sources in the project area were movement of trucks, excavator, people and animals in the proximities of the survey lines.

Layers were assigned by identifying crossover points, which occur where the slope (1/v) changes. The crossover point separating vesicular basalt and basalt is minor, but the change in slope between the top soil and bedrock is distinct. After the layer assignment, a time-term inversion model can be run. Velocity is calculated, and from the model depth is inferred. Velocity models for each spreads were generated using different first arrival picks in order to gain an understanding of model sensitivity.

This was done for the seven spreads and for each of the source. See a typical example of figure 4.11 and figure 4.12.

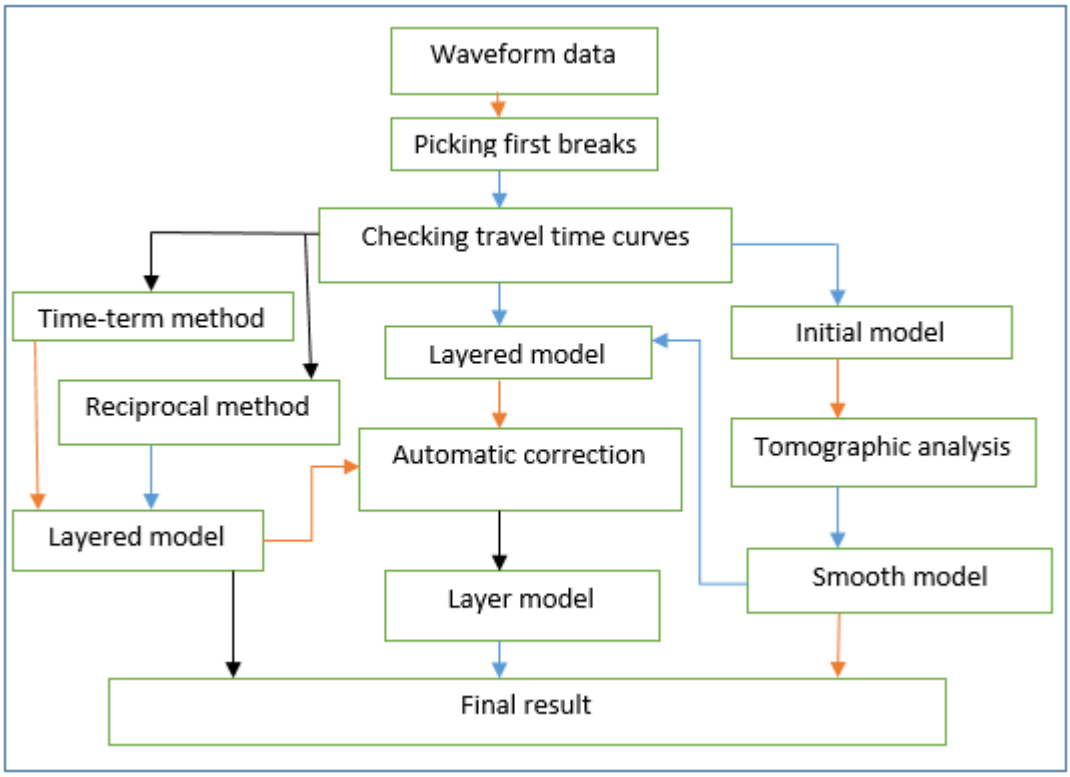

Figure4.10. Processing flowchart for seismic refraction data analysis

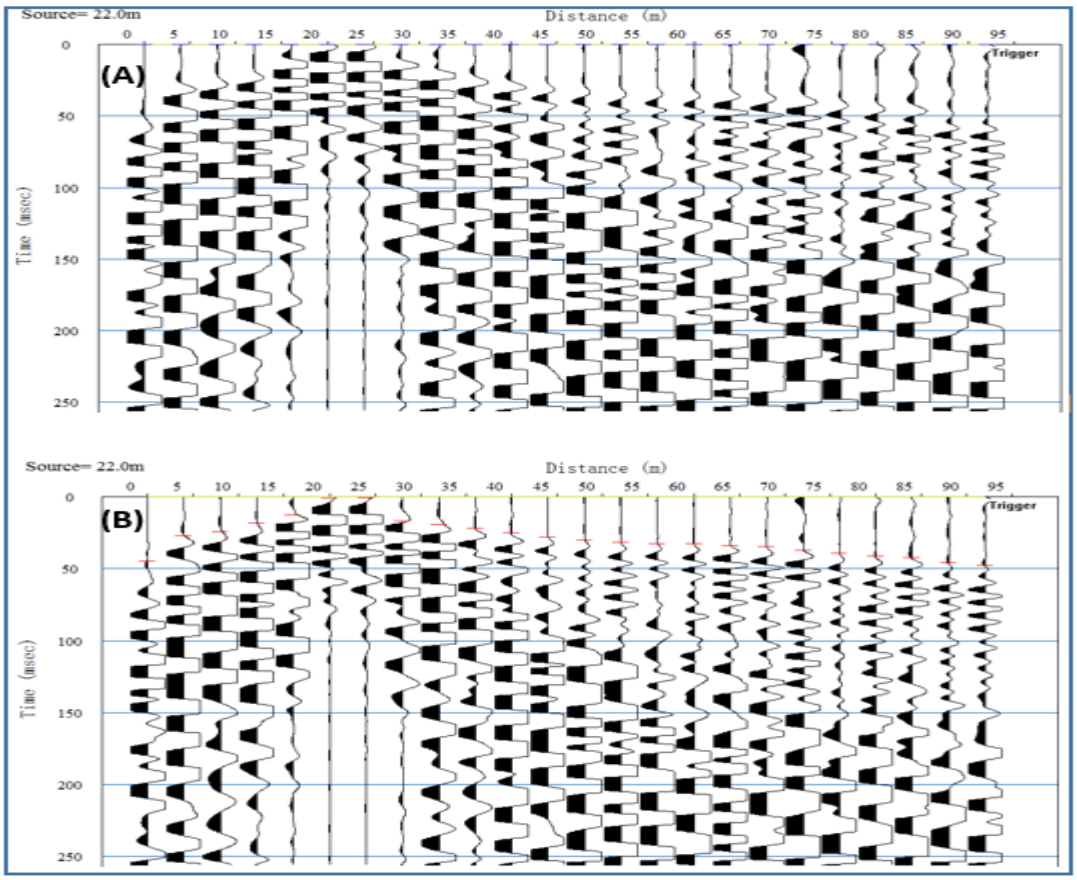

Figure4.11. Sample of waveform (A) and a waveform with picked first breaks (B)

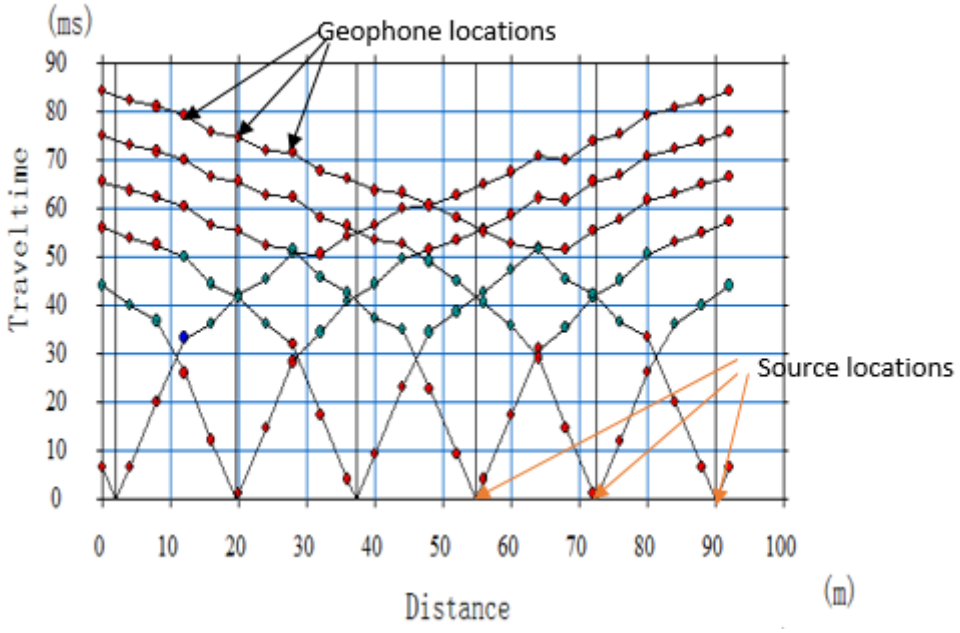

Figure 4.12.Time-distance plot of the Spread

4.4 Magnetic Survey

Magnetic method is a geophysical technique that measures the total magnetic field intensity of the Earth. The magnetic method is capable of mapping various geologic features, such as igneous intrusions, faults, some geologic contacts and lithology. In the present study Magnetic method is employed for subsurface study to outline lithological contacts and structural zones which could be associated with faults and fractures that may affect the building foundation.

Magnetic methods comprise of three major activities;

- Measurement of the specific field value at the ground (Data acquisition)
- Processing of the measured data (Data processing)
- Interpretation of the processed data qualitatively and quantitatively in terms of the rock property variations within the known geology (Data interpretation)

4.4.1 Field data acquisition and Data instrumentation

The land magnetic data acquisition in the area were done by using GSM-19T proton precession magnetometer for acquiring primary data for this research. The total magnetic data collected during the field work was 153 data points. At the field survey three magnetic readings were taken for the base station and then average of this readings were used for the diurnal correction. All the magnetic data were collected for one day during the morning time.

Figure4.13. Magnetic data acquisition using the GSM-19T magnetometer.

At the very beginning, before establishing base stations the first thing that was done is to look for appropriate location with very less magnetic noises such as cars, houses with iron roof, roads, power lines and others and a point close to the survey area. At each station the magnetometer reading, recording time, location in UTM coordinate and elevation (meter) were recorded. For this study the base station reading were reoccupied within one hour interval for the correction of diurnal variation. The positions of the survey stations and the station elevations were determined using the GPS receiver, Garmin. Hence we have one base station located at a UTM coordinate of 271672 Easting and 1211169 Northing. In each time magnetic data reading was started and ended up at this base station.The distribution of magnetic data in the study area is shown in Figure4.11.

4.4.2. Magnetic Data Processing and Presentation

The magnetic data were collected and processed for effective interpretation of the subsurface condition of the building site. Observed magnetic field data, coordinate data, elevation data and time were manually entered into a computer after the completion of the field work using Microsoft excel worksheet. Before processing the data the field magnetic data should undergo different corrections.

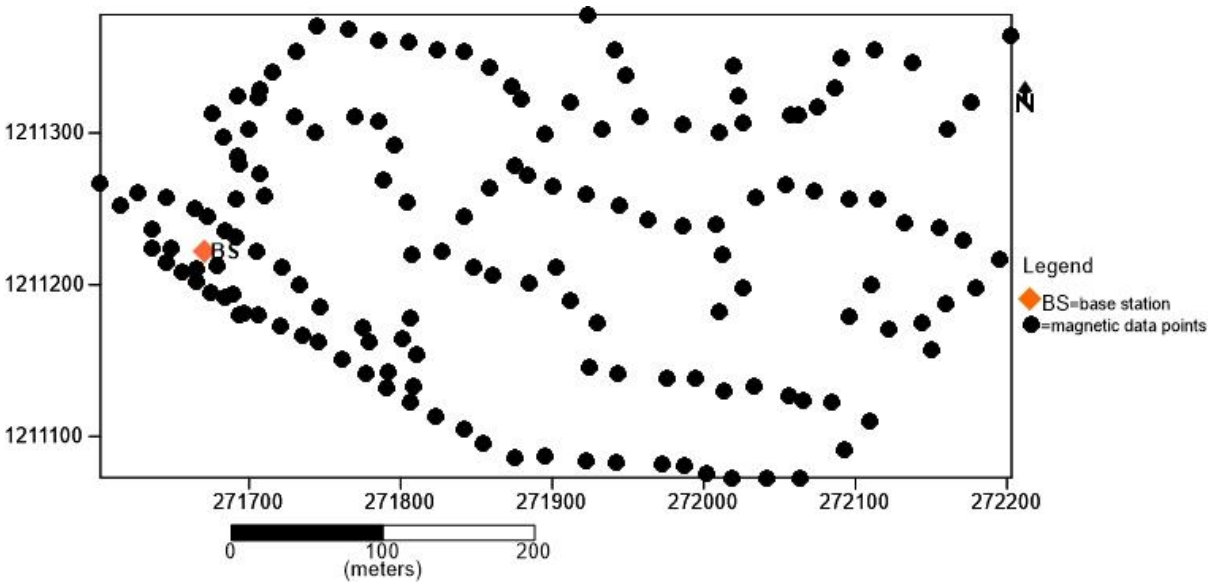

Figure 4.14.Magnetic data distribution of the survey area

Variation of the Earth's magnetic field with time, due to the rotation of the earth and with respect to the solar wind, which may last several hours to one day, is called diurnal variation. The magnetic data processing started by correcting the raw data for diurnal variation. In spite of great improvements in instrumentation, Diurnal variation will be corrected and data

enhancement techniques are applied in order to extract maximum information from the magnetic data. Repeated readings were taken every one hour of the magnetic measurement at the base station. After the data collection, the diurnal effect was calculated and the magnetic data were filtered.

The formula applied for diurnal correction is

$$M_c = M_i - \frac{((M_2 - M_1))}{(T_2 - T_1)}(T_i - T_1)$$

Where M_1 and M_2 are magnetic field readings at the base station at the beginning and at the end of the magnetic survey, T_1 and T_2 are the corresponding time respectively. M_c is the corrected magnetic data, M_i is magnetic data observed along the traverse, T_i is the corresponding time.

Magnetic survey involves measurement of the sum of magnetic field produced by both local and regional magnetic fields. The regional magnetic field, often referred to as geomagnetic field needed to be subtracted from the acquired total magnetic field to obtain the magnetic field anomaly (residual) caused by local source.

After subtracting the diurnal effect from the original magnetic data observed, the geomagnetic field was calculated using the mathematical model of Earth's magnetic field called the International Geomagnetic Reference Frame (IGRF) model 2005 in Geosoft Oasis Montaj 6.4.2 software. This model is calculated based on the dates, elevation and geographical location (latitudes and longitudes) of the observed magnetic data with the generated average geomagnetic field of 36150nT. The IGRF values were subtracted from the observed magnetic values for each station to determine the residual magnetic field due to anomalous contribution from local magnetic sources in the area.

The corrected magnetic data were then gridded and the results were then contoured using computerized mapping and processing software (Geosoft Oasis montaj version 6.4.2). To produce different maps for both potential methods magmap application were found to be very important. The corrected magnetic data were plotted, after which the possible noisy data were removed. For effective interpretation of the obtained magnetic data, further enhancements were carried out using various filtering techniques.

The commonly used data enhancement techniques including the analytical signal method and tilt derivative method are employed here. As a result, the analytical signal magnetic map and the tilt

derivative magnetic map are produced from values of total magnetic anomaly map compiled for the study area.

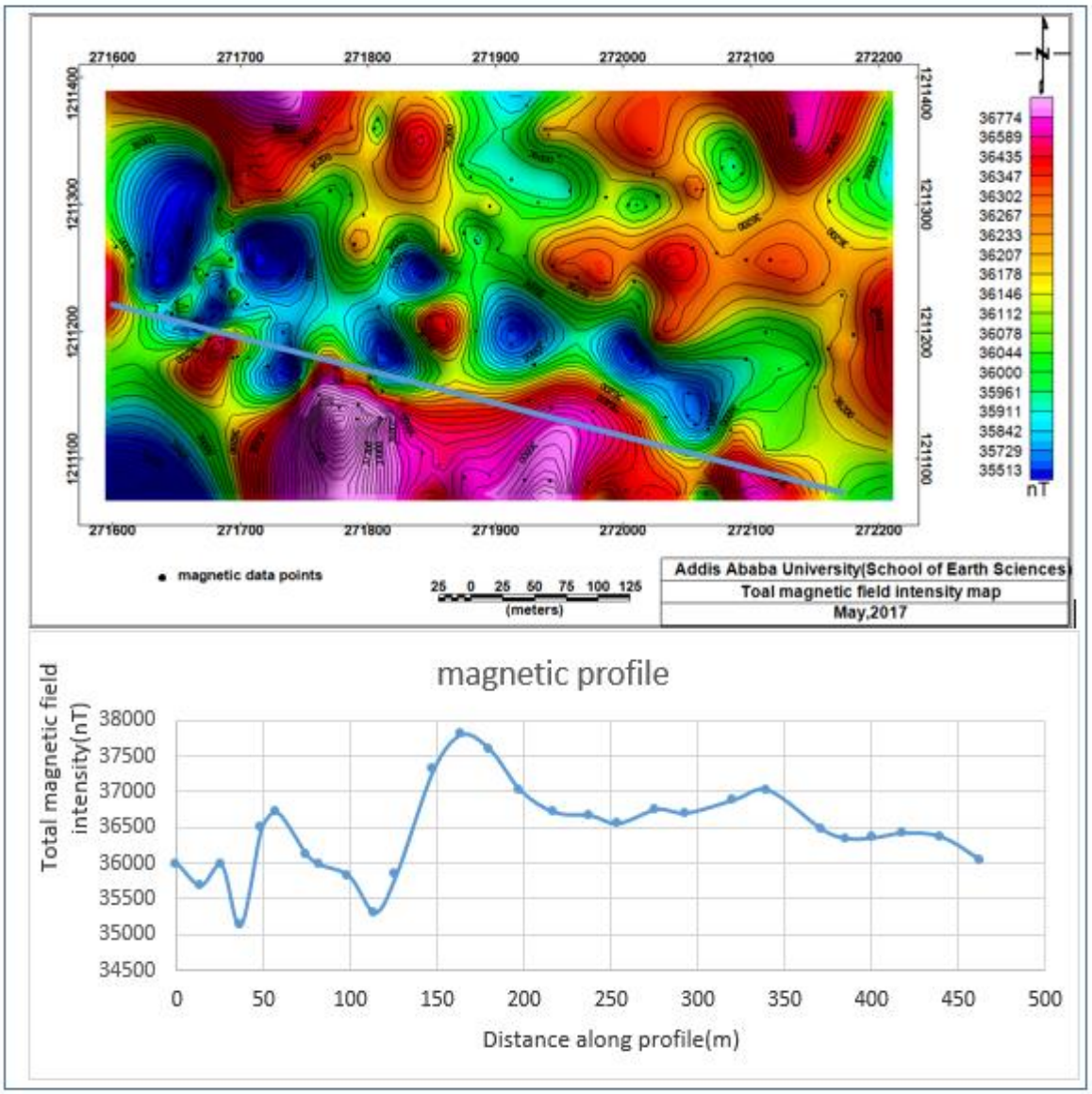

Figure 4.15.Total magnetic field intensity anomaly map (a) and magnetic profile plot for survey profile one (b)

CHAPTER V

5. RESULT, DISCUSSION AND INTERPRETATION

5.1 Introduction

In this thesis work interpretation has been made based on integration of results from electrical sounding, seismic refraction and magnetic data with the help of a borehole lithological log and dug test pits data. The borehole data helps to understand the vertical geological section of the study area and to correlate these different units with the electrical and seismic refraction velocity model sections. The depth of the boreholes used for lithological correlation is 296m; whereas the depths of the geoelectric section and seismic velocity model are about maximum depth 20-35m, i.e. the depth of the geophysical sections is smaller as compared to the depth of the borehole depth. A borehole used in the interpretation of the geophysical data is found near the boundary of the study area drilled by Amhara design and supervision works enterprise collaboration with Amhara water, irrigation and energy bureau for water supply purpose to Injibara University for the coming year consumption.

In addition, apparent resistivity pseudo depth section and sliced stacked map were prepared from the resistivity sounding data to examine the general picture of the subsurface to larger depths.

This section includes the interpretation of geo-electric sections, apparent resistivity sliced-stacked map, Pseudo depth section maps p-wave velocity models, magnetic anomaly maps, analytical signal map, tilt derivative map which have been developed using different geophysical plotting and processing softwares.

In the following sections, interpretation of the electrical resistivity, seismic refraction and magnetic data for each survey was done. The thorough interpretation of the study goes as follows:

5.2 Interpretation of resistivity survey data

5.2.1 Resistivity Sounding Data

The resistivity sounding survey have been conducted at thirteen sounding points along four profiles with half current electrode spacing (AB/2) of 150m. The individual VES are interpreted to get the layer parameters (resistivity and thickness of the subsurface layers) using win resist and IPI2win as given in Figure 4.4.

Surfer (Version 10), Oasis montaji (6.4.2) and MapInfo softwares were used to plot the presented pseudo-sections, slice-stacked map and geo-electric section based on which both qualitative and quantitative interpretations are conducted. The VES data are presented in the form of apparent resistivity pseudo depth sections, geoelectric section and slice- stacked map have been discussed separately in the following sections.

5.2.1.1 Profile-1

Apparent resistivity pseudo-depth section map

Pseudo depth maps are prepared by taking raw apparent resistivity data show resistivity variation of the subsurface both in lateral and vertical directions without introducing the bias of data filtering. They do not reflect the actual depths of anomaly sources however they are good means of displaying the vertical distributions of resistivity values and also can be used as guide when the geo-electric sections are produced.

The apparent resistivity pseudo depth section (Figure 5.1) is prepared from the VES surveys carried out along Profile-1 includes VES3, VES1, VES2, VES7, VES8 and VES13 from NW to SE respectively.

The pseudo depth section (Figure 5.1) indicates that the top most part of the study area has higher resistivity value that ranges from 450Ω-m to750Ω-m. This is likely to be the response of the compacted top soil composed of the mixture of clay, silt, sand, gravel and sediments derived by river action. In between VES-8 and VES-13 high resistivity value is observed extending to shallow depth to deep. Furthermore, relatively medium resistivity values are shown at deep and covering most of the area below each VES points. This intermediate resistive layer is found at higher depth under VES1, VES2, VES7 and VES8. However, very low resistive formation is found at shallow depth on these VES points. Therefore, much attention should be given in this area in the designing of building foundation. In general, the

pseudo depth map along profile one shows that in between VES2 and VES7 the study area has very low resistivity value which extends up to 100m depth. These area has a resistivity value <50Ωm and this could be the response of the weathered and fractured vesicular basalt. An intermediate resistivity value ranging from 100Ωm to 300Ωm covers the area at shallow depth beneath VES3, VES8 and VES13.

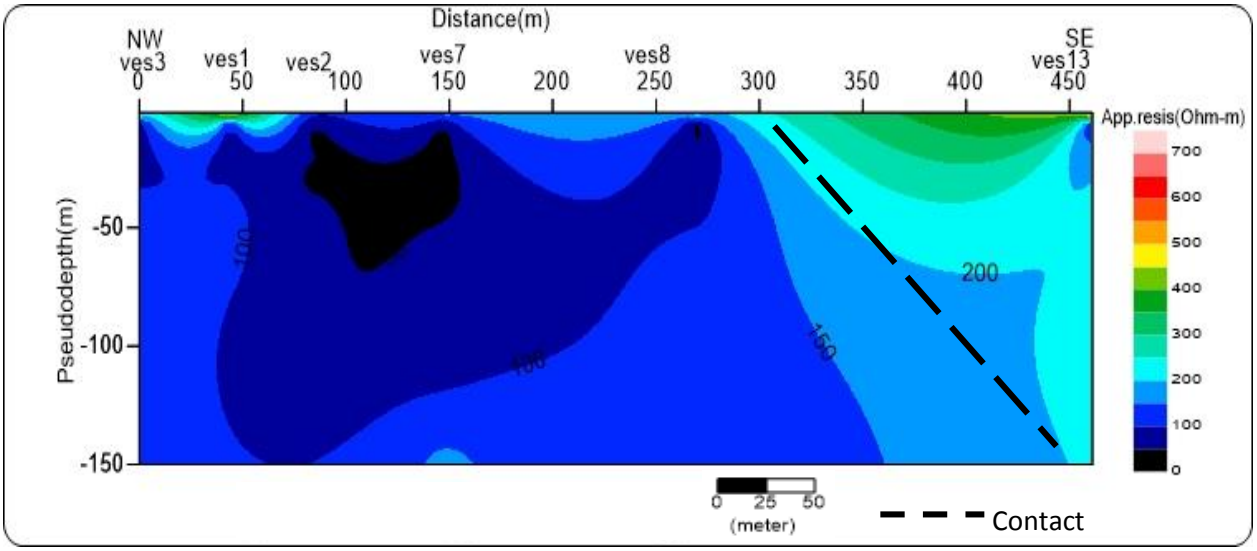

Figure5.1.Apparent resistivity pseudodepth section map of profile-1

Geoelectric section

The geoelectric section of Profile-1 is obtained from the interpreted layer parameters of VES1, VES2, VES3, VES7, VES8 and VES13 in the study area as shown in figure5.2.The geoelectric section shows three layers. The top layer that has variable resistivity ranging from about 97-427Ω-m and the thickness of this layer varies about from 2-3.5m and it is more likely to be a mixture of clay, silty and sandy soil from the lithologic log and dug pit test data. The lateral variation in resistivity is believed to be come due to variation of compactness along the profile. The variation in compactness may come from the movement of cars and animal etc. The second layer, which is over lain by the top soil, has relatively very low resistivity value ranging from 33Ωm to 60Ωm and thickness varying 5-27m beneath the VES points. This layer has a maximum thickness beneath VES2 and VES7 and is inferred as highly weathered and fractured vesicular basalt. The third layer possesses relatively high resistivity value ranging from 167-1269Ω which could be the response of the basaltic formation. This

formation is found at shallow depth at about 10m in the northwestern and southeastern part of the study area respectively, while the depth of this unit in the near central part geoelectric section just beneath VES2 and VES7 goes up to 27m.

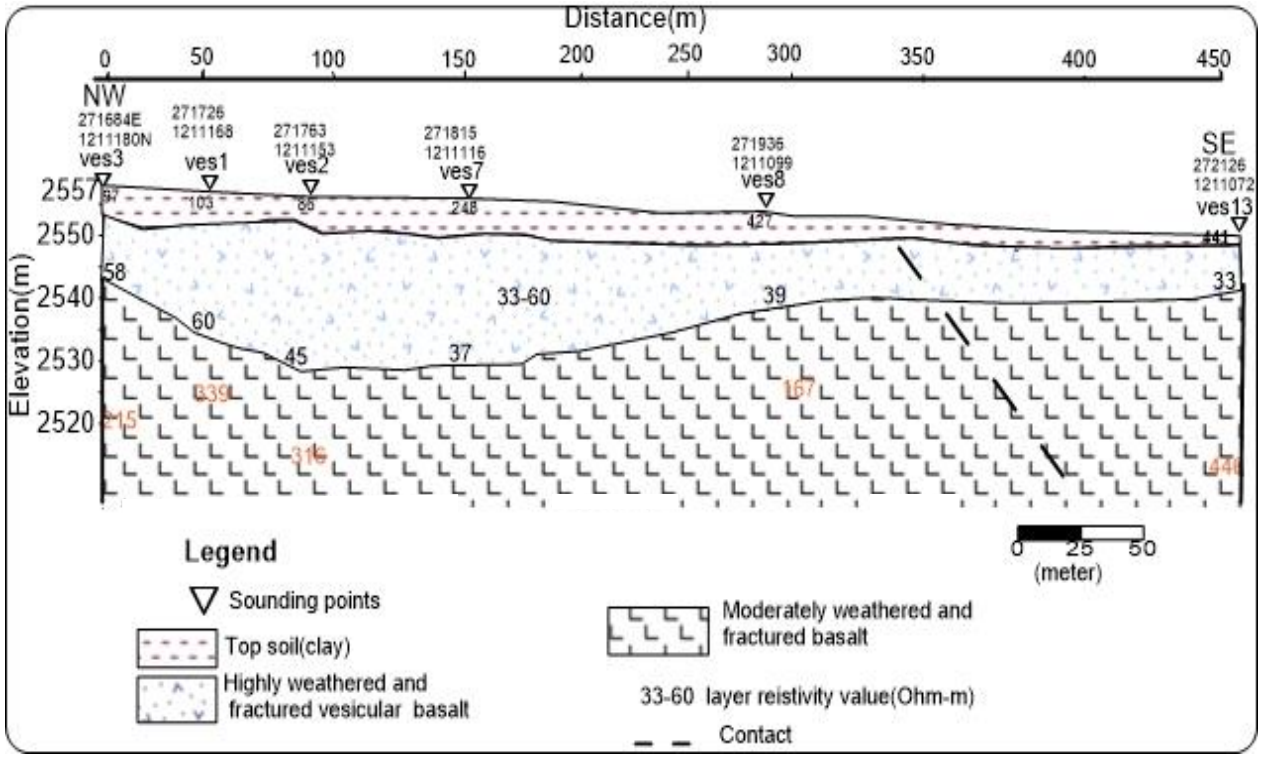

Figure 5.2.Geoelectric section map along profile-1

5.2.1.2 Profile-2

Apparent resistivity pseudodepth section map

Profile-2 of the vertical electrical sounding survey consisting of four VES points VES4, VES5, VES6 and VES9 which is almost parallel to profile one has been carried out. The distance between the four sounding points is different from one VES to the other to have a profile length of about 292m. The generalized electrical picture of the subsurface of this profile displayed by the pseudodepth section map as given in Figure 5.3. This psuedodepth section gives the electrical resistivity variation of the subsurface. The top part of the section has relatively high resistivity ranging 230-340Ωm, underlain by very low resistivity formation ranging 60-110Ωm beneath VES4 and VES5 and moderately high resistivity 120-210Ωm below VES6 and VES9.In this section map we can generalize that the northwestern part of the profile possess very low resistivity values, therefore it is not recommended to set the foundation on this area or special attention

should be taken.

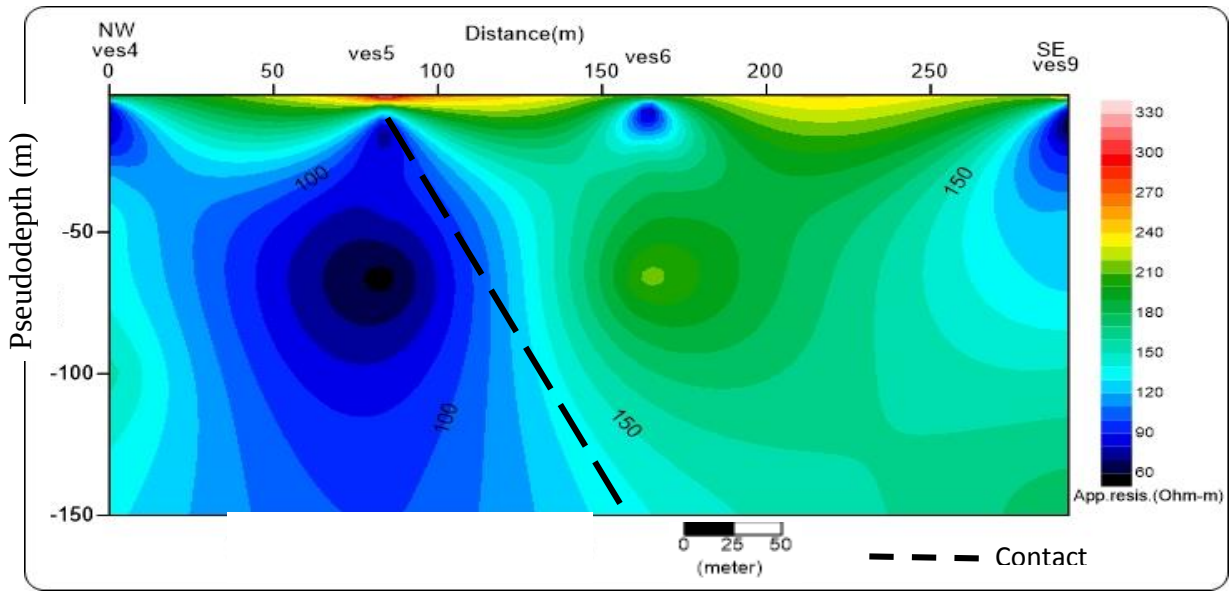

Figure 5.3.Apparent resistivity pseudodepth section along Profile-2

Geoelectric sectction

Profile-2 of the geoelectric section was obtained from the model parameters of sounding points along profile-2(VES4, VES5, VES6 and VES9).Well log and dug pit test data located around the survey area were used to constrain thickness and resistivity values these sounding points. The individual VES points VES4, VES5, VES6 and VES9 have been interpreted to obtain the layer parameter resistivity and thickness of the individual layers using a combination of the IPI2win and WinResist softwares and the results of these are given in chapter four and Appendices of the thesis. The geoelectric section constructed from interpretation of the VES along this profile (Profile-2) from the interpreted layer parameters of VES4, VES5, VES6 and VES9 is given in Figure 5.4.The first layer in this section is the top dry soil which is composed of clay, silt and sandy soil shows relatively high resistivity ranges from 190-351 Ω-m and having a thickness of about 2m.The second layer in the geoelectric section exhibits relatively low resistivity values that could be due to weathered and fractured vesicular basalt because of higher moisture content relative to the overlying and underlying layers. From the geoelectric section, the resistivity of this layer is seen to be vary from 39-70Ω-m and its depth extends to 18m.The resistivity values of the third layer are in the range of 173- 363Ω-m, this relatively higher resistivity response could be due to the weathered basalt which is considered to be the competent bedrock in the survey area.

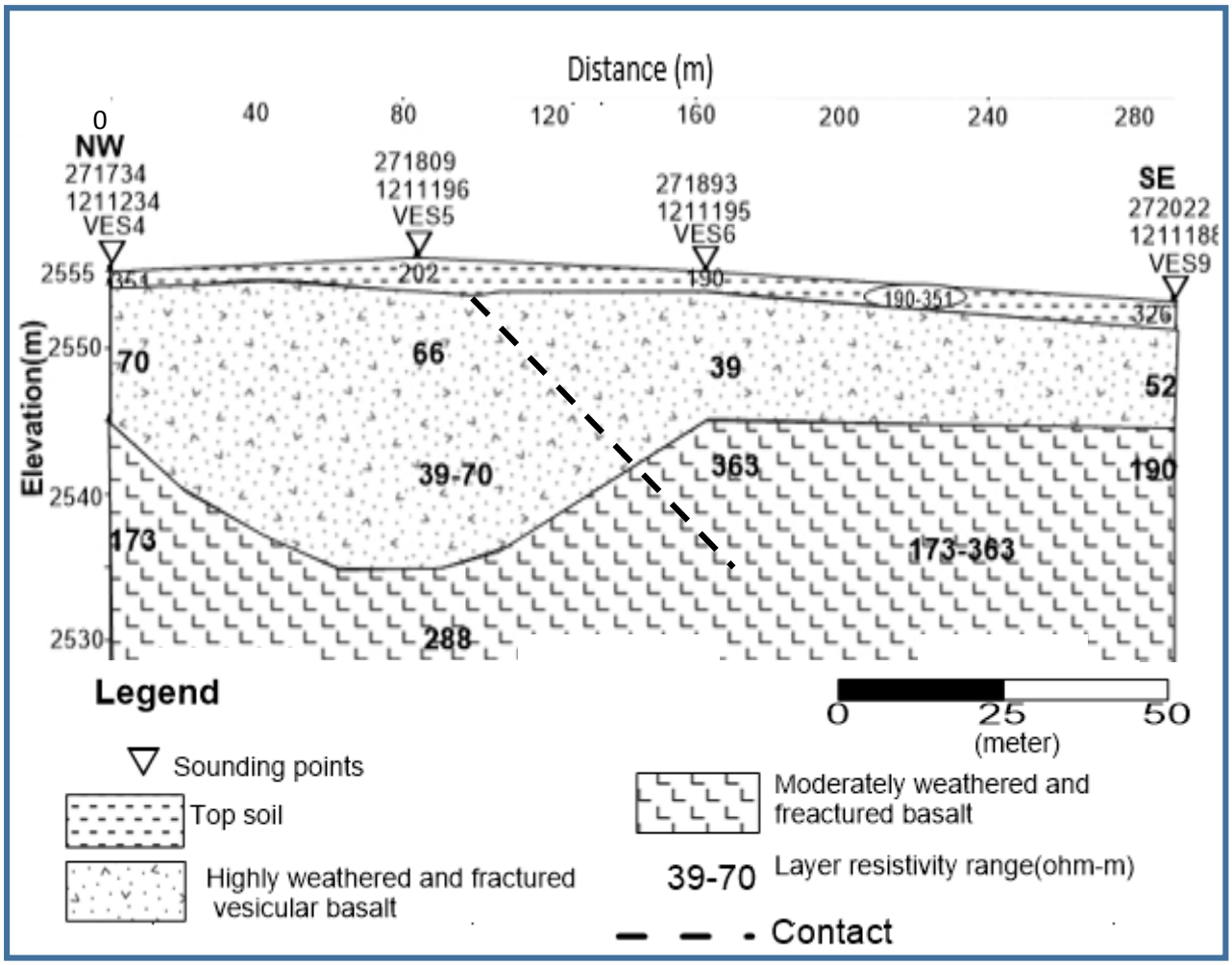

Figure 5.4.Geoelectric section map of Profile-2

5.2.1.3 Profile-3

Apparent pseudo depth section map

In profile-3, three sounding points has been carried out and the pseudo-depth section developed from VES10, VES11 and VES12 that lie on the survey profile is given in Figure 5.5. The figure shows that, the vertical resistivity variation increases as one goes to deep except just beneath each VES points at shallow depth. The highly resistive region at the top of the section shows that the presence of compacted top soil, while the shallower level which is dominated by a low resistivity values, interpreted as a likely response of weathered and fractured vesicular basalt. The deeper level with high resistivity value from 190-250 Ohm-m is may be the presence of massive basalt formation which has an implication for building foundation in the survey area.

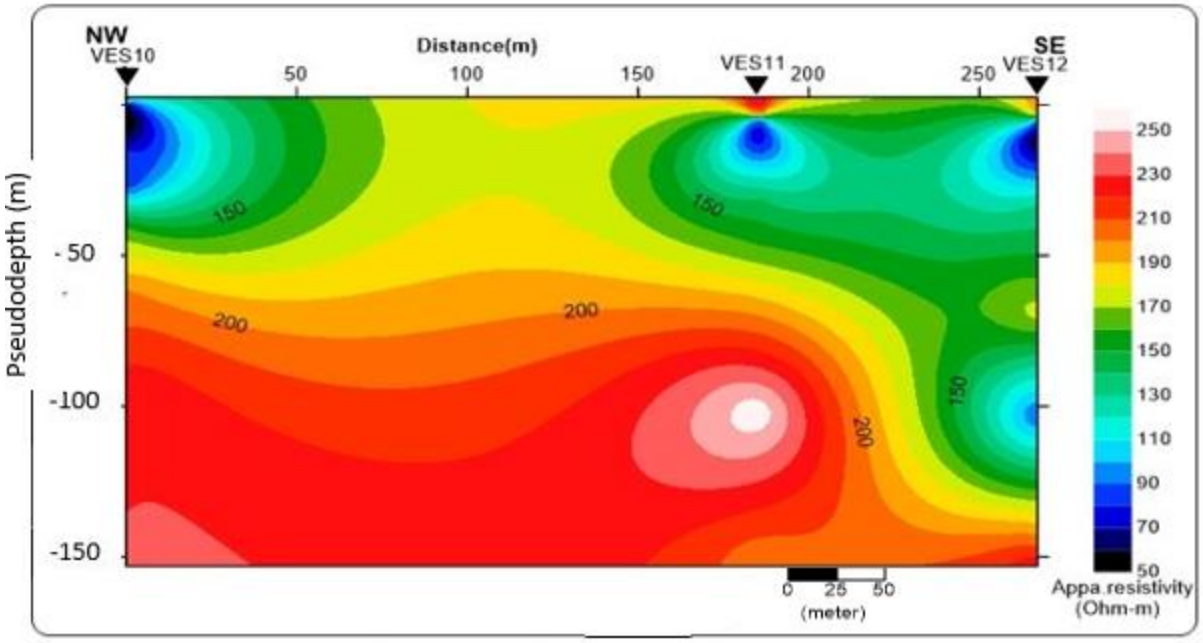

Figure5.5.Pseudodepth section along profile-3

Geoelectric section

The geo-electric section of profile three was constructed from model parameter of VES point data along profile three (VES10, VES11 and VES12). The resistivity parameters found from one dimensional inversion from IPI2win and win resist software of each VES point data were used to prepare geoelectric section shown below in (Figure 5.6). The geoelectric section shows that the shallow subsurface lithological units found along line three which are represented by three VES points. The three geoelectric units have a relative resistivity in accordance with the following patterns, $\rho_1>\rho_2<\rho_3$ with resistivity values ρ_1 (198-286) Ω-m, ρ_2 (44-53) Ω-m, ρ_3 (266-445) Ω-m.

The first geoelectric layer that has resistivity ρ_1 (198-286) Ω-m and the thickness varies about from 1-4m is characterized as top soil composed of clay, silt and sand. The second geoelectric layer is marked by resistivity values ρ_2 (44-53) Ω-m is likely correlated with highly weathered and fractured vesicular basalt. The resistivity of the third geoelectric layer that corresponds to moderately weathered and fractured massive basalt has a resistivity value ρ_3 (266-445) Ω-m. From the section, the third layer is relatively a competent bed rock in the study area. This geoelectric layer is at shallow depth in the northwestern flank relative to the southeastern one. Therefore, along this profile setting the building foundation in northwestern part is more advisable in order to minimize risk. The lateral variation in resistivity along the first, second

and third horizon possibly associated to the variation in degree of weathering, intensity of fracturing and geological structures.

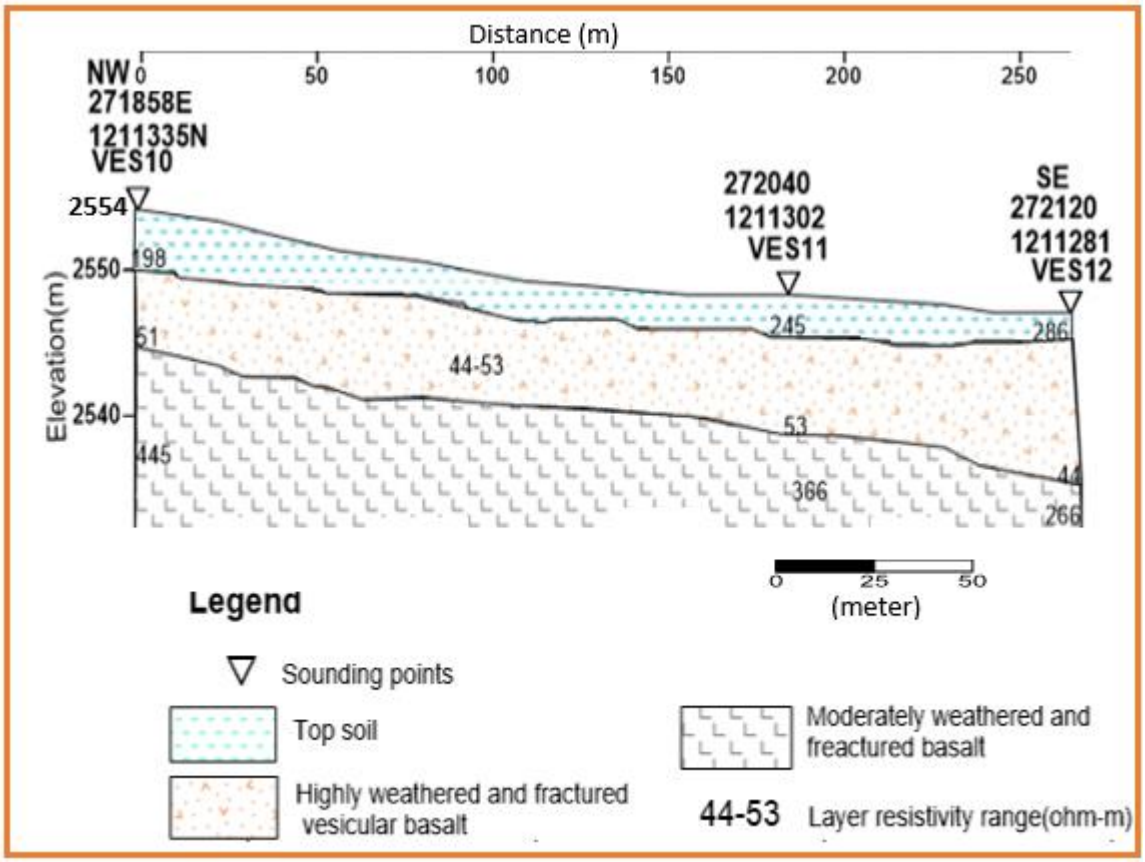

Figure 5.6.Geoelectric section map along profile-3

5.2.1.4 Profile-4

Apparent pseudo depth section

This section is constructed using the VES points VES7, VES6 and VES11that lie on the traverse line four as given in figure 5.7.According to this figure, the resistivity of the section increases with increasing depth of the investigation in between VES6 and VES11. The central part of the section is dominated by a high resistivity value extends to from shallow depth to deep, while the shallow zone of the section beneath VES7 and VES11 is dominated by low resistivity value. In the pseudo-depth section (Figure.5.7) we can observe that southwestern and northeastern flank is dominated by low resistivity and high resistivity formation respectively. As a result, along this profile it recommended that to set the building foundation on the northeastern flank of the study area and use southwestern flank for parking purpose.

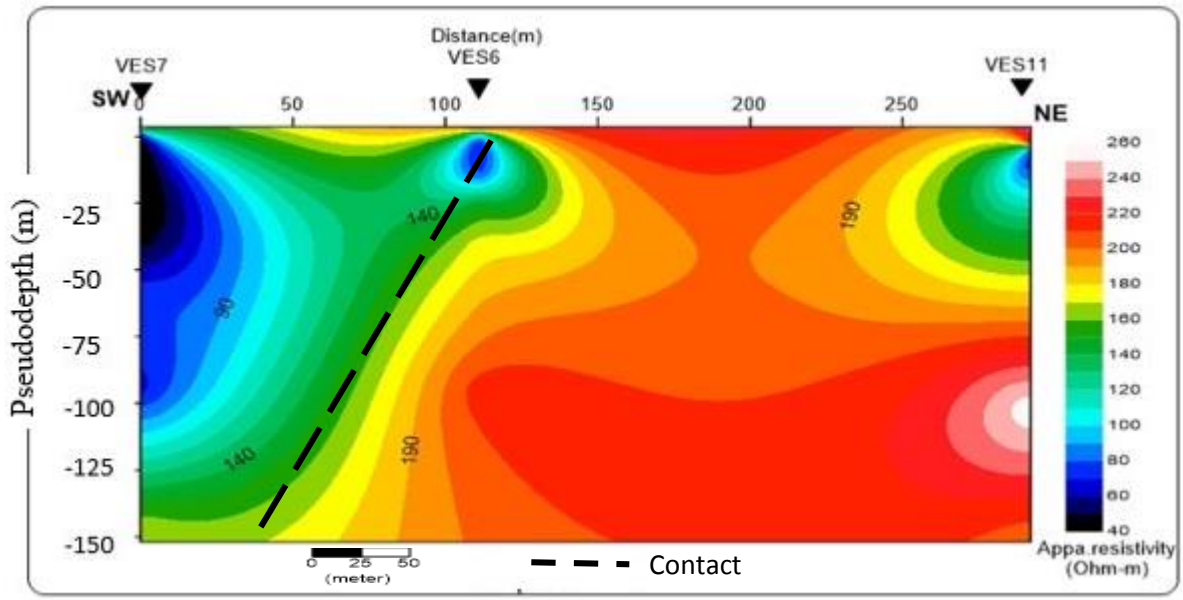

Figure 5.7 Apparent resistivity pseudodepth section map along profile-4

Geoelectric section

The resistivity sounding geoelectric section along profile-4 is constructed from the interpreted layer parameters of VES7, VES6 and VES11. It shows that the area is underlined by different layers beneath each point and the resulting geoelectric section is presented in (figure 5.8). The geoelectric section figure 5.8shows, VES7, VES6 and VES11 have three layers with different thickness of each layer. The top most part of the geoelectric section has resistivity values that range from 103 to190Ω-m with thickness varying from 1-2m. This layer is probably related to dry top soil mixture of clay, silt and sand.

The second layer has relatively low resistivity values ranging 35-58 Ohm-m which may possibly the response of the highly weathered and fractured vesicular basalt. This horizon shows different thickness beneath each VES points ranging 10-18m. The resistivity of the third layer ranges from 339-1200Ωm which may be the response of moderately weathered and fractured basalt. It lies at a depth of 25m in the vicinity of beneath VES7, at a depth of about 10m beneath VES6 and under VES11 the depth about 18m. Along this profile line possibly this layer would be the competent bedrock in the study area.

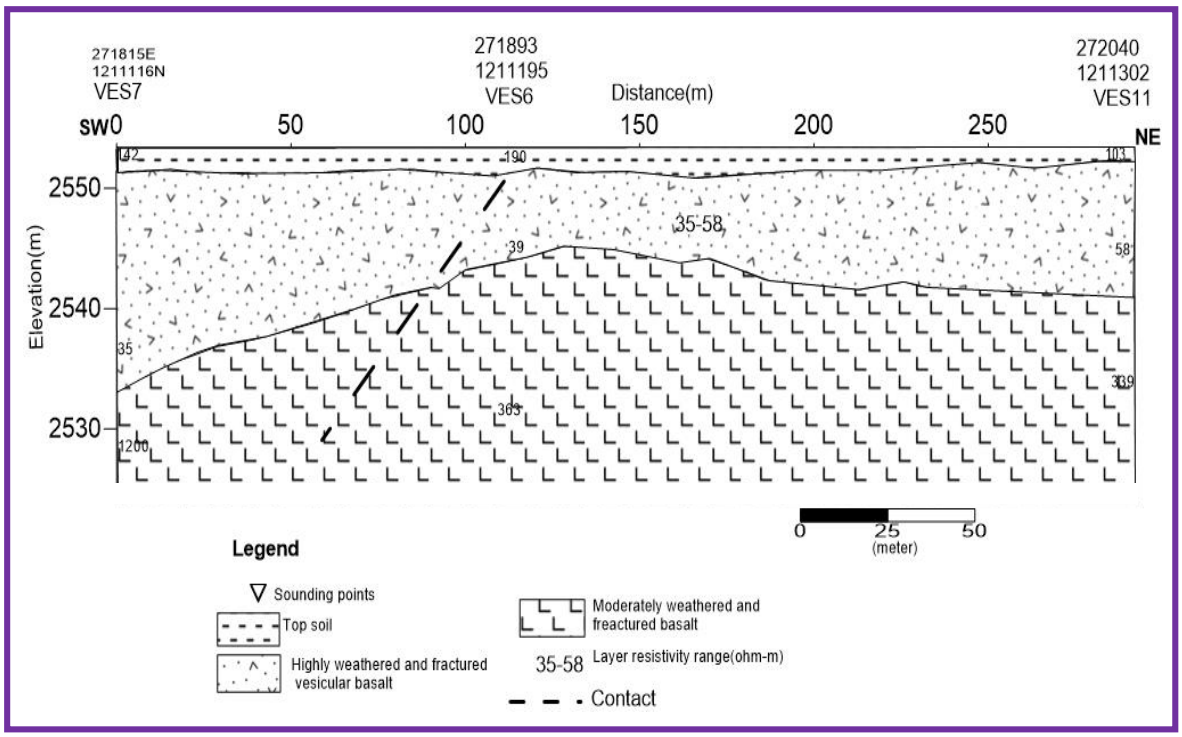

Figure 5.8. Geoelectric section map along Profile-4

From this geoelectric section, the thickness of the first layer becomes thin towards northeastern and the second layer has increased in thickness towards SW and NE direction from the center of the survey area. This is may be due to sliding problem, accumulation of clay soils and slide deposits at this location. Therefore, in this area setting the building foundation in between VES6 and VES11 is more preferable because the competent bed rock is relatively found at shallow depth and the thickness of the weak zone is small as compared to the southwestern flank of the part of the survey building site.

5.2.1.5 Sliced-Stacked apparent resistivity psuedosection map

From the different AB/2 apparent resistivity value considerably varies from 10-750 Ohm-m as shown below. The stacked apparent resistivity pseudo section map (Fig. 5.9) shows that the sub-surface resistivity section of the entire study area which was constructed by extracting apparent resistivity values of all profiles at the same depth of investigations. In order to obtain a more reliable and realistic representation of the possible subsurface structures, five slices (AB/2=1.5, 9, 30, 66 and 100m) were selected from the electrical apparent resistivity sounding data to characterizes the sub-surface. The choice of such spacing depends on the variability between them and to show the vertical and lateral variations of resistivity over the study area.

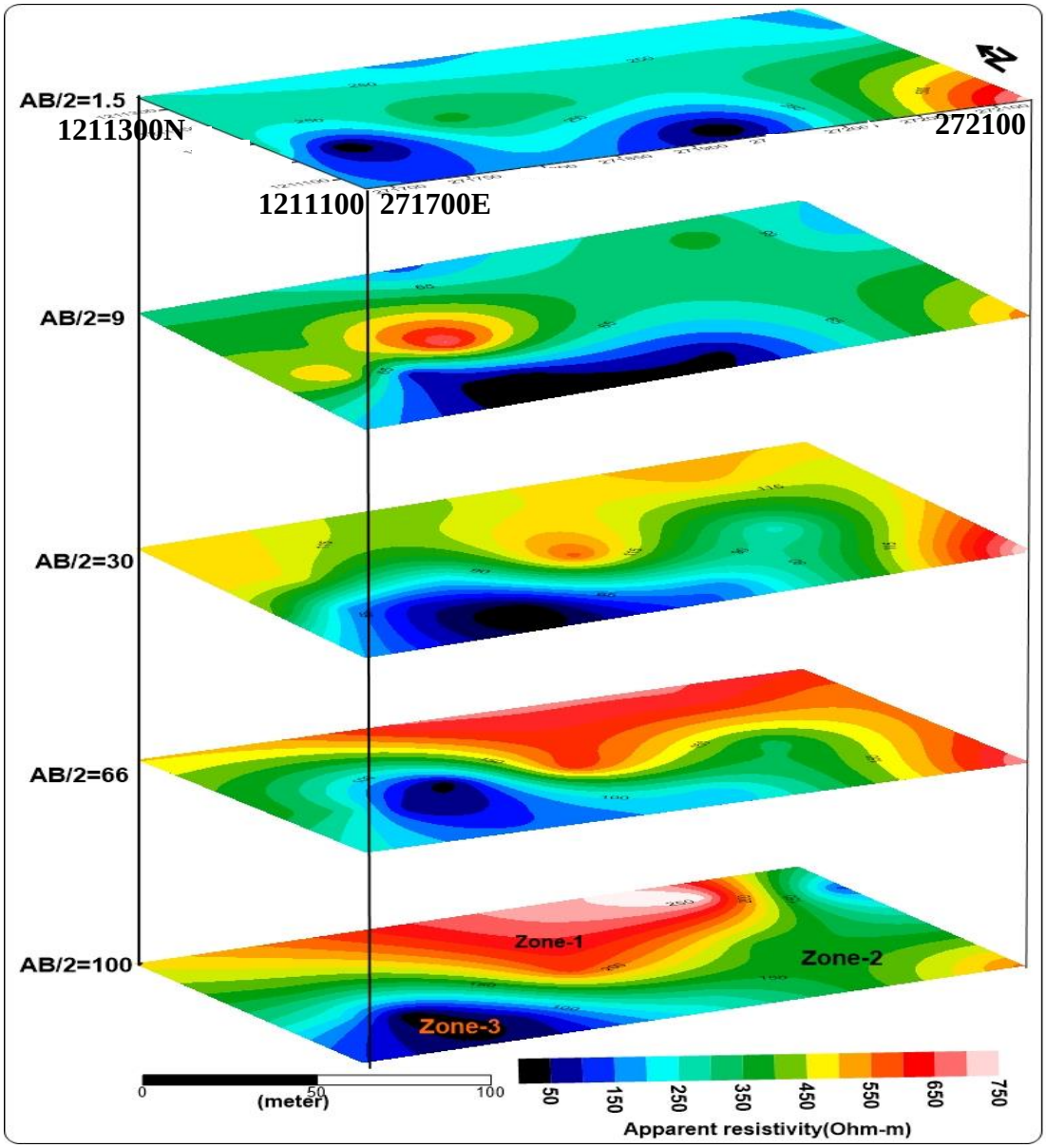

Figure5.9. Sliced-Stacked apparent resistivity map at different AB/2 of the construction site

From the sliced-stacked map (Figure5.9), it is found that most northern, northeastern and eastern part of the study area is characterized by with high resistivity ranging from 450-750Ω-m in the study area. On the other hand, relatively low resistivity value characterizes the southern, southwestern and western part of the survey.

Based on this map (figure5.9) we can see the study area into three resistivity zones (Zone-1, Zone-2 and Zone-3).

Zone-1 is characterized by relatively very high apparent resistivity value which ranges from 450Ω-m to 750 Ω-m. This high resistivity value is possibly the response of the basaltic formation in the survey area. This formation dominates the northern, northeastern, eastern and southeastern

part and it is extends to a high depth on these flanks.

Zone-2 is characterized by relatively intermediate apparent resistivity value ranging from 150Ω-m to400Ω-m.This zone covers most of the central part of the study area and its coverage increases towards the East and the West.

Zone-3 this zone is characterized by relatively low resistivity which covers the southern and south eastern part of the construction site. It is found at all depths with variable lateral extension.

In general this map shows that the southern, western and southwestern part of the construction site comprises subsurface formation which has low resistivity as a result of the presence of water saturated, weathered and fractured vesicular basalt. As a result, it is not recommended for foundation purpose and/or it requires special attention in design and construction. However, most of the eastern and northeastern part of the survey site covered by higher resistive formation. This higher resistivity values are the responses of relatively competent formations as a result it is advisable to set the building foundation in the northern, eastern and northeastern part of the study area. This result is more or less similar with the results drawn from the geoelectric section map, inversion and velocity models.

5.3 Interpretation of seismic refraction data

Data were processed using the software programs PickWin95 and Plotrefa from the SeisImager software package. These programs allow cross-sectional areas of the subsurface beneath each spread to be plotted, thus modeling the bedrock interface using a time-term inversion method was employed. A three-layer model was employed to represent the basalt bedrock, vesicular basalt and a thin top soil layer. Raw field data were imported into PickWin95 and then before picking the first arrival times, band pass frequency filter using upper and lower cut off frequency of 409.6HZ and 56.95HZ respectively was applied to remove the noise and improve signal to noise ratio. The first arrival times were picked up using the auto-pick option of the system for all records and few adjustments were made manually where it seems necessary. This was performed for each of the shot points along the spreads. Then, the first arrival data were imported into Plotrefa, and a plot of time versus distance (1/v) was generated (Fig. 4.9). Plotrefa automatically checks reciprocal times for multiple shot locations. It is best if the root mean square (RMS) error is less than 5%. Most of the data points in the spreads have RMS values below 5%; however, there are some data points with higher RMS errors.

Layers are assigned by identifying crossover points, which occur where the slope of 1/v changes. The crossover point separating vesicular basalt and basalt is minor, but the change in

slope between the top soil and bedrock is distinct. After the layer assignment, a time-term inversion model can be run, then using this results as an initial model tomographic inversion is applied. Velocity is calculated and the model depth is inferred. Velocity models for each spreads were generated using different first arrival picks in order to gain an understanding of model sensitivity.

The model produced using the above software packages were interpreted according to the area geology and the parameters determined from the model. Because of noise data of the seismic refraction spread three, first arrival picking of p-wave travel times was very difficult. Therefore, spread three was not considered in the processing and interpretation part.

5.3.1 Velocity model for Spread-1

The seismic refraction velocity model for spread one is presented as in figure5.1. This is 92m long profile which runs NW-SE direction. The model is generated using time-term inversion method. The velocity model represents seismic velocities between 280m/s and 1758m/s. The top most layer shows low p-wave velocity varies 280-520m/s and is about 1.5-3m thick with slight difference along the spread. The velocity indicates that the top layer is composed of soil deposits. The second layer is located at a depth of about2-3m.The velocity of this layer ranges 1400-1355m/s and from the lithological log in the study area this layer is probably weathered and fractured vesicular basalt. The p-wave velocity in the third layer is relatively high and from local geology and lithological log this layer is possibly moderately weathered and fractured basalt. This moderately weathered and fractured basalt is regarded as the bed rock in the building site. The velocity of the model shows that the third layer is relatively strong rock type. Its velocity is 1758m/s. The depth of this layer is varies along the spread. It extends relatively high depth to the left ends of the model (Figure5.10).

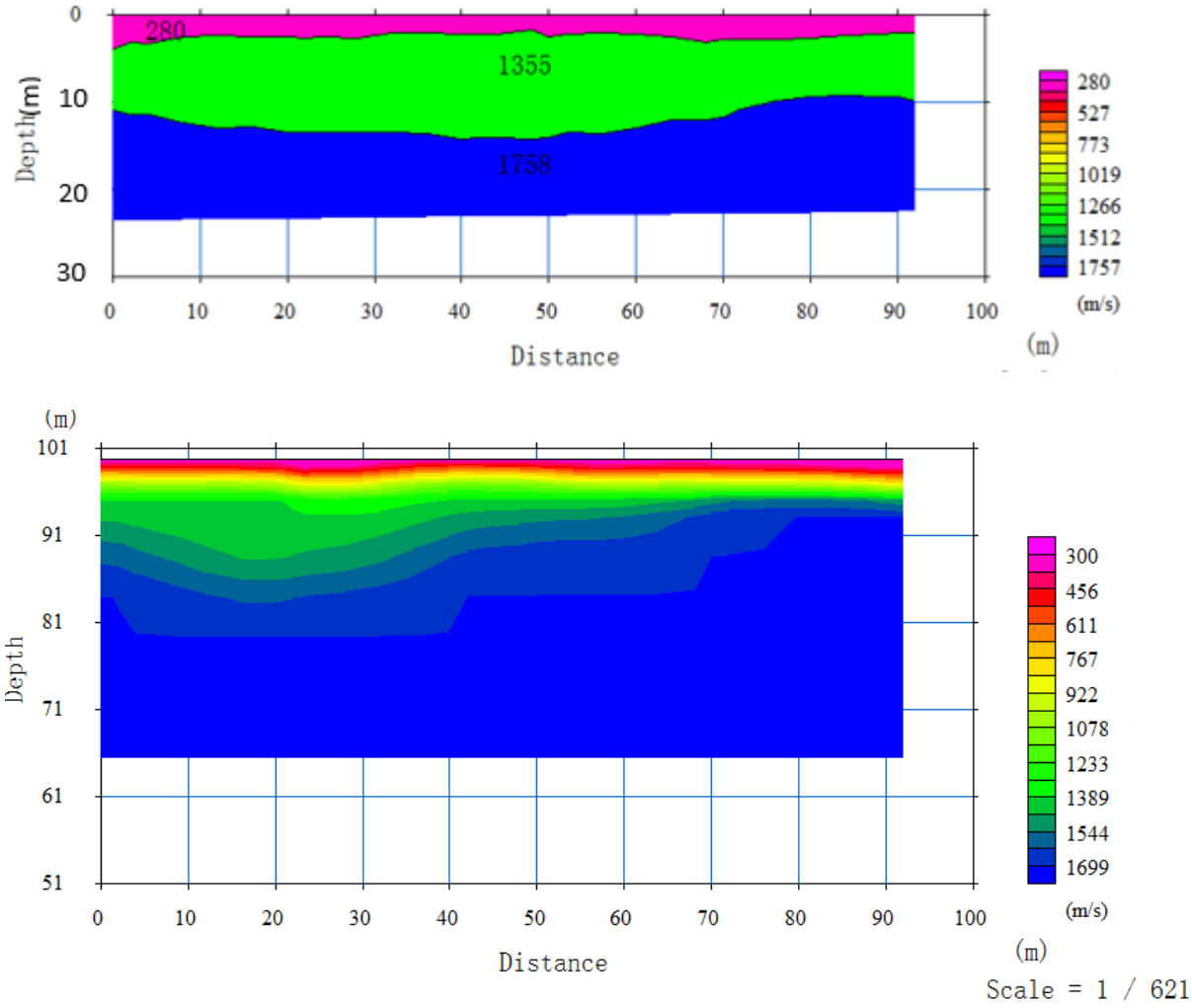

Figure 5.10.Time-term and 2D seismic tomography velocity models for spread-1

5.3.2 Velocity model for Spread-2

The seismic refraction of spread two lie in the same line as that of spread one laying in NW-SE direction and its velocity model is presented in figure5.11 with total spread length of 88m.From the velocity model generated from this profile, the time-term inversion model show three p-wave velocity layers. The model presents seismic velocities between 458m/s and 1500m/s. The top layer shows low p-wave velocity of 458m/s and the thickness of this layer is almost similar along the spread. The p-wave velocity indicates that the top layer consists soil deposits of clay, silt and sand. The p-wave velocity of the second layer is varying 900m/s-1250m/s and from the lithological log in the study area this layer more likely to be slightly weathered and highly fractured vesicular basalt. The p-wave velocity in the third layer is relatively high 1500m/s and from the lithological log this layer is probably moderately weathered and fractured basalt. This moderately weathered and fractured basalt is regarded as

the bed rock of the site. The velocity of the model shows that the third layer is relatively competent rock formation. The depth of this layer is different at the left and right ends of the velocity model. It is relatively deeper in the left side of the velocity model than towards the right end.

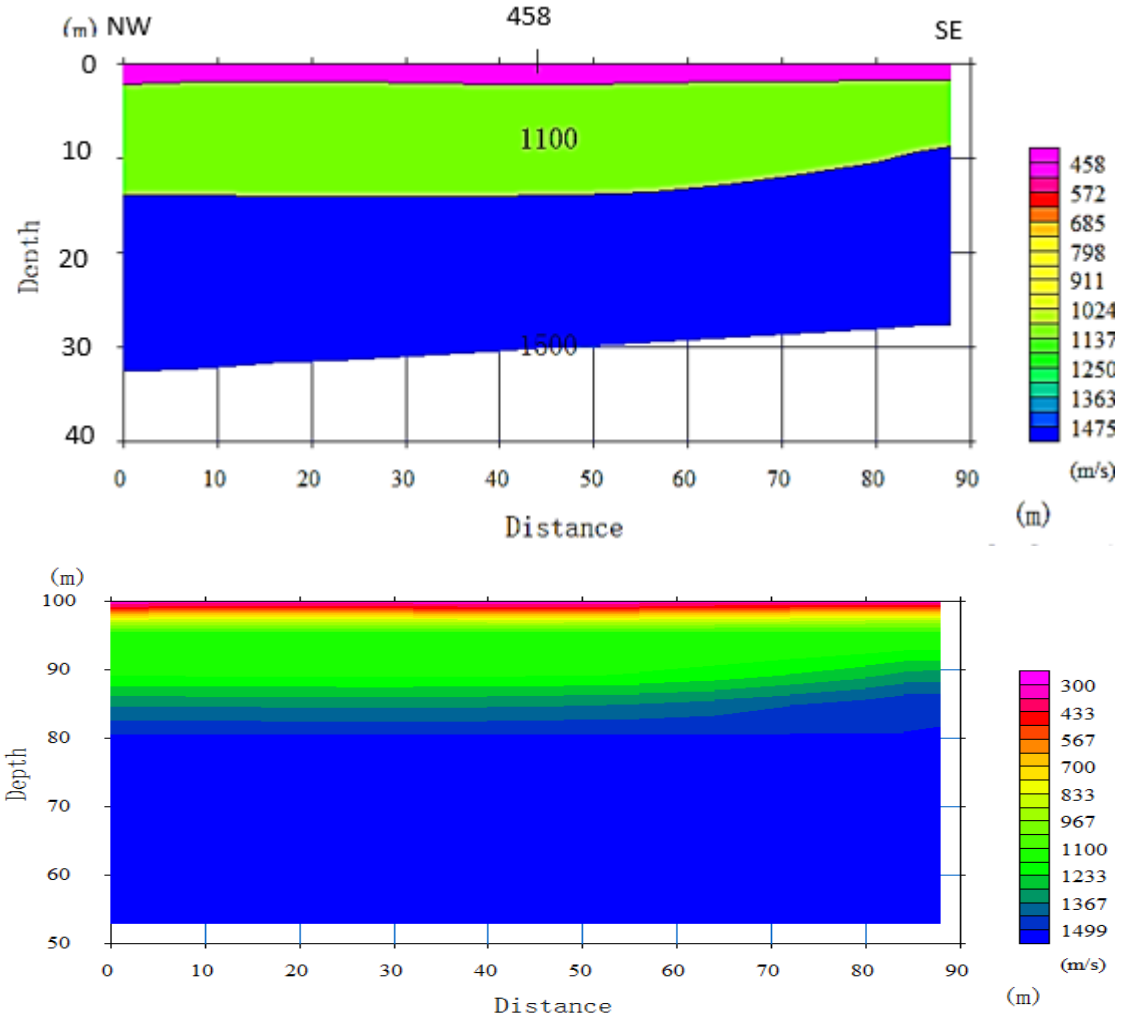

Figure 5.11.Time-term and 2D seismic tomography velocity models for spread-2

5.3.3 Velocity model for spread-4

In spread four the first Layer in the velocity model essentially shows (fig.5.12) low-velocity material overlying on medium velocity layer. This 300m/s indicates that the top layer is dominated by soil deposits of clay, silt and sand with thickness ranging from 2-3m.

The velocity of the second Layer with p-wave velocity 1200m/s indicates moderately zone which is possibly weathered and highly fractured vesicular basalt from the lithological log near by the boundary of the study area. The depth for this layer extends up to about 12m.

The third layer which has a relatively high p-wave velocity material 3000m/s at the base of the velocity model is interpreted as to represent moderately weathered and fractured basalt and it

is considered as bed rock in the area. This layer is suggested relatively good for setting civil structures.

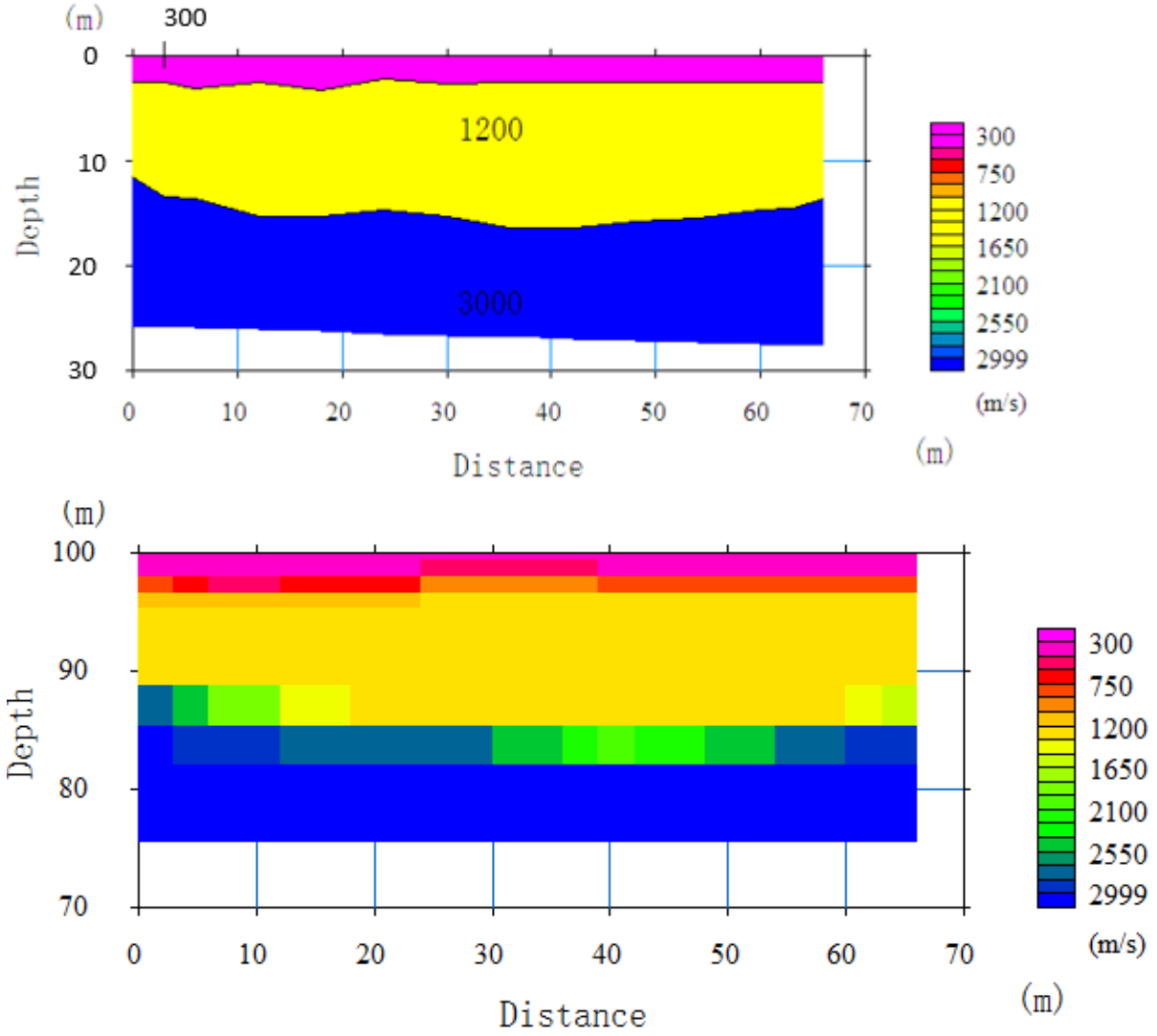

Figure 5.12. Time-term and 2D seismic tomography velocity models for spread-4

5.3.4 Velocity model for spread-5

The seismic refraction of spread five laying in E-W direction which crosses profile four of the electrical resistivity sounding survey. As shown in velocity model (Figure.5.13) the thickness of the first top layer is vary 2-3m with seismic velocity of 255m/s. Information from the lithologic log and the velocity value this layer is more likely made up of top soils of clay, silt, and sand. The second layer with p-wave velocity value 1092m/s is corresponding to weathered and highly fractured vesicular basalt. This layer from the geoelectric section has low resistivity due to its high moisture content. The third layer has relatively high p-wave velocity 2225m/s and it is found at a depth up to about 10-12m. From the calculated velocity and borehole

information, this layer may be moderately weathered and fractured basaltic formation. This layer is relatively competent and therefore it is regarded as the bed rock in the study area.

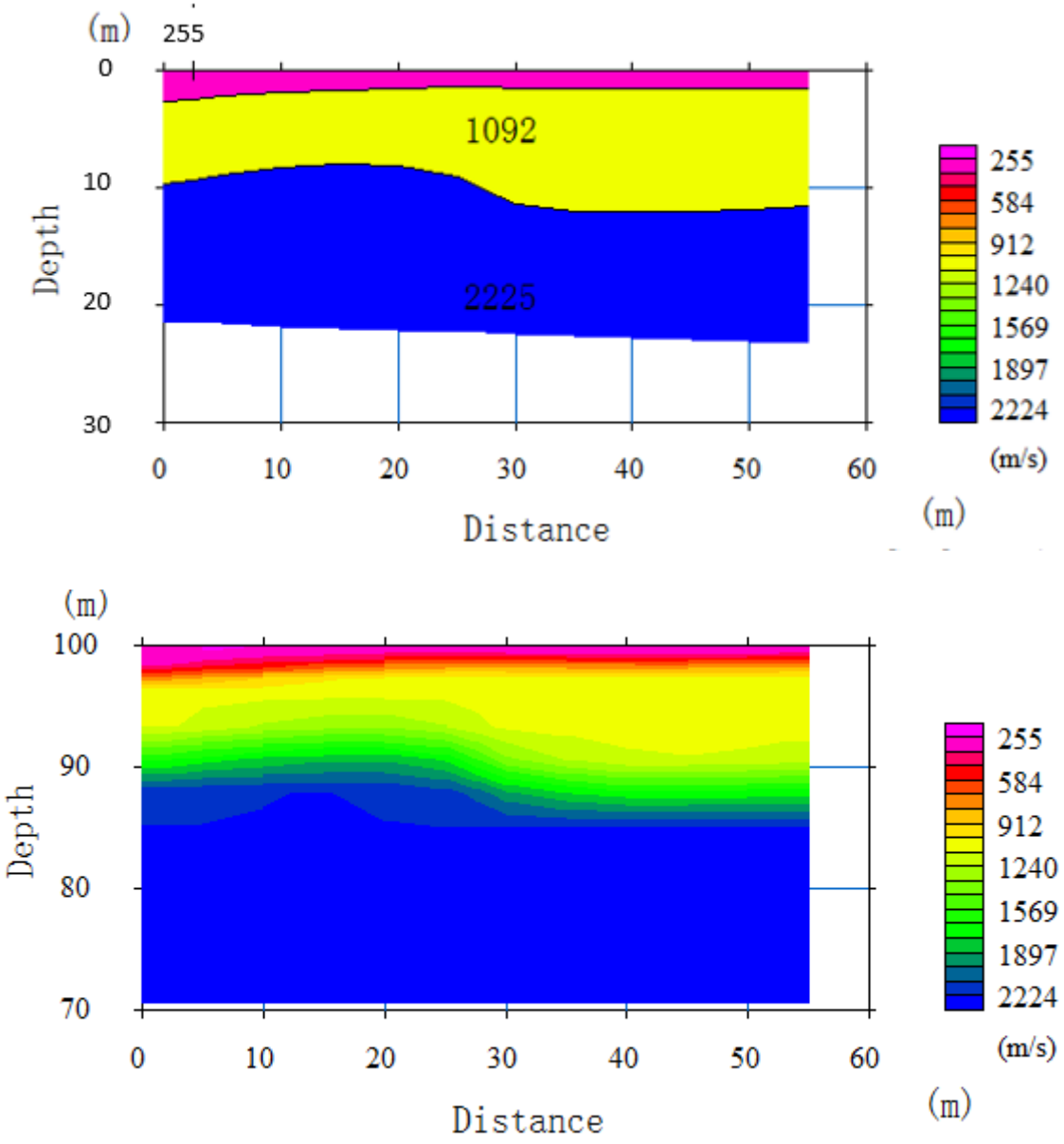

Figure5.13.Time-term and 2D seismic tomography velocity models for spread-5

5.3.5 Spread-6 Velocity model

Spread six is parallel to profile four of the resistivity sounding survey which lies along SW-NE direction. The seismic velocity model of this spread is shown in Figure5.14.The top Layer of the velocity model for spread six is about 3-4 m thick with average P-wave velocity of 510m/s. Layer 2 and 3 have average velocities of 948m/s and 2555m/s respectively. The third Layer is buried about 11-13 m deep in the spread line. The second layer of spread six has relatively low

velocity as compared to other spreads in the survey area. This may due to the presence of completely weathered and fractured vesicular basalt. Some intercalation of clay material in the vesicular basalt.

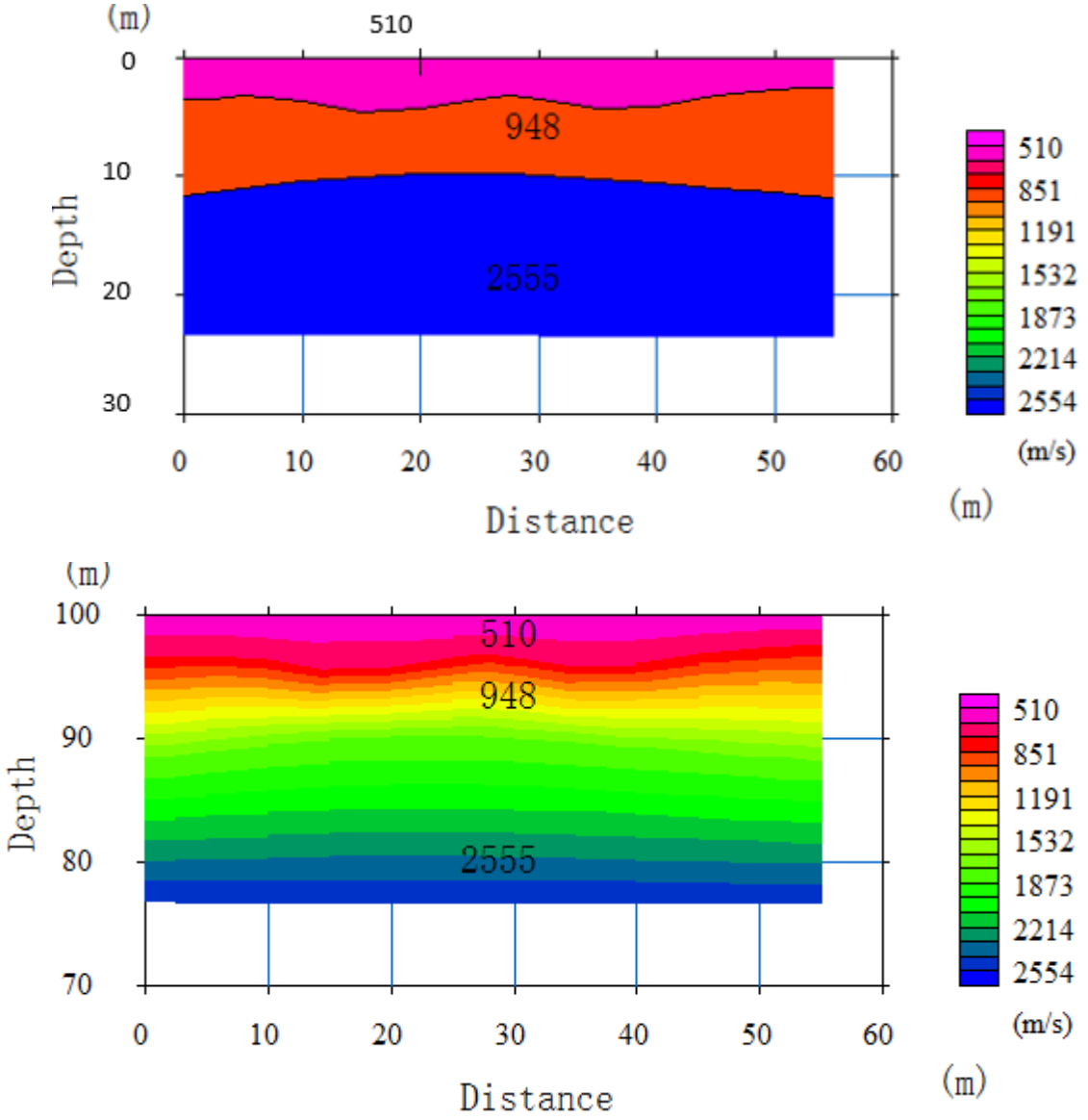

Figure5.14.Time-term and 2D seismic tomography velocity models for spread-6

5.3.6 Velocity model for spread-7

Velocity model generated for spread seven located to the northwestern end of the survey area as shown in Figure 4.5. As the p-wave velocity model Figure 5.15 shows the thickness of the top most layer varies from 2-3m with velocity of 273m/s. This very low p-wave velocity indicates the top layer is composed of clay, silt and sand deposits. From the lithological log in the study area the second layer is more likely to be weathered and highly fractured vesicular basalt with p-wave velocity varies 1400-1802m/s. This layer is mapped at depth ranges 3-15m

deep with irregular morphology. Moderately weathered and fractured basalt is mapped below this layer with velocity of 2527m/s. The p-wave velocity of this layer suggests that it is competent enough to be the bed rock of the study area and it is located at a depth of about 10-15m.From the velocity model we can point out that for each layer velocity it is changed abruptly, it does not show gradational change. Relatively this bed rock is one the most competent one. The competent rock formation is relatively at shallow depth in the left side of the velocity model as compared to right end of the spread.

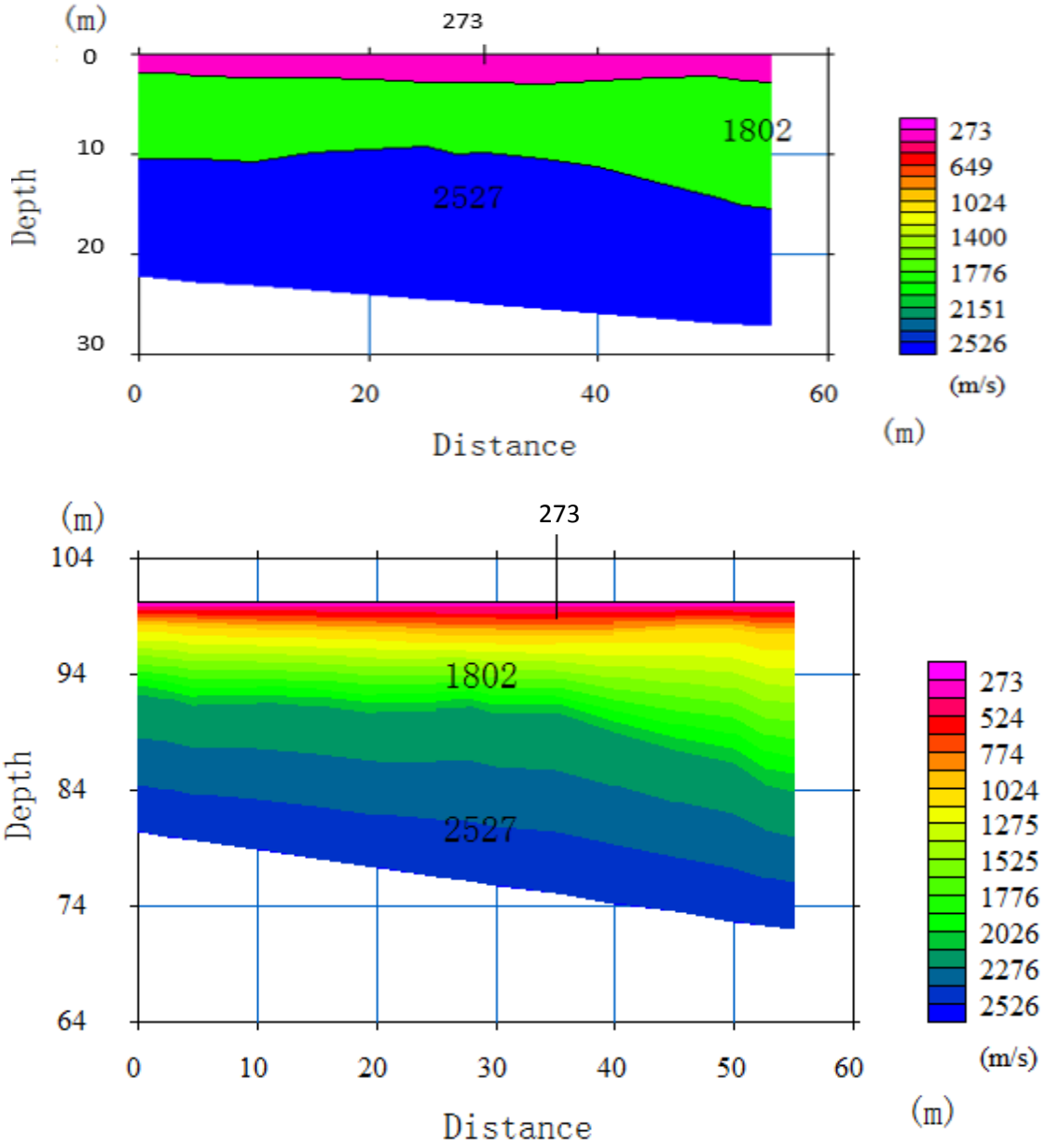

Figure5.15.Time-term and 2D seismic tomography velocity models for Spread-7

5.4 Interpretation of magnetic data

Magnetic data can be interpreted both qualitatively and quantitatively. The qualitative process is largely map-based and dominates the early stages of a study. Qualitative interpretation involves recognition of the nature of discrete anomalous bodies including intrusions and faults. Magnetic method has many applications in engineering studies is to locate contacts between different lithological units and geological structures that display magnetic contrasts such as faults or dykes. To interpret the magnetic data in terms of such subsurface indications, the magnetic data are presented in different forms. As a result, different magnetic intensity/anomaly maps that are assumed to be relevant for this thesis work were produced following the appropriate reduction procedures. All the magnetic anomaly maps were generated using Geosoft Oasis Montaj (Version 6.4.2) software.

5.4.1 Total magnetic field anomaly map

The image of the total magnetic field anomaly map of the study area is shown in figure5.16. The map is produced from the difference between the diurnally corrected total magnetic field and the expected value of the IGRF in the study area. The map is used to see the overall subsurface structure.

The anomaly map of the survey area can classified in to three regions as A, B and C. Region-A is characterized by very high magnetic anomaly and it covers the southern, northern and northeastern part of the study area.

Region-B, which have intermediate magnetic anomaly covers most of the central part, southeastern and northern of the study area. The area represented by region-C shows very low magnetic anomaly and it covers the northwestern, western and some portion of the central part of the area. In addition, this zone shows NW-SE trend on the survey area. This NW-SE trending zone with low magnetic anomaly is interpreted as weak or contact zone on the analytical signal and tilt angle derivative maps.

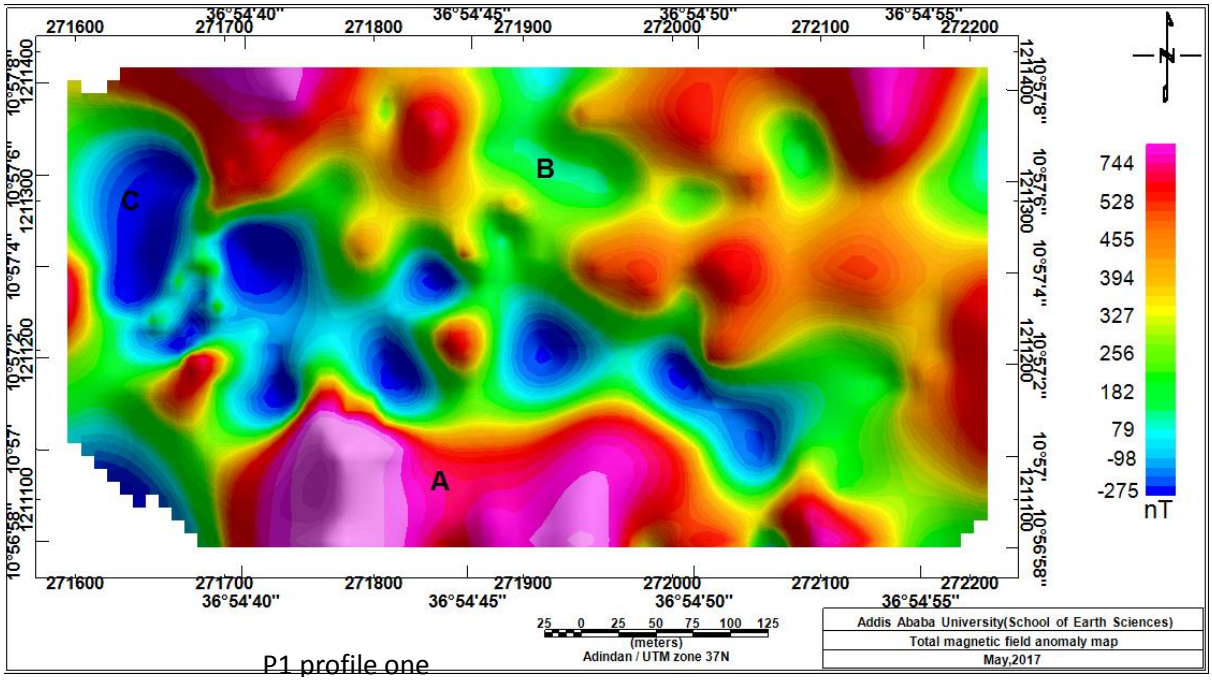

Figure 5.16.Total magnetic field anomaly map Injibara University campus construction site

5.4.2 Analytical Signal Map

The total magnetic field anomaly map obtained in the survey area is used to produce the analytical signal map (figure5.17) using the Geosoft Oasis Montaj (6.4.2) software. The analytical signal the map shows the responses of anomalous bodies in the upper part of their sources. The analytic signal map shows maximum contrast over magnetic contacts or weak zones. In the study area, possibly two aligned weak zones or contacts are identified which oriented in the same direction NW-SE as shown in Figure 5.17 with thick dashed lines.

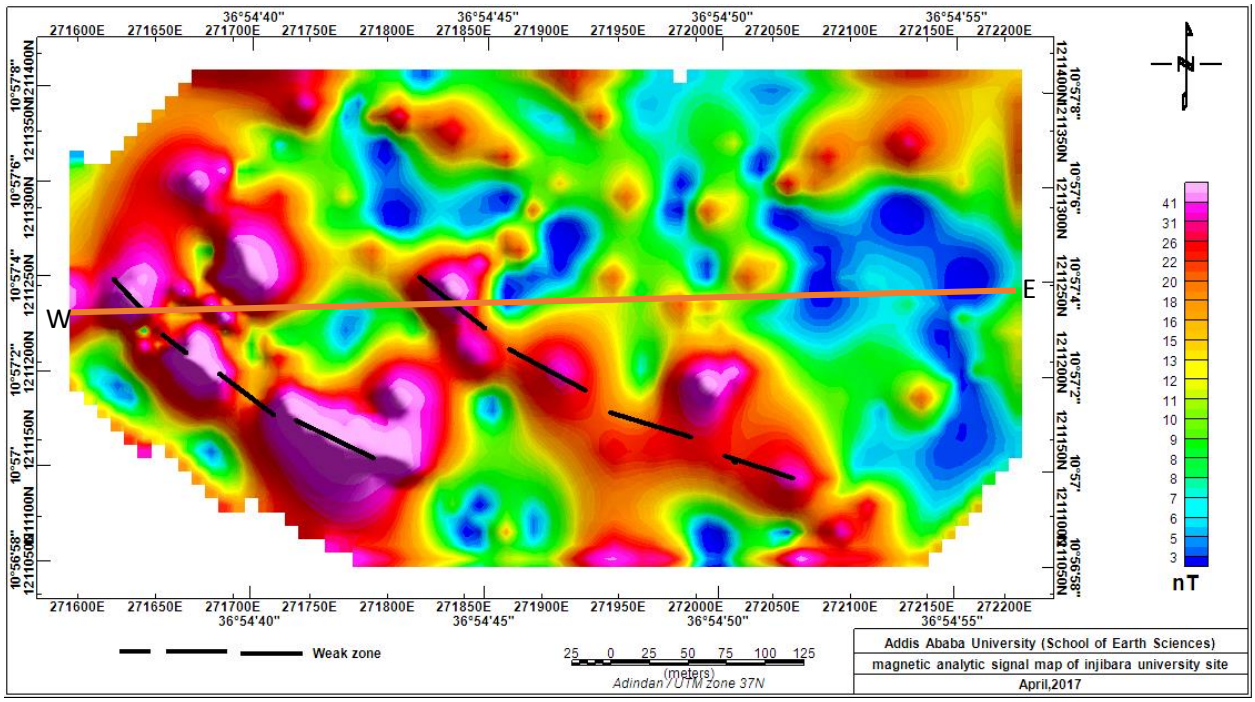

Figure 5.17. Magnetic analytical signal map Injibara University campus construction site

5.4.3 Magnetic tilt derivative map

The tilt derivative map is obtained by applying a tilt derivative filter to the magnetic analytical signal map using Geosoft Oasis Montaj (v6.4.2) software. The map is used to locate edges and geological boundaries in the study area. It produces a zero value over or near the source edges with positive values over the source and negative values outside the source (Alemayehu Ayele, 2012). The tilt angle map (Figure5.18) shows the orientation and relative position of the weak zones or contacts in the surveyed area is demarcated on the map. The orientation and position of the weak zones indicated in the tilt angle map has a similar trend with that of the analytical signal map shown above.

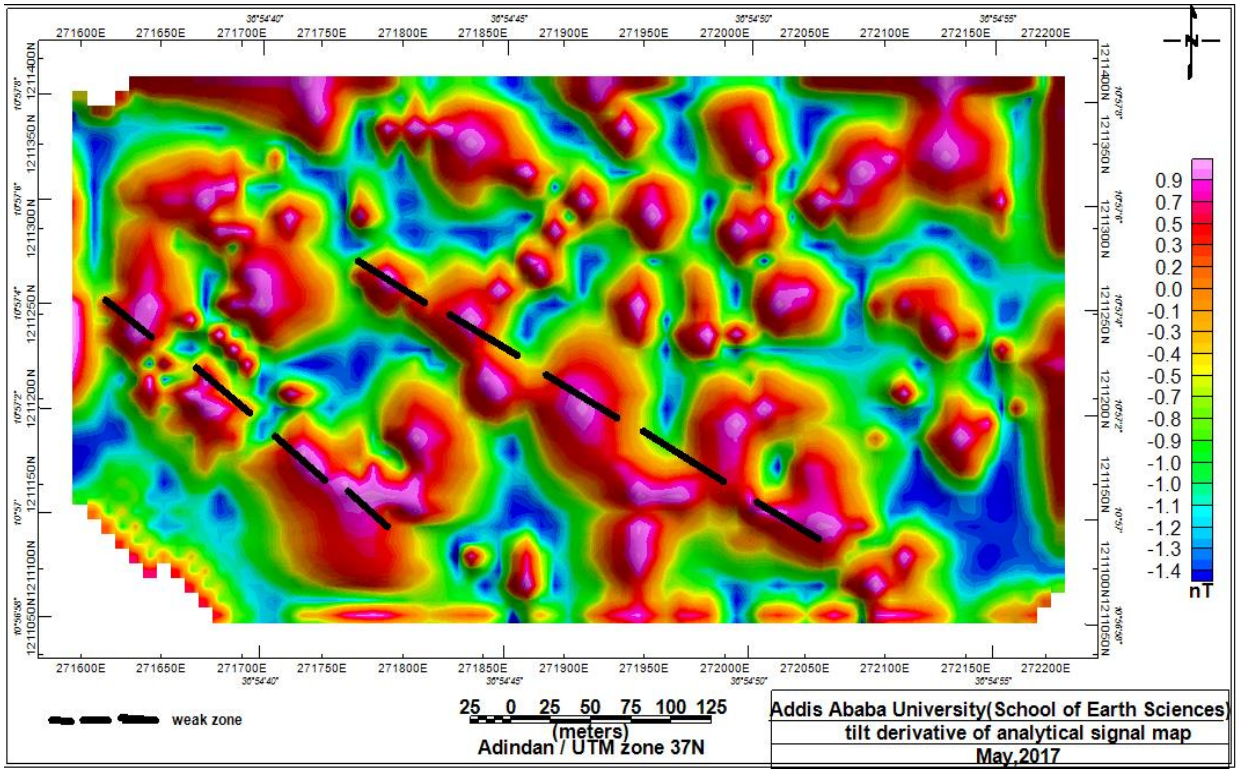

Figure 5.18.Magnetic tilt derivative map

5.4.4. Magnetic 2D modeling

The model was constructed from the anomaly values extracted from the magnetic analytical signal anomaly map (Figure5.17) using GM-SYS modeling Geosoft Oasis Montaj software. It is an interactive forward modeling program which calculates the magnetic response from a user defined hypothetical geological model. A starting magnetic susceptibility model was obtained from the standard books. Any difference between the model response and the observed magnetic field are reduced by refining the model structure. It should be noted that magnetic models are nonunique, i.e. many Earth models can produce the same magnetic response. The model (Figure5.19) shows, to the western part of the model the top soil is relatively thick as compared to the eastern end of the model. From the model the second layer which is weathered and fractured vesicular basalt is relatively thick in the eastern part of the model and the third layer, weathered and fractured basalt, is found relatively at shallow depth in the western part of the model as compared to the eastern.

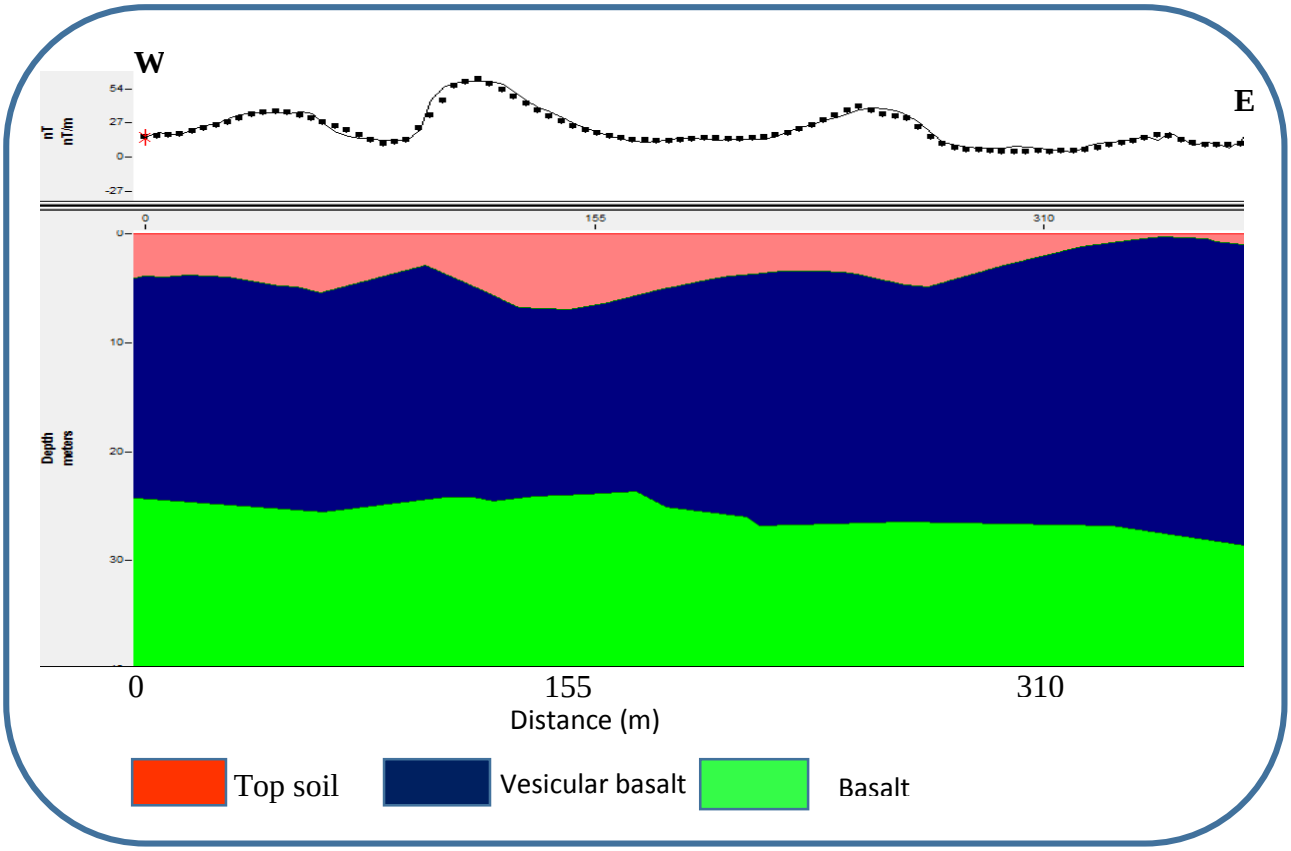

Figure 5.19. Magnetic 2D modeling along selected profile of Injibara University building site.

5.5 Combined Interpretation of resistivity and seismic refraction data

Profile-1

Relatively high resistivity layer 97-441Ω-m on the geoelectric section of profile-1 (Figure 5.20(A)) is found from the top of the profile. This layer has almost similar thickness up to 300m along the profile. After 300m the thickness of this layer considerably decreases towards southeastern part. The low resistivity layer underlie by the top layer extend to depths of about 27m just beneath VES2 and VES7 in areas where weak zone is present. The third layer show high resistivity and corresponds to a relatively competent formation.

The velocity-depth model of profile-1 (Figure5.20 (B)) shows with an average velocity of 369m/s and thickness of about 1.5-3m for the first layer. The second layer recorded an average elastic wave velocity of 1227.5m/s in a depth range of 1.5-13m. Velocity of 1758m/s may a signature of the hard underlying bedrock on this profile was found at depth ranges 10-13 meters.

From figure 5.20 we can conclude that the resistivity and refraction survey gives almost similar result but not quite uniform. The depth and the overall trend of the three layers from the both methods are almost similar.

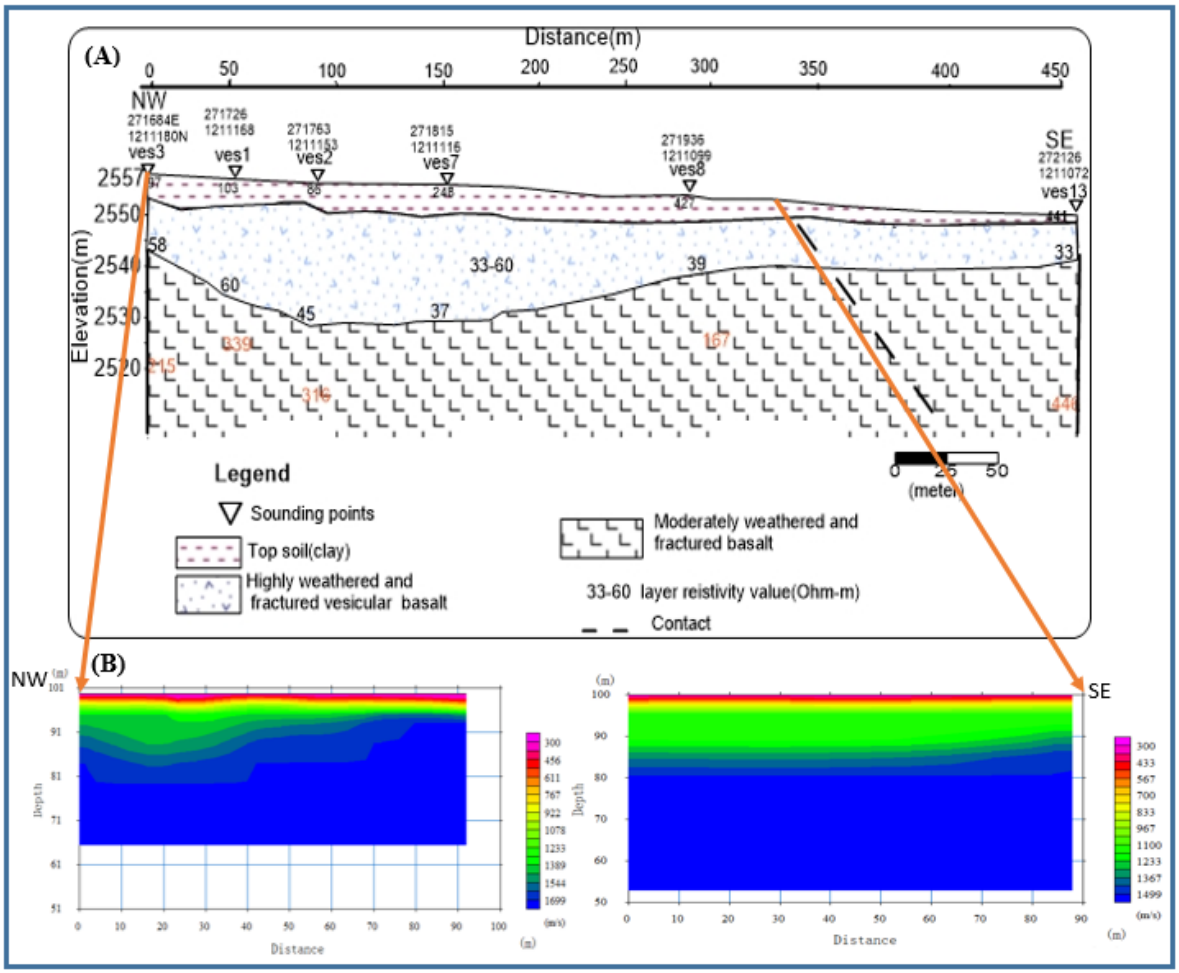

Figure5.20.Combined interpretation of Geoelectric section and velocity-depth model of Profile-1

Depth to bedrock estimated in both methods show considerable difference this may come due to the resolution difference in vertical depth. Both methods have also their own limitations, the resolution of the resistivity method decreases exponentially with depth and the image becomes increasingly fuzzier with depth. Refraction seismic has a limitation to see very thin layer and low velocity zone at depth.

The resistivity profiles 1-4 in study area show a series of very low resistive zones, which can be related to local fracture and weathering. For example, Profile 1, 2 and 4 shows a deep low-resistivity zone in between high resistive zones. Such an anomaly can be caused by a water-saturated fracture or weathering and have been observed on different profiles and can probably

be used to trace the weak zone in the study area. By comparing the two we can easily distinguish the overburden from the bedrock. However, only two spreads in the seismic survey correlate to anomalies in the resistivity profile.

5.6 Combined interpretation of resistivity and magnetic data

Profile-1

Variation of magnetic anomaly profile conducted along profile-1 ranges nearly from -41 to 78nT as shown figure5.21a.These low and high peaks, which indicate the presence of weak zone or local fractures and high anomaly zones, appear at a distance of about 99m and 163m respectively. The low peak anomaly in the profile almost coincides with the discontinuities or local fractures displayed on the geoelectric section of this profile. Therefore, there is a positive correlation between magnetic anomaly plots with the geoelectric section of the same profile.

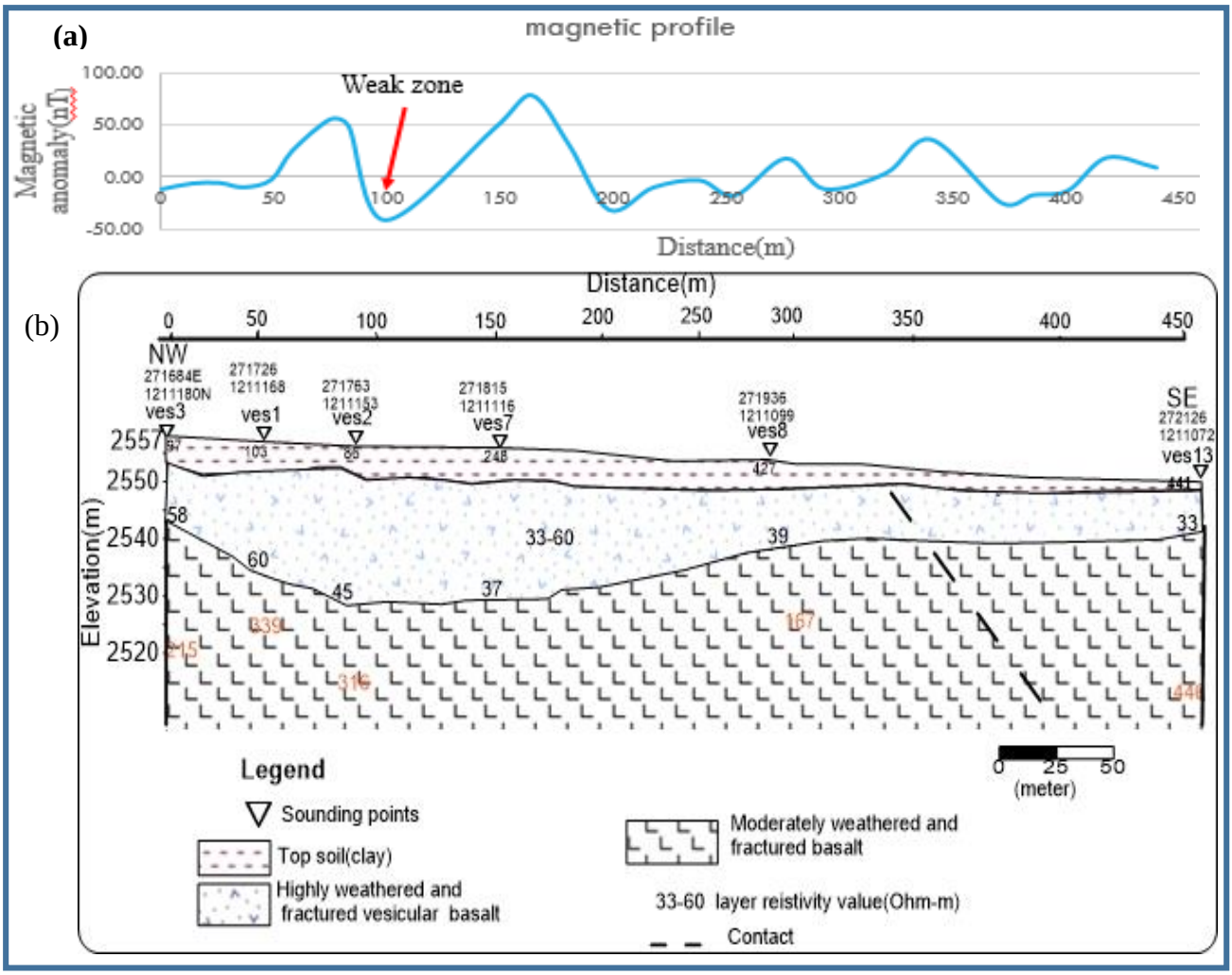

Figure5.21.Combined interpretation of Geoelectric section and magnetic anomaly of profile-1

CHAPTER VI

6. CONCLUSION AND RECOMMENDATIONS

6.1 Conclusions

Integrated geophysical studies involving electrical resistivity, seismic refraction and magnetic methods were carried out for engineering site characterization of the building construction site at Injibara University, southwest of Injibara town, Northwestern Ethiopia. Based on the results of collected data the following conclusions are made:

a) Based on geoelectric and seismic seismic velocity contrasts, i.e.,33-1,200Ω–m for resistivity and 255-3,000 m/s for p-wave velocity ranges, three distance layers underlying the study area are delineated. The top soil, characterized by 97-441Ω-m resistivity and 255-510 m/s p-wave velocity ranges, is associated with the response of the upper layer composed of clay, silt and sand. The relatively wide resistivity and p-wave velocity variations are due to heterogeneous nature of these top soils in terms of their compositions, degree of compactions and moisture contents. Over the area its thickness varies from about 1 at the SE part to 4m on NW flank of the study area. The second layer attributed to the highly weathered and fractured vesicular basalt is characterized by 33-70Ω-m resistivity and 948-1802 m/s P-wave velocity range and revealed somewhat undulating morphology. Such low resistivity rang (<70Ω-m) associated with this bed suggests its strongly weathered nature with possible content of significant amount of fluid. The third layer in the study area is described by relatively high resistivity p-wave velocity (on average >718Ω-m and 2250 m/s) values which are interpreted as responses of a moderately weathered and fractured basaltic bedrock, which is assumed to acquire suitable geotechnical characteristics to bear loads from heavy civil engineering structures. The depth to the surface of this competent formation ranges from about 10m in the NW end and SE part to 27m near to the central part of the study area.

b) The apparent resistivity pseudo-depth section maps show that NW part of the study area possesses relatively very low resistivity except profile-1 that may exhibit poor bearing capacity for the building set on. However, most pseudo-depth section maps indicated that the southeastern part of the study area shows high resistive formation which may provide better bearing capacity for the building foundation.

c) The sliced-stacked apparent resistivity section map indicates that the northeastern and southeastern portions of the study area may provide better bearing capacity for building foundation than the western and southwestern portion. Further, it is also anticipated that the strata with low resistivity may pose corrosive potential which may severely affect the steel structures in building foundation. Therefore, while designing the footing for proposed buildings proper care must be taken to protect it from the possible corrosive effect within strata of low resistivity.

d) The magnetic map shows high anomaly contrast. The analytical signal and the tilt derivative maps have clearly outlined localities of high magnetic gradient that probably are due to structural discontinues (weak zones) or may be lithologic contact zones.

From this it may be deduced that high magnetic anomaly responses are the results of relatively fresh igneous rocks whereas low magnetic anomaly responses are resulted due to weak zones and high degree of weathering in rocks. The dominant structural trend in the study area is inferred to have NW-SE orientation. These lineaments may have an adverse effect on the stability of building foundation.

e) Analytical signal map and tilt derivative of analytic signal show that the area associated with geological contacts or weak zone in the western and southwestern need special design for engineering foundation heavy civil structures.

6.2 Recommendations

The following recommendations are made based on the results and discussions, critical examination of the resistivity sections, seismic velocity models and magnetic anomaly maps obtained from the underground models and the external features found on the study area.

a) The subsurface near the central part to southwestern parts is highly weathered and fractured. Besides, the second layer that represents the fractured and weathered vesicular basalt with low resistivity values is inferred to contain considerable amount of moisture/water content. This relatively low resistivity bed with significant fluid content could be susceptible for displacement of foundation structures depending on the degree of groundwater level fluctuation. Therefore, the construction of students' dormitories or other office buildings at this specific location requires appropriate engineering measures to avoid any unexpected incidents from potential geo-hazard events.

b) Relative to the near central part of the area, the SE part, where more competent bedrock occurs at shallower depth, is more suitable for building foundation. Therefore, it is recommended to erect particularly student dormitories over such stable placed to ensure safety of human life against any geo-hazard consequences.

c) The second layer representing the fractured and weathered vesicular basalt with low resistivity is inferred to contain considerable amount of moisture/water content. May have a potential adverse effect on the suitability of designing foundation.

d) Localized anomaly distortions observed on analytical signal and tilt derivative maps at western and SW parts of the survey area are associated local fracture/weak zones. Therefore, these places need special attention during preparation of designs for foundation of heavy civil engineering structures.

e) The present study covered only some part of the university construction site. Therefore, to ensure the safety and sustainability of the buildings to be constructed in the future, additional investigations must be conducted at places where the University compound will be expanded.

REFERENCES

1. Alemayehu Ayele, (2012).Integrated geophysical and geotechnical investigations for the building site characterization of Wolkite University, Gubre, Wolkite,Ethiopia. Unpublished MSc Thesis, Addis Ababa University, Addis Ababa, Ethiopia.
2. Alhassan, D.U., (2010).Seismic refraction investigation of the subsurface structure at the southern part of the Niger state college of education, Minna, Nigeria.
3. Amhara design and supervision works enterprise, (2016).Hydrogeology and geotechnical work process.
4. Bernard, J. (2003): Short notes on the principles of geophysical methods for groundwater investigations.
5. EIGE. (2008).Geological report of bure map sheet (NC-37/5).
6. Emmanuael, T. (2015).Geotechnical site investigation using Seismic refraction and resistivity Techniques, Kwame Nkrumah University of Science and Technology.
7. Ethiopian Building Code Standard (1995). Code of Standards for Seismic Loads. Ministry of Work and Urban Development, Addis Ababa, Ethiopia.
8. Gerhard et al. (2007).Environmental Geology Handbook of Field Methods and Case Studies.
9. John Milsom, (2003).Field geophysics, the geological field guide series, University college of London.
10. Johnson, R.B and Degraff, J.V, 1991, Principles of Engineering Geology, John Wiley and Sons, New York.
11. Kearey, P., Brooks M., and Hill, L. (2002).An Introduction to Geophysical Exploration. Third edition. Blackwell Science Ltd, UK.
12. Kieffer B., Nicholas A., Henriette L., Florenece B., Delphine. B. Arnaud P., Gezahegn Y Dereje A., Dominique W., Dougal A.J, Francine K., and Claudine M., (2004). Flood and shield Basalt from Ethiopia magmas from the African supers well Journal of petrology 45,793-834
13. Loke, M.H (1999). Electrical Imaging Surveys for Environmental and Engineering Studies. A practical guide to 2-D and 3-D surveys. Penang, Malaysia, pp 57.
14. Loke, M. H. (2001). Electrical Imaging Survey for Environmental and Engineering Studies.
15. McCann, D.M., Jackson, D.D. and Culshaw, M.G. (1987). The Use of Geophysical Methods in the Detection of Natural Cavities and Mineshafts. Journ. Eng. Geol. London

16. Miller, H.G. and V.Singh, (1994). Potential Field Tilt. A new concept for location of potential field source: Journal of Applied Geophysics, 32; 213-217.
17. Mohor, p. (1963). The Ethiopian Cenozoic lavas p a study of some trends: spatial, temporal and chemical. Bulletin of the Geophysical Observatory, Addis Ababa, **6**, 103 – 144.
18. Mohar, P.A., (1971). The Geology of Ethiopia University College of Addis Ababa Press.
19. Mohr, P. 1983a. Ethiopian flood basalt province.
20. Mohr, P. A. (1971).The Geology of Ethiopia .253p Hailslassie I University, Addis Ababa.
21. Mohr, P.and Zanettin,B.(1988). The Ethiopian flood basalt province. In Macdougall, J.D. (ed.), Continental flood basalts. Kluwer Academic Publishers, Dordrecht.
22. Reynolds, (1997). "Introduction to Applied and Environmental Geophysics," John Wiley and Sons Ltd. England.
23. Reynolds, J. M. (2011). An introduction to applied and environmental geophysics. John Wiley & Sons.
24. Salem, A. and Ravat, D. (2006).A combined analytic signal and Euler method for automatic interpretation of magnetic data, Geophysics.
25. Sharma, P.V. (1997). Environmental and Engineering Geophysics. Cambridge Univ.Press.
26. Sheriff, R. E. (2002). Encyclopedic dictionary of applied geophysics.
27. Solomon Gerra, 2000.A short introduction to the geology of Ethiopia.
28. Telford, W.M., L.P. Geldart, R.E. Sheriff and D.A. keys, 1990. "Applied Geophysics, 2nd edn." Cambridge University Press, London.

Appendices

Appendix-1

Table 1: Lithological log of Awi University well

Depth(m)		Lithologic Description
From	To	
0	4	Top soil(clay)
4	8	Slightly weathered & fractured vesicular basalt
8	12	Slightly weathered & highly fractured vesicular basalt
12	18	Highly fractured & weathered vesicular basalt
18	24	Slightly weathered & Highly fractured vesicular basalt
24	28	Highly fractured and moderately weathered basalt
28	32	moderately weathered & highly fractured basalt
32	36	Moderately weathered & fractured basalt
36	44	Massive basalt
44	50	Scoracious basalt
50	52	clay
52	54	Moderately fractured scoracious basalt
54	56	Highly fractured & weathered scoracious basalt
56	58	Highly weathered & slightly fractured scoracious basalt
58	62	moderately fractured & highly weathered basalt
62	66	highly weathered & Slightly fractured basalt
66	68	Highly weathered & moderately fractured basalt
68	76	Slightly fractured & moderately weathered basalt
76	78	Slightly fractured & weathered basalt
78	80	Highly weathered & moderately fractured basalt
80	82	paleo soil
82	84	Highly weathered & slightly fractured basalt
84	86	Moderately fractured & weathered basalt
86	90	Slightly fractured & highly weathered basalt

Appendix-2

Figure1: Samples of resistivity sounding curves

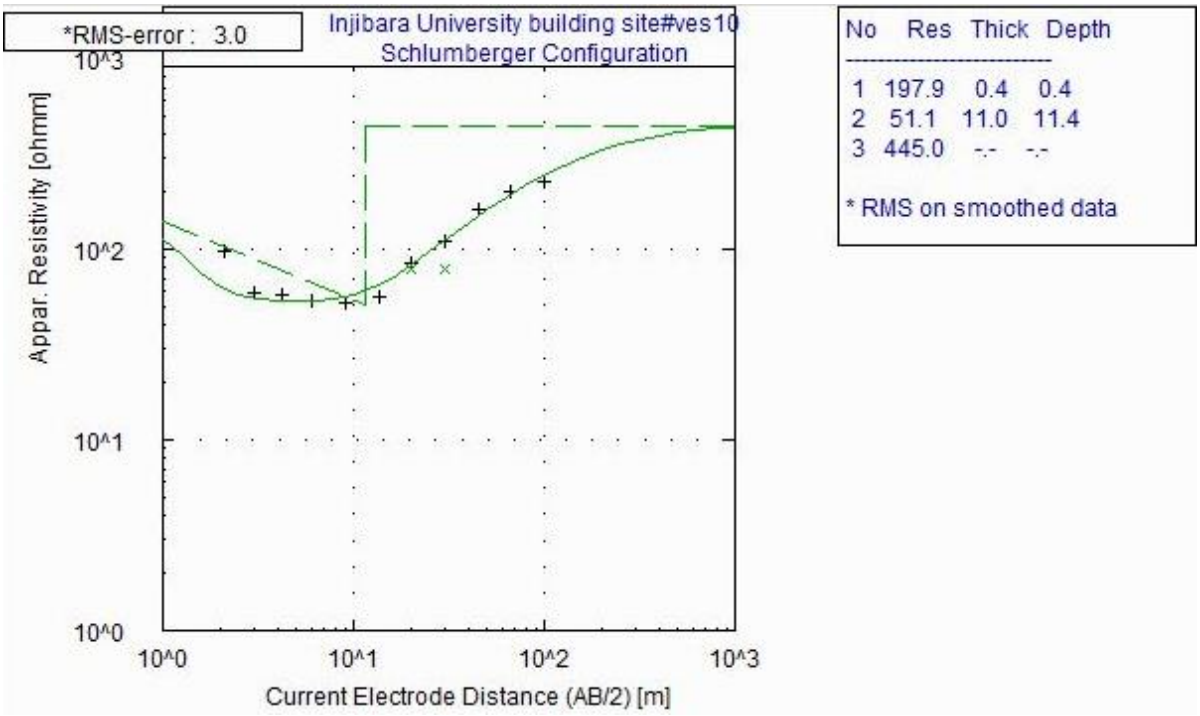

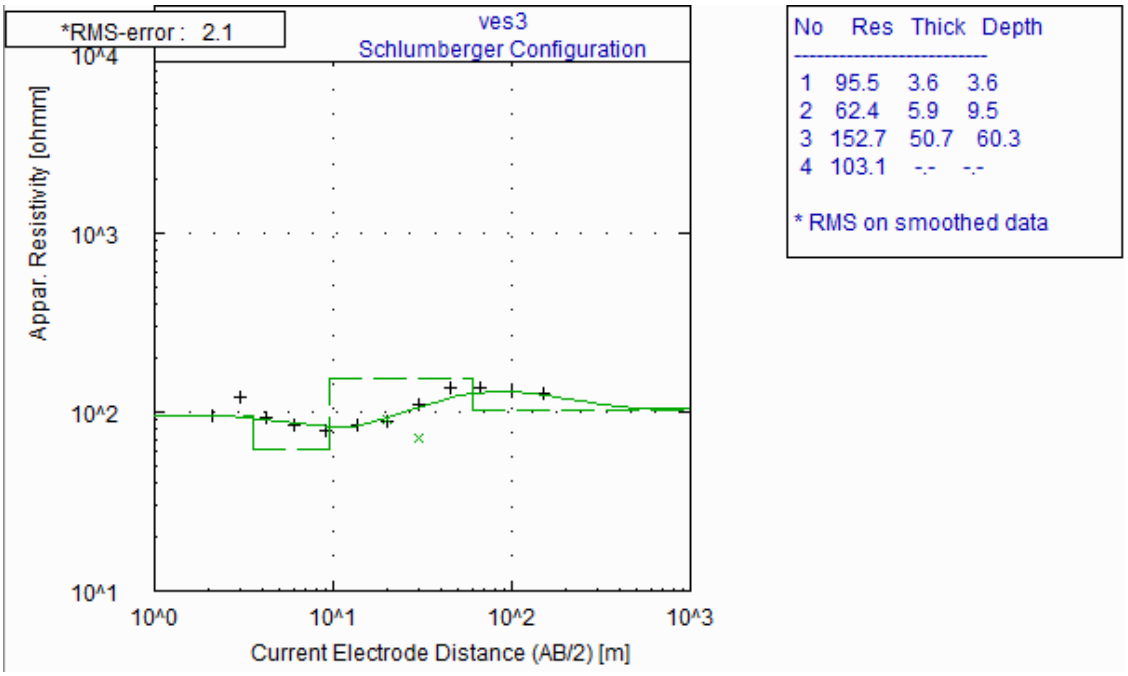

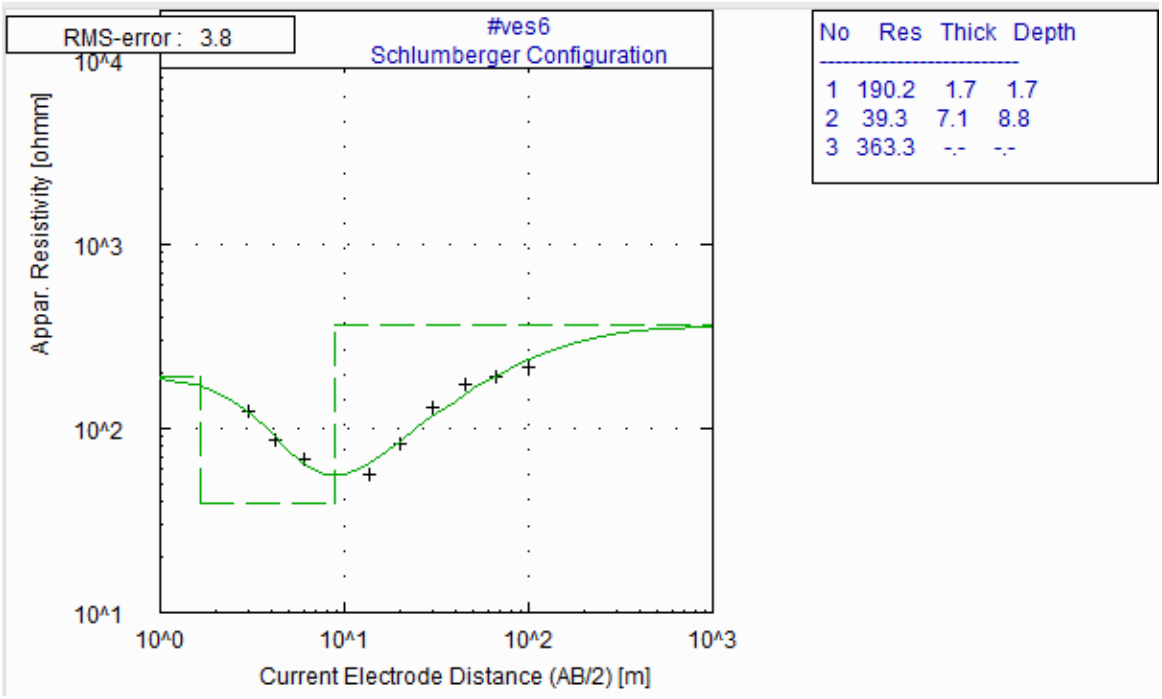
RMS-error : 3.8
#ves6
Schlumberger Configuration
Appar. Resistivity [ohmm]
10^4
10^3
10^2
10^1
10^0
10^1
10^2
10^3
Current Electrode Distance (AB/2) [m]
No Res Thick Depth
1 190.2 1.7 1.7
2 39.3 7.1 8.8
3 363.3 -.- -.-

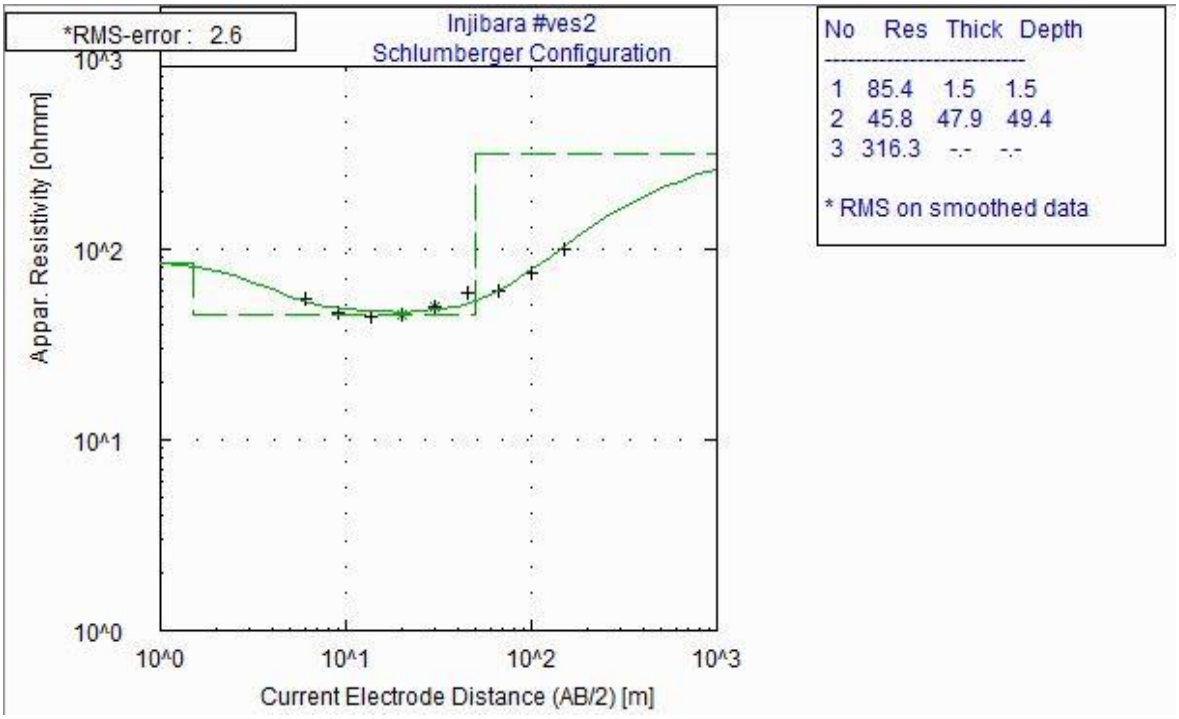
*RMS-error : 2.6
Injibara #ves2
Schlumberger Configuration
Appar. Resistivity [ohmm]
10^3
10^2
10^1
10^0
10^1
10^2
10^3
Current Electrode Distance (AB/2) [m]
No Res Thick Depth
1 85.4 1.5 1.5
2 45.8 47.9 49.4
3 316.3 -.- -.-
* RMS on smoothed data

Appendix-3

Figure2: Travel time-distance curves

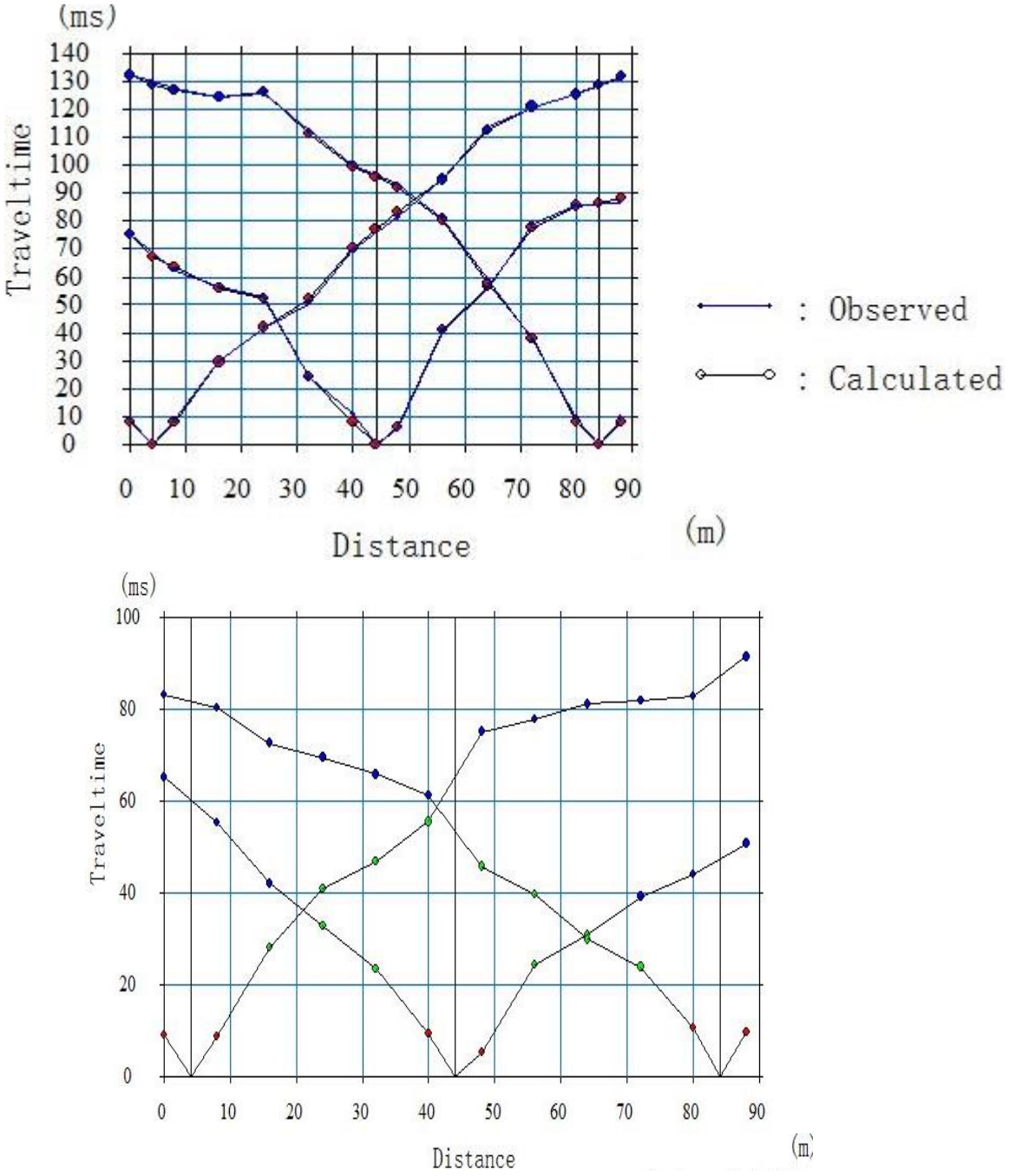

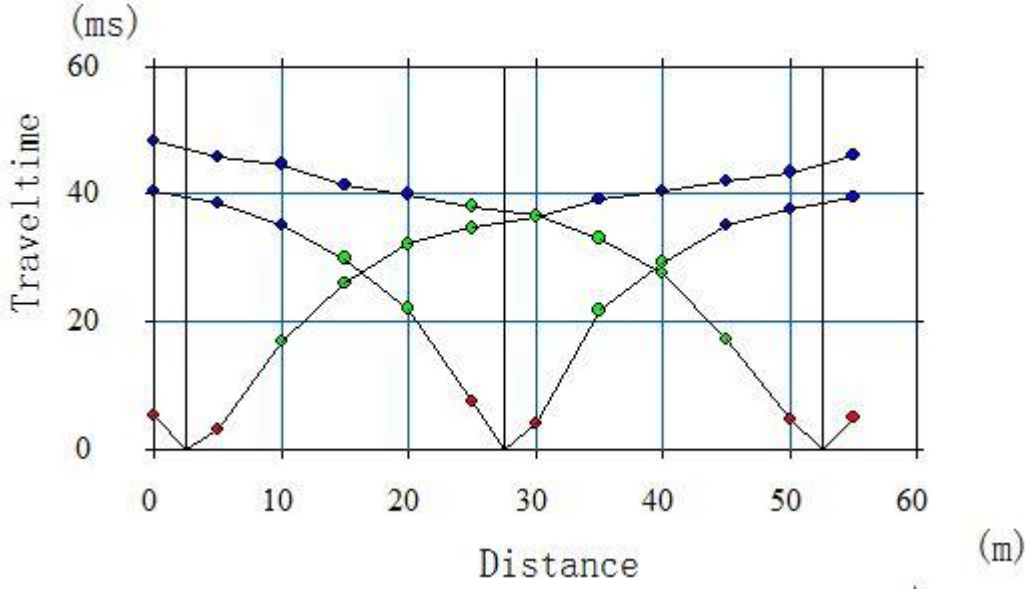
(ms)
60
40
20
0
Traveltime
0
10
20
30
40
50
60
Distance
(m)

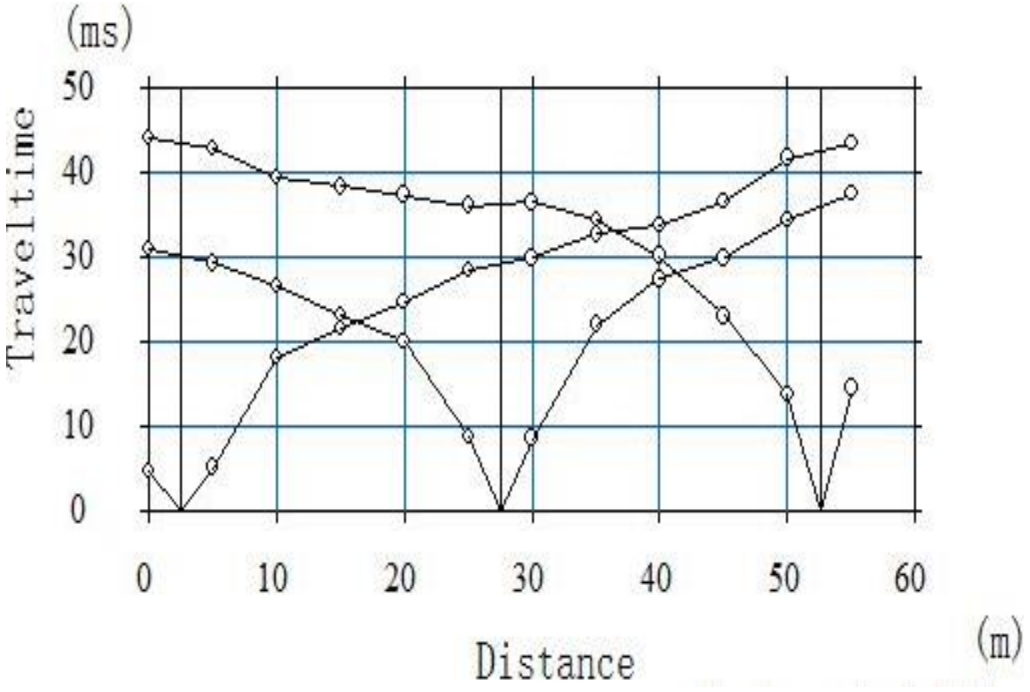
(ms)
50
40
30
20
10
0
Traveltime
0
10
20
30
40
50
60
Distance
(m)

Appendix-4

Table2: Resistivity of common rocks

Common rocks	Resistivity(Ω-m)
Topsoil	50–100
Loose sand	500–5000
Gravel	100–600
Clay	1–100
Weathered bedrock	100–1000
Sandstone	200–8000
Limestone	500–10 000
Greenstone	500–200 000
Gabbro	100–500 000
Granite	200–100 000
Basalt	200–100 000
Graphitic schist	10–500
Slates	500–500 000
Quartzite	500–800 000

Appendix-5

Table 3: P-wave velocities of different materials (Gerhard, 2005)

Earth materials	$V_{p(}$m/s)
water	1450-1530
Petroleum	1300-1400
loess	300-600
Soil	100-500
Snow	350-3000
Solid glacier ice	3000-4000
Sand loose	200-2000
Sand (dry, loose)	200-1000
Sand (water saturated loose)	1500-2000
Glacial moraine	1500-2700
Sand and gravel (near surface)	400-2300
Sand and gravel at 2km depth	3000-3500
Clay	1000-2500
Estuarine mud's/clay	300-1800
Flood plain alluvium	1800-2200
Permafrost quaternary sediments	1500-4900
Limestone (soft)	1400-4500
Limestone (hard)	2800-7000
Dolomites	2500-6500
Anhydrite	3500-5500
Rock salt	4000-5500
Gypsum	2000-3500